General Disclaimer

One or more of the Following Statements may affect this Document

- This document has been reproduced from the best copy furnished by the organizational source. It is being released in the interest of making available as much information as possible.

- This document may contain data, which exceeds the sheet parameters. It was furnished in this condition by the organizational source and is the best copy available.

- This document may contain tone-on-tone or color graphs, charts and/or pictures, which have been reproduced in black and white.

- This document is paginated as submitted by the original source.

- Portions of this document are not fully legible due to the historical nature of some of the material. However, it is the best reproduction available from the original submission.

LOW COST POINT FOCUS SOLAR CONCENTRATOR

**FINAL STUDY REPORT
PHASE I, PRELIMINARY DESIGN**

PREPARED FOR

JPL, PASADENA, CALIFORNIA

BY

GENERAL ELECTRIC COMPANY

ADVANCED ENERGY PROGRAMS

March 16, 1979

CONTRACT P.O. 9552 10

LOW COST POINT FOCUS

SOLAR CONCENTRATOR

FINAL STUDY REPORT

PHASE I, PRELIMINARY DESIGN

PREPARED FOR

JET PROPULSION LABAROTORY

BY

GENERAL ELECTRIC COMPANY - AEP

TABLE OF CONTENTS

SECTION 1.0

INTRODUCTION

1.0 INTRODUCTION

1.1 Program Overview

This report documents the activities and results relating to General Electric's approach to the preliminary design of a low cost point focus solar concentrator. The program spanned twenty-two weeks, six weeks of parameter analysis and sixteen weeks of analysis, design and production assessment activity. The overall schedule of activity is shown in Figure 1-1. The first task, Parameter Optimization, involved the modelling and trade-offs associated with predicting the concentrator performance and establishing the subsystem design requirements. Once a set of subsystem design requirements were set, the preliminary design (Task 2) and the production assessment (Task 4) commenced. The primary objective of this activity was to develop subsystem designs that were responsive to the established application requirements, compatible with volume and prototype production techniques and offered low cost solutions to meeting the subsystem requirements. Task 3 documented the appropriate interfaces with the receiver and engine and with the ground.

Prior to initiating activity on Phase I, a set of objectives were established for the Program. These objectives are:

1) Develop a preliminary design for a low cost point focus solar concentrator. The key phrase is low cost. Since the index of performance for the design was cost/performance, significant attention was placed on evolving a design that was as cost effective as possible.

2) Demonstrate critical material/process systems. A novel aspect of the design is the use of moldable plastic parabolic dish segments. It was deemed necessary to demonstrate at the sample specimen level that the material that we recommend in the design did indeed produce a plastic molded mirror.

	MOS	1		2		3			4		5	
	WKS.	1 2 3 4	5 6 7 8	9 10 11 12 13	14 15 16 17	18 19 20 21 22

| Task	Schedule
TASK I PARAMETER OPTIMIZATION	weeks 1–6
TASK II PRELIMINARY DESIGN	weeks 8–20
TASK III INTERFACE REQUIREMENTS	weeks 8–17
TASK IV ASSESS PRODUCTION IMPLEMENTATION	weeks 14–20
TASK V PROGRAM MANAGEMENT	weeks 1–22
TASK VI REPORTING	△ wk 6, ▲ wk 9, ▲ wk 14, ▲ wk 18, ▲ wk 22
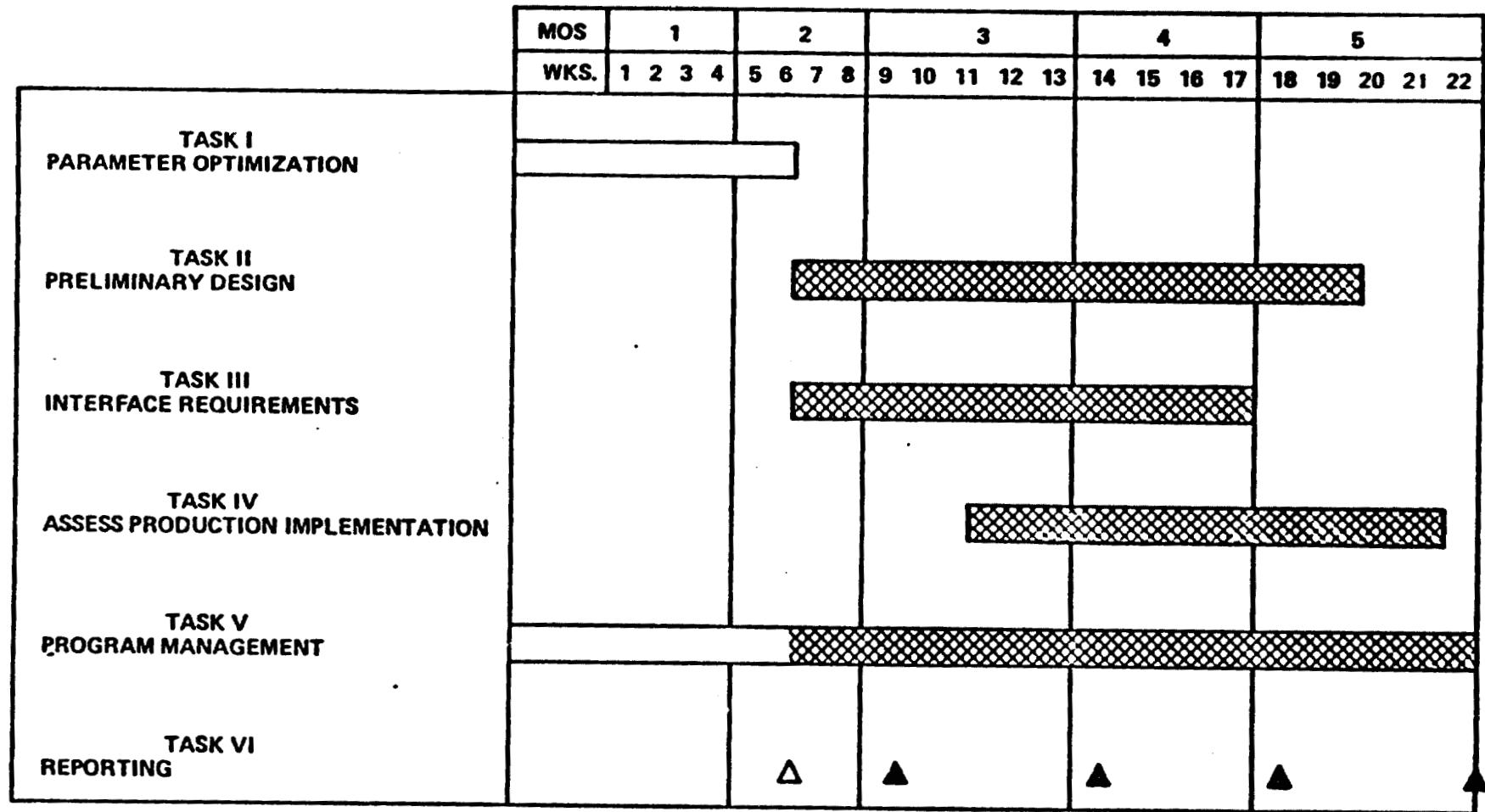
Figure 1-1. Phase I Program Schedule

3) Assess volume production requirements. With low cost as the major theme in the Program, it was important to investigate the manufacturing implications of the design and assess the types and nature of the equipment that would be needed to produce the concentrator in high volumes. (100,000 units/year baseline).

4) Establish a Phase II/Phase III manufacturing approach. Since there is a near term requirement for the concentrators, it was required that the concept lend itself to near term production. Thus alterations/compromises in the concept would have to be identified, however, an evolution would have to be established from prototypes through to production.

With these objectives in mind analysis, design, testing and manufacturing assessments commenced for Phase I of the Low Cost Point Focus Solar Concentrator Program.

1.2 Preliminary Design Methodology

There are a number of elements to General Electric's preliminary design methodology which warrant some discussion. These elements represent a unified and systematic approach to the design activity. They are:

1) design to cost

2) requirements examination

3) efficient structural design

4) reference diameter design

The first concept is that of design-to-cost. In principle, this approach establishes subsystem cost goals relative to an overall system cost goal. As the subsystems are designed they have a specific target cost that they must meet. This design to cost approach is shown schematically in Figure 1-2. Using the General Electric TC-600 parabolic dish concentrator as a baseline design, the
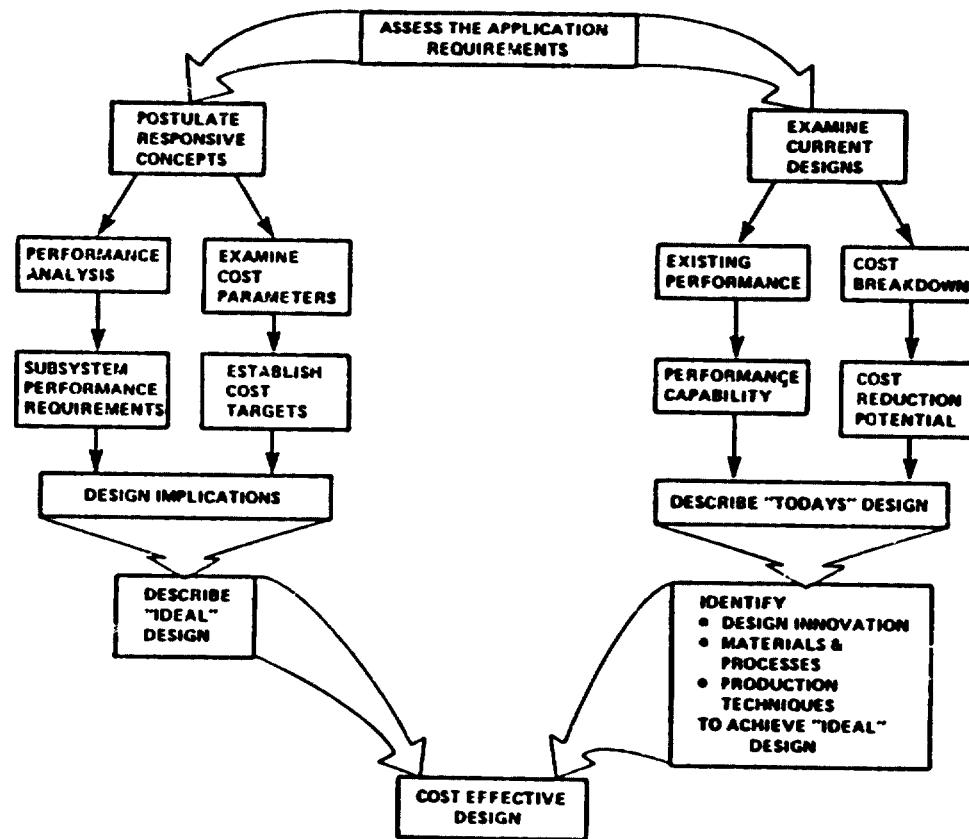
Figure 1-2. Design-To-Cost Methodology

costs were examined (Figure 1-3). It became obvious that certain subsystems were high cost centers and different approaches would have to be taken if lower cost solutions were to be found. In this instance the dish/structure, mount subsystem and assembly costs were definite high cost areas. As a result the low cost point focus concentrator design presents more cost effective solutions in these areas. The actual cost targets were established in the proposal and represent a balance between subsystem cost and subsystem function.

The second major element of General Electric's design methodology involves a careful examination of the design requirements. By understanding the weight and cost implications of all the major design requirements, cost effective relaxation of those requirements can be made. Specific requirements that were studied during this phase of the program were:

- operating and survival wind loads
- ice and snow loads
- AISC code requirements
- Seismic loads
- operation and orientation requirements
- life and reliability

While some of these requirements had little impact on cost, others had major impacts and forced a re-thinking of some of the subsystem design approaches.

The third major element of the design was to recognize that efficient structural designs yield low weight components and, as long as "exotic" materials are not used, low weight yields low cost. This principle, more than any other, significantly shaped the configuration of the concentrator. The design that evolved is very efficient for all subsystems, and through the use of low cost per pound materials, has resulted in a low cost design.
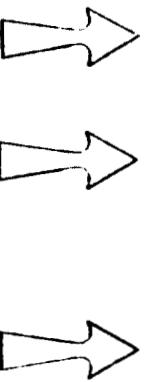
SUBSYSTEM	CURRENT DATA BASE GE TC-600		PROPOSED COST GOALS		STUDY RESULTS	
	$/FT^2	%	$/FT^2	%	$/FT^2	%
DISH/STRUCTURE	6.90	23	2.25	22.5		
REFLECTOR	2.10	7	1.75	17.5		
MOUNT	5.10	17	1.50	15		
DRIVE	3.0	10	3.0			
TRACKING/CONTROL	1.80	6				
ASSEMBLY	11.10					

DEFINED KEY SUBSYSTEMS
FOR COST REDUCTION

Figure 1-3. Cost Examination

Finally, the preliminary design phase calls for a diameter "optimization". Since performance varies little within size range of interest, cost trends will establish a diameter recommendation. In order to fully understand the implications and costs of diameter effects, it was first necessary to complete a preliminary design in all its aspects. For this reason a reference diameter was chosen and detailed analysis and design data were generated. Then members and components were resized under the new diameter conditions. This way meaningful cost versus size information can be generated. The reference size was chosen to be 7 meters based on General Electric's related experience at that size. The range studied was 7-12 meters.

With this methodology, the preliminary design evolved for General Electric's approach to a low cost point focus concentrator. Section 2 presents a brief description of the recommended design as it evolved. Section 3 presents the results of the Parameter Analysis and Subsystem Requirements Development. Sections 4 through 10 discuss the details of the concepts that were investigated and Sections 11 and 12 the production assessment and concentrator economics. Section 13 presents the results of the diameter scaling and Section 14 discusses the approach to the near term prototypes.

SECTION 2.0
CONCENTRATOR DESCRIPTION

2.0 CONCENTRATOR DESCRIPTION

There are a number of characteristics of General Electric's approach to a low cost concentrator. The concentrator is a point focus, single reflection exposed parabolic concentrator which tracks the sun in two axis. In an attempt to reduce cost and increase performance, the concentrator dish is constructed of injection molded plastic mirror segments. The degree of mold replication of the molding process insures a high accuracy light weight part. Injection molding is desirable as a volume production technique. Furthermore, the design freedom inherent in the use of moldable plastics permits many time saving and cost reduction features.

Another feature of General Electric's approach is to make the reflector system an integral part of the dish structure system. The reflector is to be molded into the plastic part, thus eliminating a field assembly operation. The entire reflector/dish then becomes a high volume production, light weight unit. The light weight of the dish translates into cost savings across the entire concentrator. Mount structure, drive motor sizes and foundation requirements can all be reduced.

To help facilitate an understanding of the preliminary design approach taken with the low cost concentrator, a scale model was constructed. This model is shown in Figures 2-1 through 2-3.

The concentrator has been divided into major subsystems. The dish is constructed of molded glass reinforced epoxy with an integral structural rib pattern on the back side to provide for stiffness. There are eight internal ribs within the dish to provide for support and alignment of the dish gore segments as well as added strength to the assembled parabolic dish. These internal ribs add considerable stiffness to the design while minimizing the loads and thus weight of plastic material in the gores. The additional blockage is small (see Figure 2-2) and the weight reduction benefits are well worth their inclusion. The reflector material

2-1
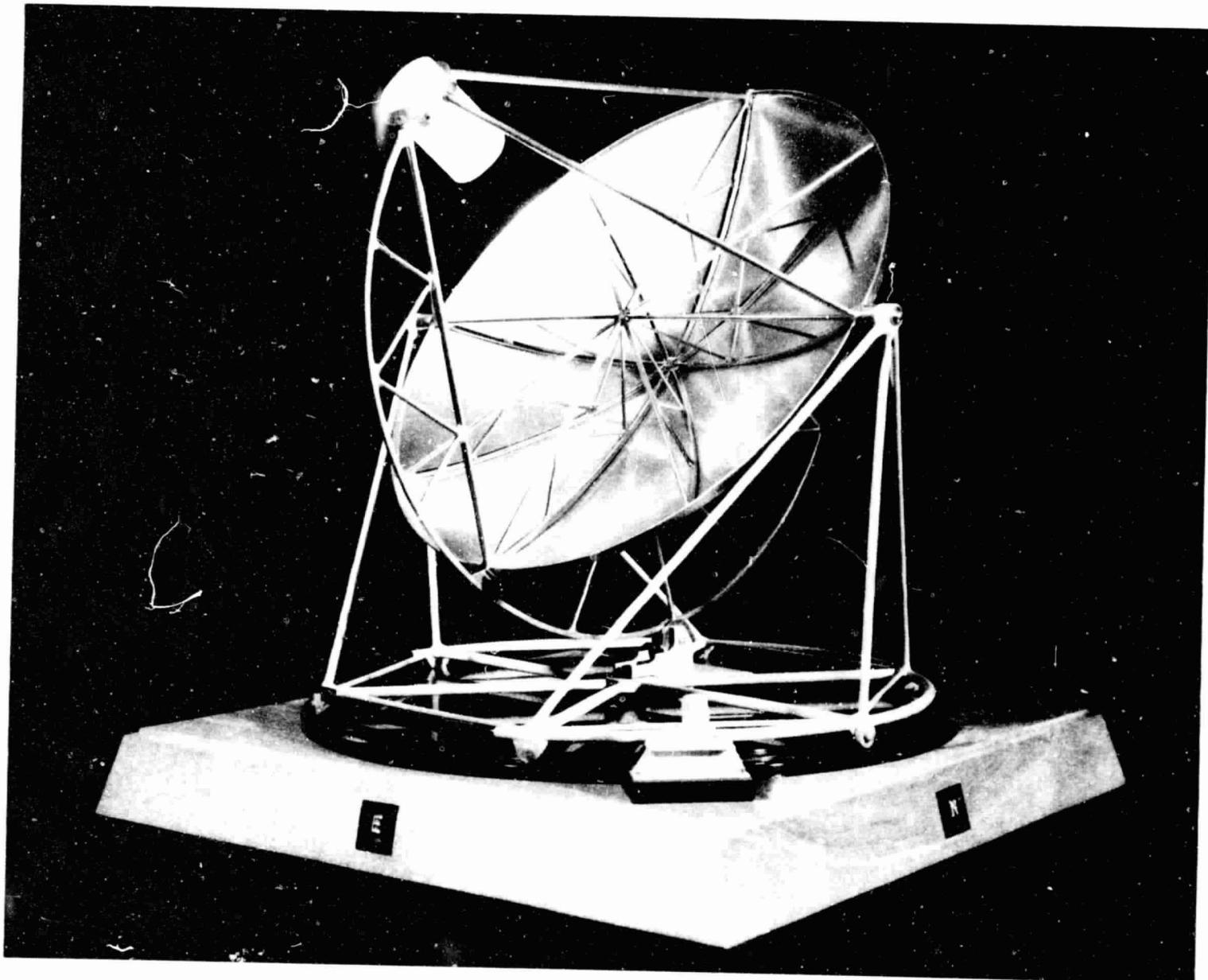
Figure 2-1. Sun Tracking Mode (VF-79-117C)
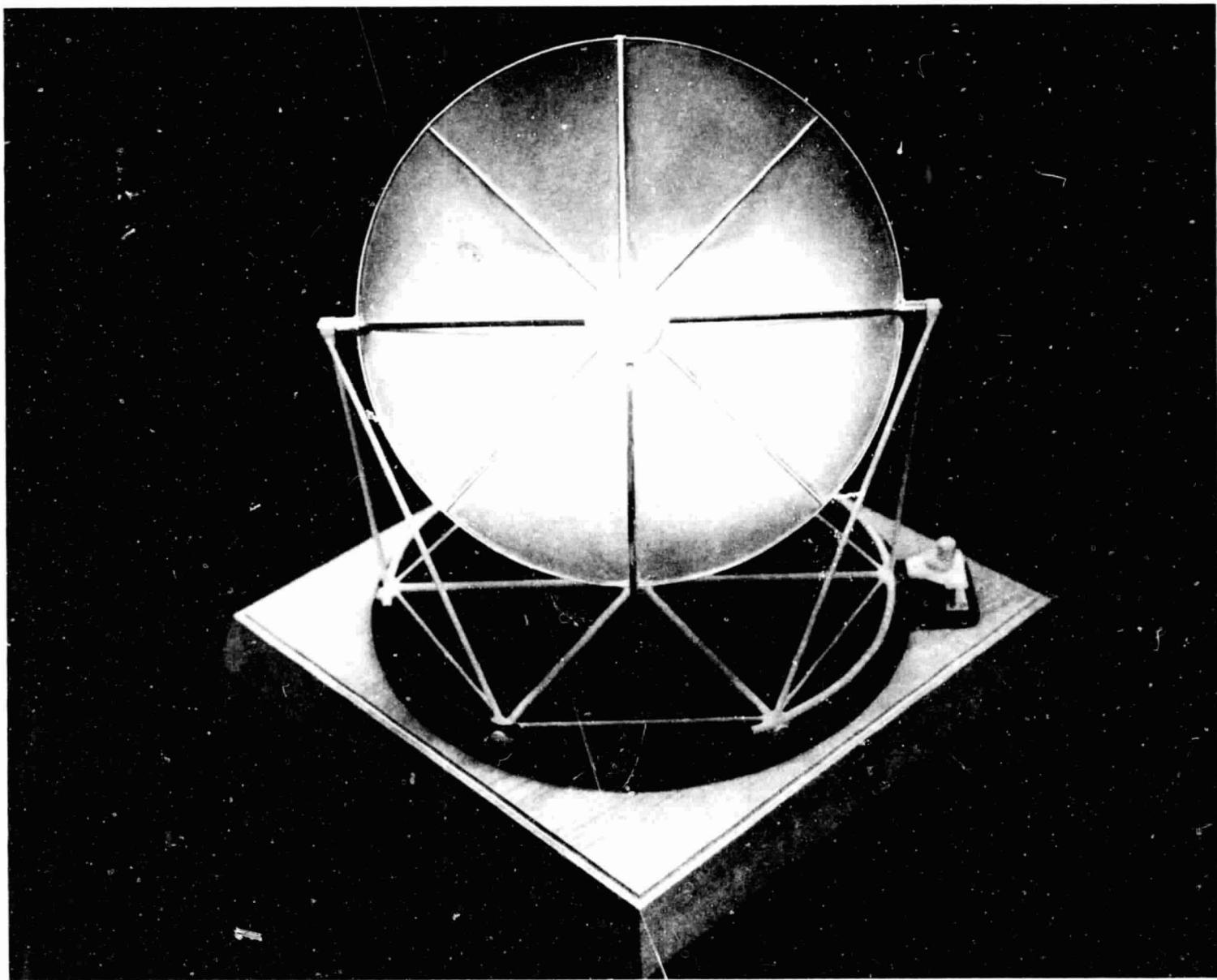
Figure 2-2. Sun View of Concentrator (VF-79-117A)
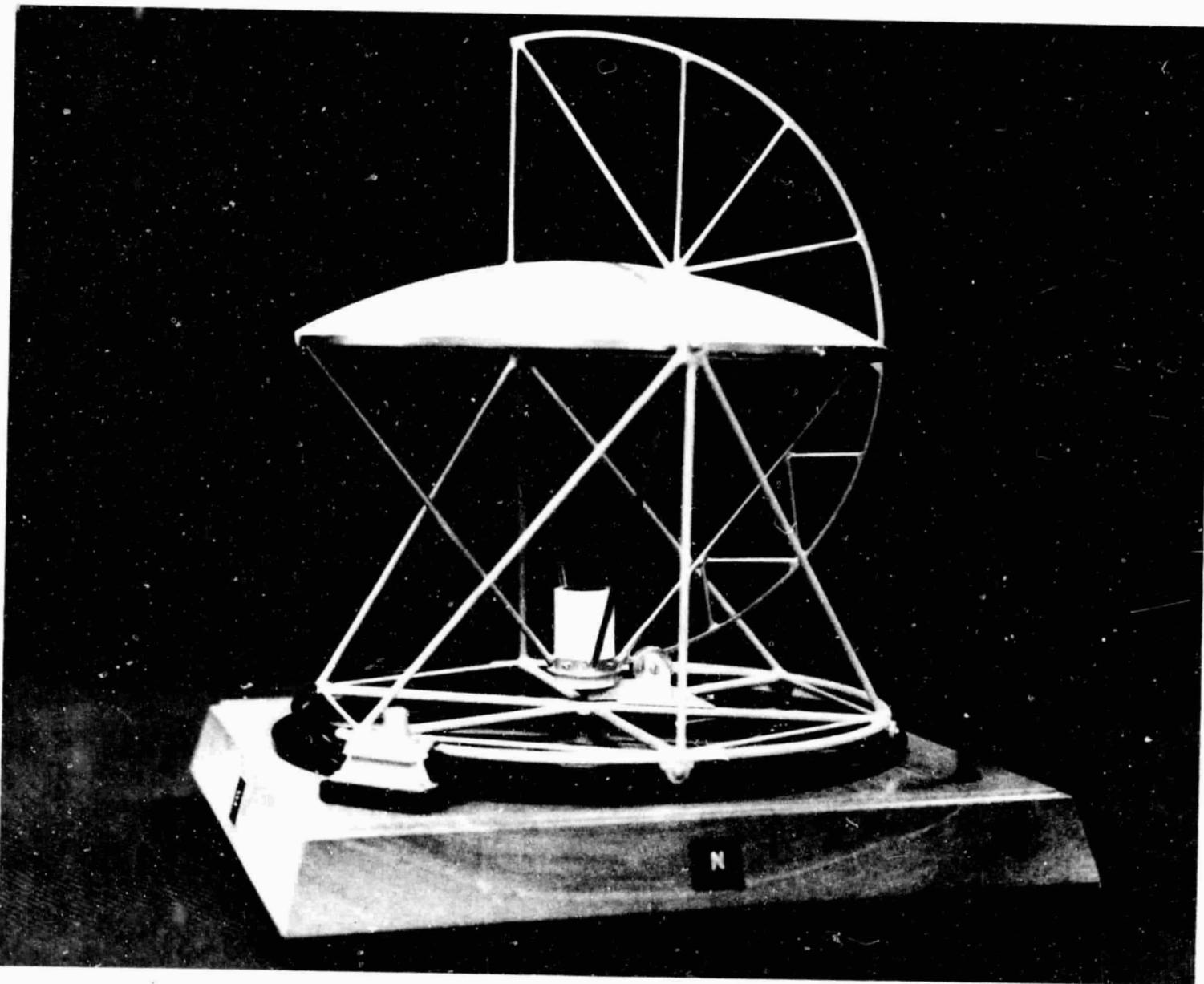
Figure 2-3.   Stow Position (VF-79-117B)

selected for near term prototypes is an aluminized polyester film that has been molded in place. This film is UV resistant, conforms to the double curvature of the paraboloid, has excellent specularity and very low cost. An advantage of the molding process is that the substitution of silvered systems as they are developed is readily permitted. Thus, higher performance potentials exist.

The mount subsystem selected is an azimuth-elevation configuration. A significant advantage of this mount approach is that it permits the stow orientation depicted in Figure 2-3. The inverted stow significantly reduces survival wind loads, provides for convenient access to the receiver/engine and offers good protection for the reflector surface. Being an efficient structural design, the selected mount configuration provides for low cost. The inverted night time stowage of the reflector provides for minimum cleaning of the reflector film. Another feature of the mount subsystem is that no field welding is required.

The drive subsystem that was selected consists of a cable and drum. The cable is provided with a rolled guide from receiver to counterweight. This track also acts to provide extra stiffness in the receiver/engine mount. Major features of this approach are low cost, low motor parasitic power, high drive stiffness and insensitivity to environmental factors.

The foundation subsystem that was selected is a rolled I-beam section mounted on simple concrete pilings. The foundation is dispersed and thus concrete is minimized. This approach to the foundation lends itself to quick assembly and a minimum of site preparation.

The control subsystem selected is a hybrid system with a position predictive mode for coarse control and then a fiber optic based closed loop control on the receiver for final positioning.

The details of the selected approaches and their cost predictions are presented in the following sections, and it is significant to note that the selected design meets the cost/performance goals established by JPL in the RFP. Figure 2-4 depicts the evolution of costs from current solar thermal concentrators to estimated subsystem costs. In several key areas, namely the dish, reflector, mount and assembly, substantial gains have been made. Both the reflector and the drive system are well below the cost goals established in the proposal.

The following sections will discuss the subsystem design selection in depth. Included are analysis, design details, production assessments and costing assessments for General Electric's preliminary design of the low cost point focus solar concentrator.

	CURRENT DATA BASE GE TC-600		PROPOSED COST GOALS		STUDY RESULTS	
	$/FT^2	%	$/FT^2	%	$/FT^2	%
DISH/STRUCTURE	6.90	23	2.25	22.5	2.62	31
REFLECTOR	2.10	7	1.75	17.5	0.20	2
MOUNT	5.10	17	1.50	15	1.42	17
DRIVE	3.0	10	3.0	30	0.99	12
CONTROL	1.80	6	0.50	5	0.75	9
FOUNDATION	--	--	--	--	1.49	17
ASSEMBLY	11.10	37	1.00	10	1.08	12
PERFORMANCE	18.1 KW$_{th}$		24.6 KW$_{th}$		23.1	
$/KW$_{th}$	686		168		153	

DESIGN MEETS
JPL ESTABLISHED
COST/PERFORMANCE
GOAL

Figure 2-4. Concentrator Data Summary

SECTION 3.0

SUBSYSTEM REQUIREMENTS DEVELOPMENT

3.0 SUBSYSTEM REQUIREMENTS DEVELOPMENT

The objectives of the subsystem requirements development activity were to:

1) identify the performance and cost parameters

2) determine the performance and cost sensitivity to variations in the key parameters

3) assess the first order performance/cost trends and provide direction in "optimizing" subsystem preliminary design selections.

By starting with specified system requirements and modelling and analyzing the concentrator performance and cost, a set of subsystem design requirements were established to ensure that the subsystem design approaches were consistent with the concentrator application requirements. The details and results of this system analysis are presented in this section.

3.1 System Requirements

The design of the concentrator must meet the specified application requirements as given in the RFP. These requirements are summarized in Table 3-1. The key operating requirement is the receiver operating temperature of 1700°F. In order to achieve this operating temperature and still minimize radiation losses from the receiver, large concentration ratios and an accurate optical surface are required. The design of the dish subsystem must also maintain its optical integrity under the specified environmental requirements. The loads and deflections caused by wind, ice and snow not only impact performance, but also have a direct impact on cost since they determine the weight and strength of the structural elements in the concentrator design. In this area, considerable attention has been paid to the design implications of these environmental requirements and, where appropriate, recommendations have been made as to their validity.

Table 3-1. System Requirements

CATEGORY	REQUIREMENTS
Configuration	• Point Focus Concentrator • Two Axis Tracking • 5-15 Meters Diameter • State-of-the-Art
Performance	• 0.004 - 0.012 Kwth/$ • 30 Years Life • High Reliability
Operation	• Design Insolation = 800 Watts/M^2 • Receiver Temperature = 1700°F • Receiver Shadowing = 1%

Environment	• -20°F → 140°F Ambient Temperature
	• 0% - 100% Relative Humidity
	• 3/4" Hail Impact
	• 1" Ice/12" Snow Blanket
	• Wind: 30 MPH + 20% Gusts Operating
	         60 MPH Slew-to-Stow
	        100 MPH Survival

3.2 Subsystem Parameters

The parameters used in the analysis of the concentrator are identified in Table 3-2. The key parameters in the analysis are the dish diameter, focal length, concentration ratio, surface slope error and total reflectivity of the dish surface.

Table 3-2. Subsystem Parameters

|	KEY PARAMETERS	DESCRIPTION
CONFIGURATION	Diameter	Dish Aperture Diameter
	F/D	Focal Length/Diameter
	η_s	Shadowing Factor
	η_c	Construction Factor ("Crack" Losses)
	t	Dish Material Thickness
OPERATIONAL	Slope Error	Deviation of Surface from True Parabola
	Specular Error	Spread of Energy Off of Reflector Surface
	Concentration Ratio	Receiver Aperture Area/Dish Aperture Area
	Dish Deflection	Deflection of Dish Slope under Wind Loads
	Tracking Error	Misfocus Due to Pointing Inaccuracies

3.3 Subsystem Models

In order to make the necessary trade-offs and establish the criteria for the preliminary design selections, analytical models were developed to define the optical, thermal and structural performance characteristic of the concentrator.

3.3.1 Configuration Model

A simple configuration model is provided to mathematically relate the geometric variables to the optical and thermal parameters used in the systems analysis. The three key geometric variables are:

1) The rim angle (Θ_0) of the dish, which is used to determine the optical performance;

2) The parabolic surface area, which is used to determine the cost and weight of the dish; and

3) The aperture diameter of the dish which is used to scale system performance, cost and weight characteristics

The geometric profile of a parabolic dish is defined as a function of the focal length, f, by $R = 2f/(1+\cos\theta_0)$, where
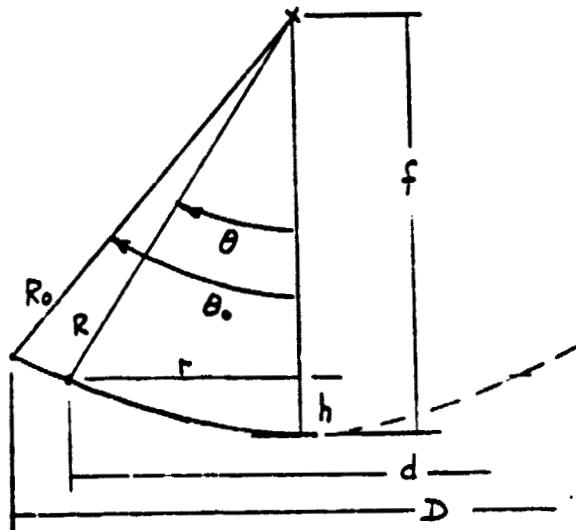
Aperture Dia., $d = 2r = 2R\sin\theta$

Dish Depth, $h = f - R\cos\theta$

$$\therefore \frac{d}{2\sin\theta} = 2f/(1+\cos\theta)$$

$$f/D = \frac{1+\cos\theta_0}{4\sin\theta_0} \text{ for } \theta = \theta_0$$

Therefore, the rim angle, θ_0, is solely a function of the non-dimensional focal length, f/D.

The surface area of a paraboloid is defined geometrically by the relationship,

$$A_S = \frac{2\pi D}{3h^2}\left[\left(\frac{D^2}{16}+h^2\right)^{3/2} - \left(\frac{D}{4}\right)^3\right]$$

The surface area can then be expressed in the non-dimensional form of surface-to-aperture area ratio, A_S/A_A.

$$A_S/A_A = \frac{8}{3h^2 D}\left[\left(\frac{D^2}{16}+h^2\right)^{3/2} - \left(\frac{D}{4}\right)^3\right]$$

where $h = f - R_0\cos\theta_0$ & $R_0 = D/2\sin\theta_0$

$$\& \; h = D\left[\frac{f}{D} - \frac{R_0\cos\theta_0}{D}\right] = D\left[\frac{f}{D} - \frac{1}{2}\cot\theta_0\right]$$

substituting gives,

$$A_s/A_A = \frac{8}{3(f/D - \frac{1}{2}\cot\theta_0)^2} \times \left\{\left[\frac{1}{16}+\left(\frac{f}{D}-\frac{1}{2}\cot\theta_0\right)^2\right]^{3/2} - \left(\frac{1}{4}\right)^3\right\}$$

which allows the surface-to-aperture area ratio to be expressed as a function of the focal length, f/D, and the rim angle, θ_0, as shown in Figure 3-1.
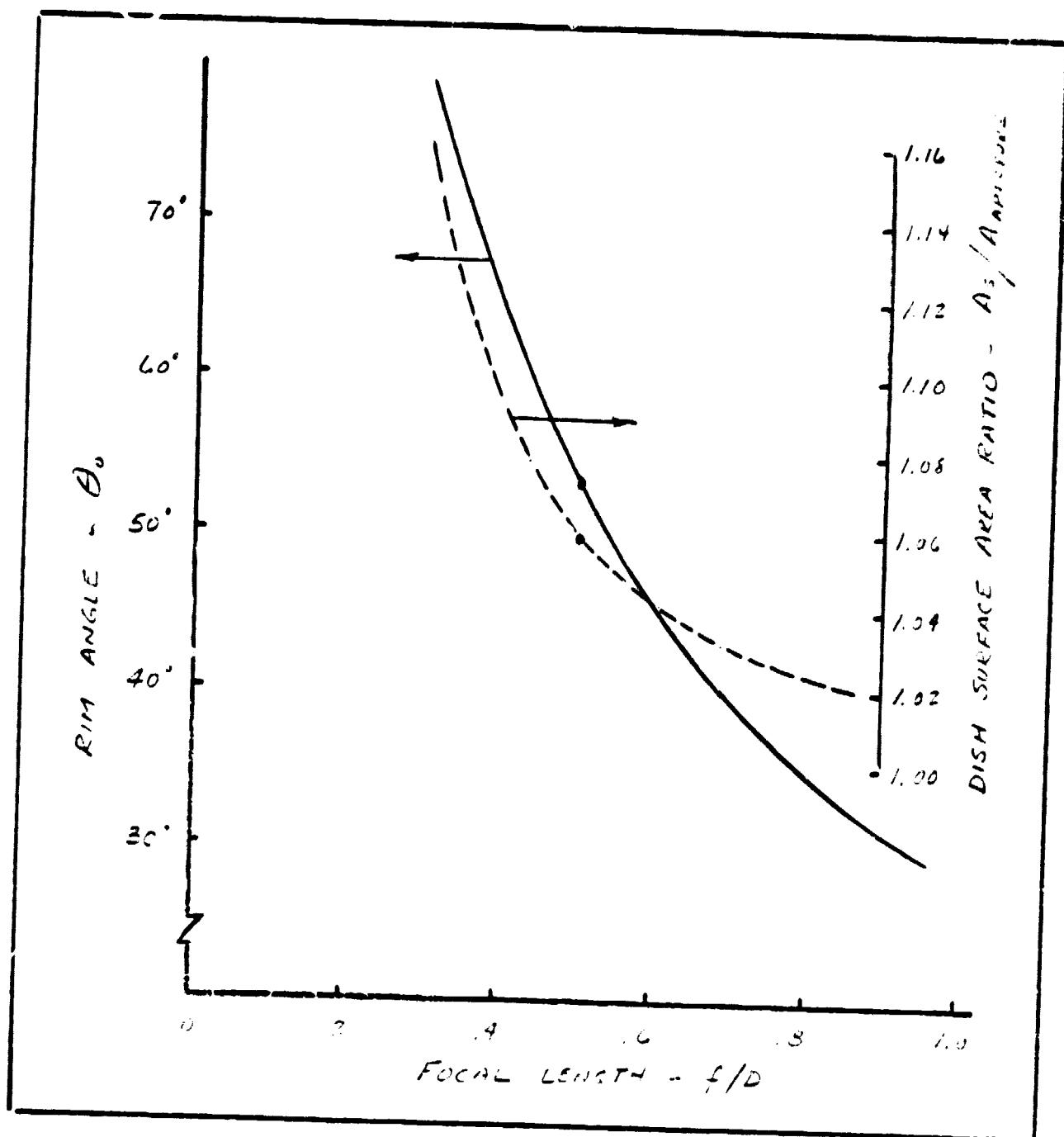
Figure 3-1. Reflector Dish Geometry - Non-Dimensionalized

3.3.2 Optical Model

The optical model is based on an analysis by A. C. Ku and is described in detail in Appendix A-1. Mathematical equations are derived which give the spatial spread of the reflected energy as a function of the RMS optical error and the rim angle of the dish. The major assumption of the analysis is that the optical error is random in nature and can be described by a Gaussian distribution function. Also, it is assumed that the reflected beams are symmetric with respect to their respective axis.

Using this analysis, the optical intercept factor is defined by

$$\eta_\tau = 1 - e^{-B}$$

where

$$B = \frac{1}{2CR\left(2f/D\right)^2\left(\delta \times \sigma/f\delta\right)^2}$$

CR = concentration ratio

f = focal length, ft.

σ = STD deviation in flux distribution, ft.

δ = STD deviation in optical error, rad.

D = dish aperture diameter, ft.

θ_0 = dish rim angle, deg.

and where:

$$\left(\sigma/f\delta\right)^2 = \frac{8(1+\cos\theta_0)}{\sin^2\theta_0}\left\{\frac{1+\cos\theta_0}{\cos\theta_0} - 4\ln\left|\frac{1+\cos\theta_0}{\cos\theta_0}\right|\right.$$
$$\left. - \frac{6\cos\theta_0}{1+\cos\theta_0} + \frac{2\cos^2\theta_0}{(1+\cos\theta_0)^2} - \frac{\cos^3\theta_0}{(1+\cos\theta_0)^3} + 3.3143\right\}$$

and

$$\delta = \sqrt{\sigma_{ss}^2 + \left(2\sigma_{sL}\right)^2 + \sigma_{sp}^2}$$

σ_{ss} = const. = .0024 rad.

σ_{sp} = const. = .0030 rad.

σ_{s1} = 1/8° to 1/4° = .00218 to .00436 rad.

Some simplifying assumptions are made in the optical model with regard to the optical errors. Deflection and tracking errors are treated as a bias, being depended on time and environment, and do not directly impact the optical trade-offs. Both errors are considered as they impact other design criteria.

Optical spreads due to the solar source and specularity distributions are assumed at nominal values. Since slope error is the dominate optical parameter compared to the source and specular spreads, deviations in their RMS values will not significantly affect the analysis. All of the RMS optical, source, and mechanical errors are assumed to be normally distributed over the aperture area of the dish. The surface slope error, σ_{SL} is identified as the independent variable in the analysis and values of $1/8°$ (.00218 rad.), $3/16°$ (.00327 rad.) and $1/4°$ (.00436 rad.) were selected as being a representative variation for a high quality, manufacturable optical surface.

3.3.3 Thermal Performance Model

The thermal performance model is defined by the net thermal energy delivered to receiver less the thermal energy losses in the receiver, as defined by the application requirements. The thermal energy delivered is a function of a design solar insolation rate of 0.8 KW/m² (as specified), the dish diameter or aperture area, the surface reflectivity, the optical intercept factor, and geometric factors in shadowing and construction that reduce the effective aperture area. The receiver thermal energy losses at the required temperature levels are a function of the aperture area of the receiver, as defined by 119 KW_TH per m², which can be redefined in terms of concentration ratio, CR, and aperture area of the dish. The resulting mathematical model for thermal performance is defined as follows:

$$KW_{TH} = \frac{\pi D^2}{4}\left[.8\, \eta_c \eta_s \eta_e \eta_r - \frac{119}{CR}\right]$$

where

D = aperture diameter of dish

CR = concentration ratio

η_s = shadow factor - f (struts, receiver)

η_c = construct factor - f (no pieces, "cracks")

η_R = reflectivity - f (materials coating)

η_I = intercept factor - f (optical model)

Several simplifying assumptions were made in the thermal performance model. The dish diameter was identified as an independent variable so that the thermal performance could be redefined in terms of KW_{TH}/m^2 of dish aperture area. Likewise, shadow and construction factors were assumed constant and independent of diameter in terms of area percentage, respectively at 0.986 (1% receiver shadow by definition) and 0.998 (assuming 1/8 to 1/16 inch "cracks"). Surface reflectivity is also identified as an independent variable in the analysis and was assumed to be a constant at 0.90, as an average value for candidate reflector options.

3.4 Optical Trade-Offs

The key parameters in the optical model are the non-dimensional focal length, f/D, the surface slope error, σ_{SL}, and the concentration ratio, CR. These parameters are varied independently to determine the optical intercept factor and the intercept sensitivity to variations in each of the key parameters.

Typical variations in the intercept factor with focal length are shown in Figure 3-2. The results indicate that the optimum intercept factor is obtained at a focal length, f/D, of 0.5, for any given slope error or concentration ratio. These results also demonstrate the importance of small slope errors in achieving good optical performance, suggesting that the variations of other optical errors,
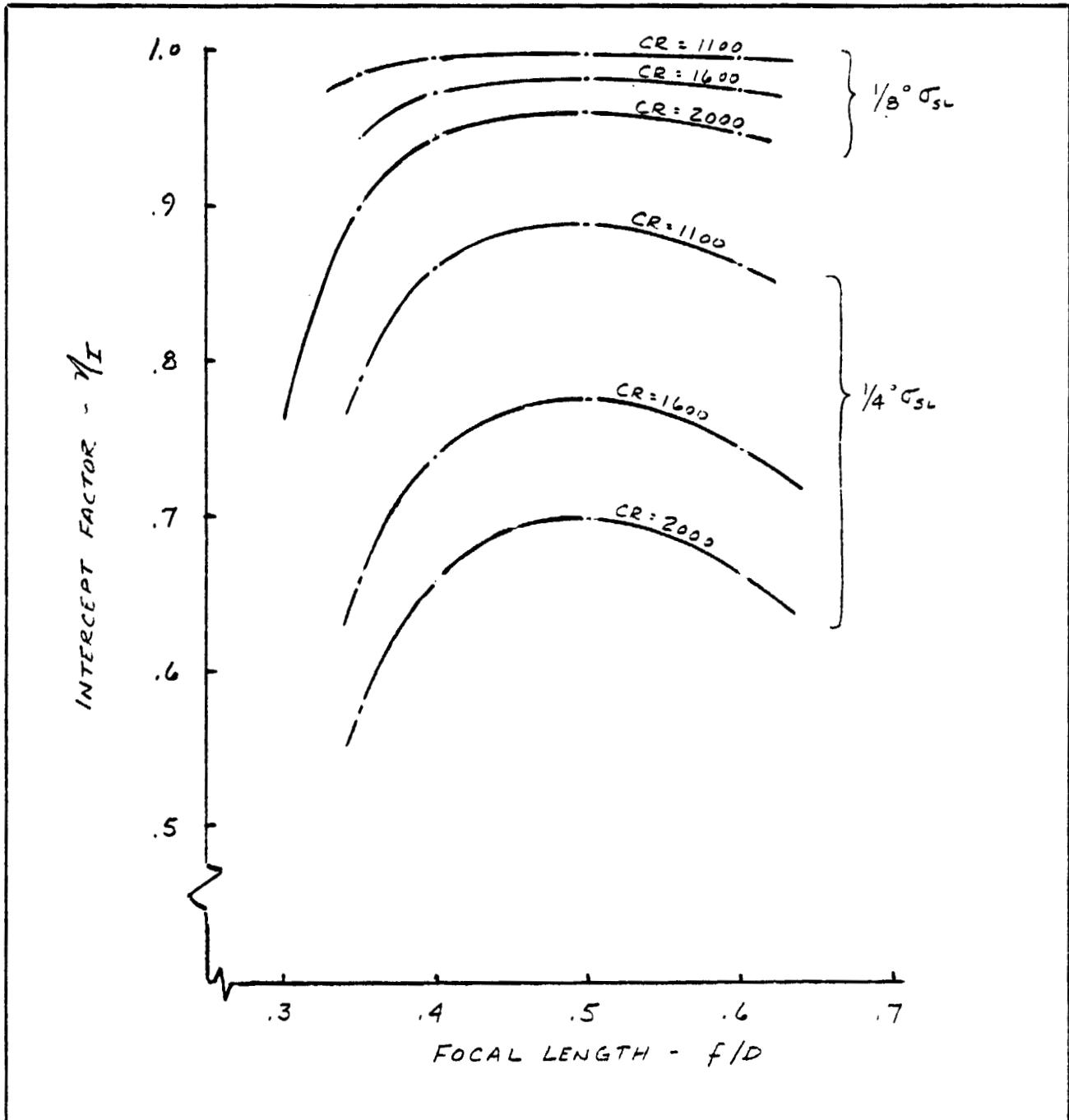
Figure 3-2. Intercept Sensitivity to Focal Length

such as specularity, only become significant when the small slope errors can not be obtained. Variations in the intercept factor with focal length also demonstrate that with small slope errors, the focal length could vary from 0.35 to 0.70 without a significant compromise in optical performance. With higher slope errors, in the order of a 1/4-degree, the effects of focal length and concentration ratio on optical performance become more pronounced.

Typical variations in optical performance with slope error and concentration ratio are shown in Figure 3-3 for a focal length of f/D = 0.5. These results demonstrate the importance of small slope errors in achieving the optical performance with high concentration ratios, as required for the specific engine applications. Also, the results indicate that for the appropriate range in concentration ratio (1100-2000) for the application, an RMS slope error of 1/8-degree will provide good optical performance and further reductions in slope error will not significantly enhance performance. Variations in the optical intercept factor with concentration ratio also demonstrates that low concentration ratios are required with the higher slope errors for good optical performance. However, good optical intercept performance at the lower concentration ratios will be compromised by poor thermal performance, which is addressed and optimized in Section 3.5.

3.5 Thermal Performance Trade-Offs

The key parameters in the thermal performance modelling are the optical intercept factor and the concentration ratio. As a dependent variable, the intercept factor was derived in Section 3.4 as a function of focal length (f/D), the slope error (σ_{SL}), and the concentration ratio (CR), all of which are retained as independent variables in the thermal analysis. Other independent variables in the thermal analysis include the surface reflectivity (η_R), a dish construction factor (η_C), and a shadowing factor (η_S), all of which are assumed as constants
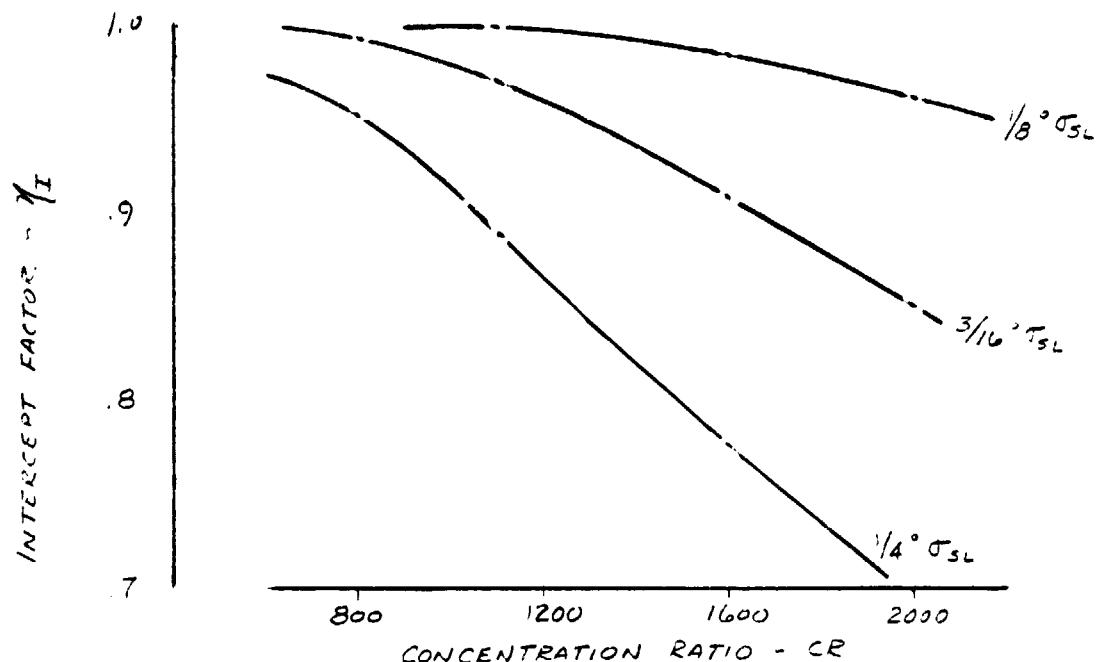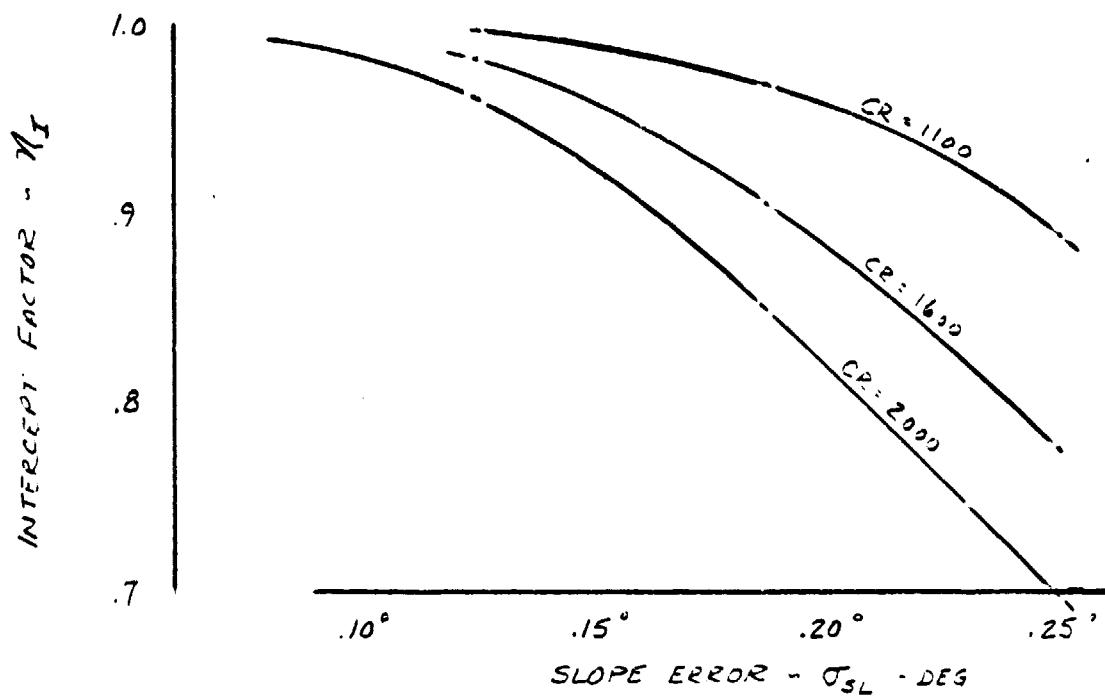
Figure 3-3. Intercept Sensitivity to σ_{SL}, CR
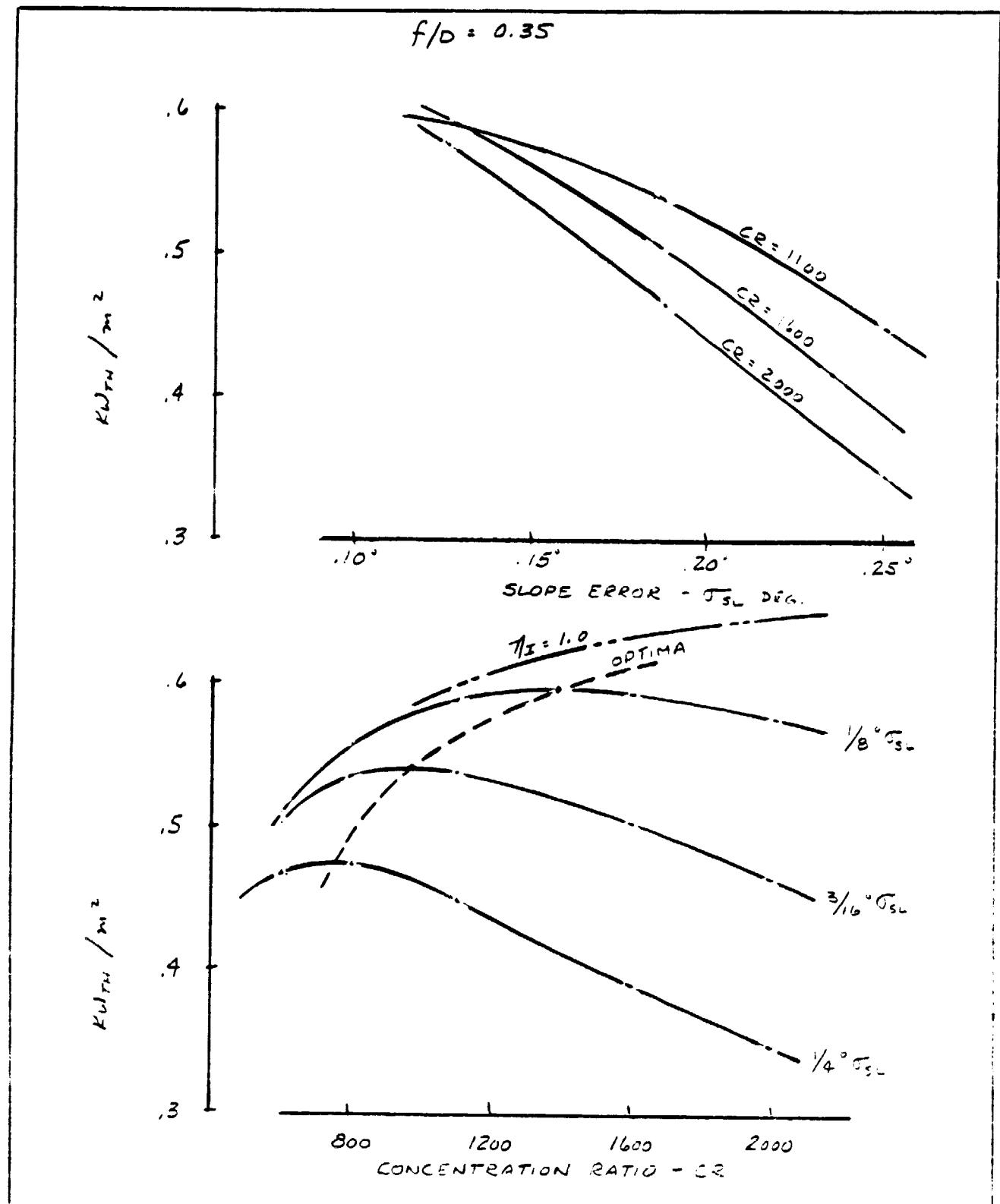
Figure 3-4. Variation in Thermal Performance with CR, σ_{SL}
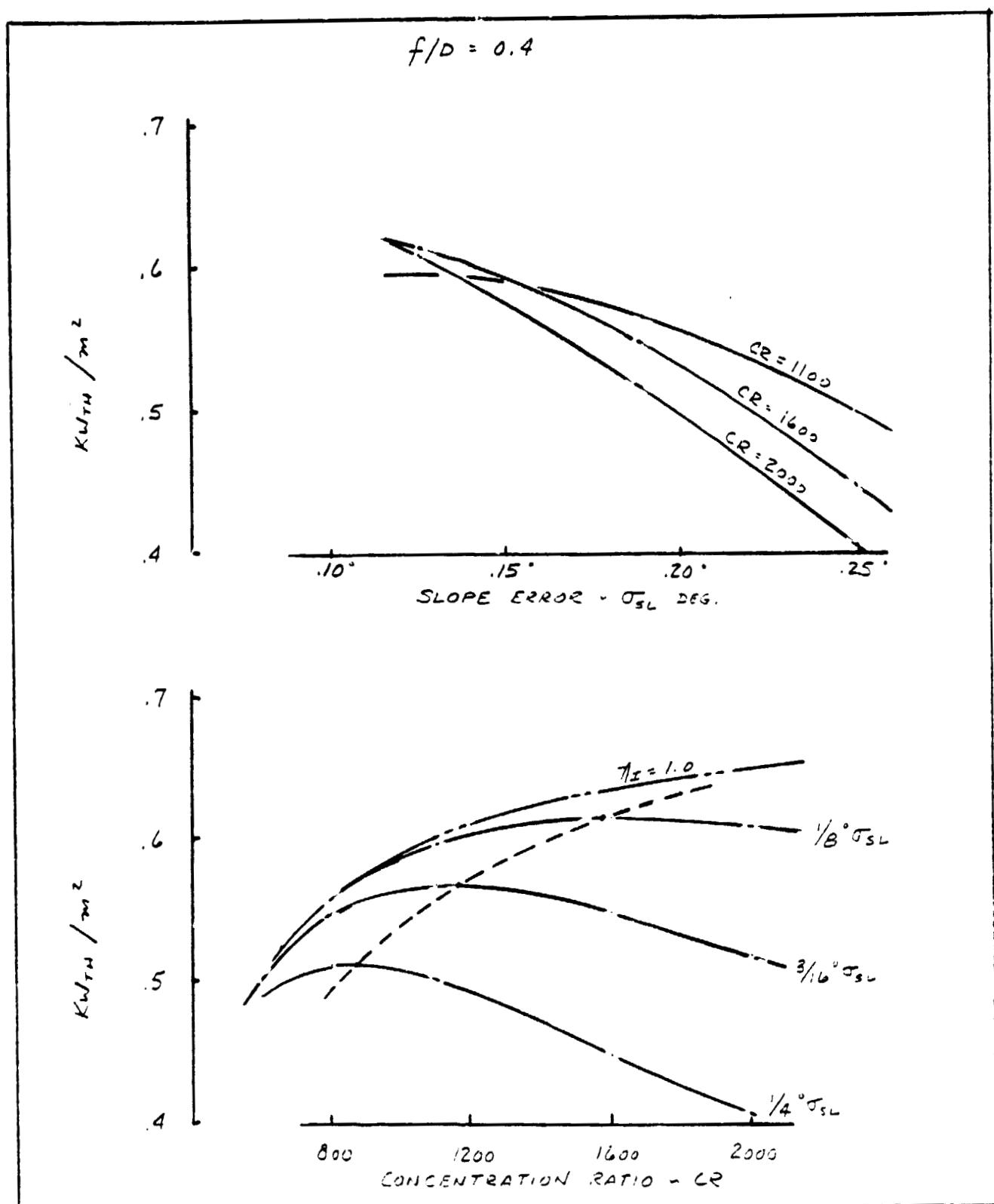
Figure 3-5. Variation in Thermal Performance with CR, σ_{SL}

affecting only the performance level and not the trends or trade-offs. The design solar insolation level and the engine thermal losses are application requirements, as specified.

Typical variations in the thermal performance (KW_{TH}/m^2) with slope error and concentration ratio are shown in Figures 3-4 through 3-7 for focal lengths of 0.35, 0.40, 0.50 and 0.60, respectively. These results indicate an optimum thermal performance and an optimum concentration ratio for any given focal length and slope error. In optimizing thermal performance, the concentration ratio is also optimized and thus becomes a dependent variable in the analysis.

Variations in the optimum thermal performance with slope error are shown in Figure 3-8 as a function of focal length. For a given slope error the effect of focal length on the optimum thermal performance is demonstrated and indicates that maximum thermal performance is obtained with a focal length of $f/d = 0.50$. The optimum concentration ratio is also shown in Figure 3-8 as it depends on slope error and focal length.

Variations in the optimum thermal performance with focal length are shown in Figure 3-9 as a function of slope error to demonstrate the performance sensitivity to focal length. The results show that for any given slope error, the focal length could vary from 0.4 to 0.6 without a significant compromise in thermal performance. Also, Figures 3-4 through 3-7 indicate that with small slope errors, an "off-optimum" ($CR_{OPT} \pm 200$) concentration ratio will not significantly compromise thermal performance.

A very significant observation is made in Figure 3-9 that the optimum concentration ratio is dependent on focal length and not vice versa. It is clearly demonstrated in Figure 3-6 that any concentrator design that starts with a specific concentration ratio could be driven to higher focal lengths with enhanced
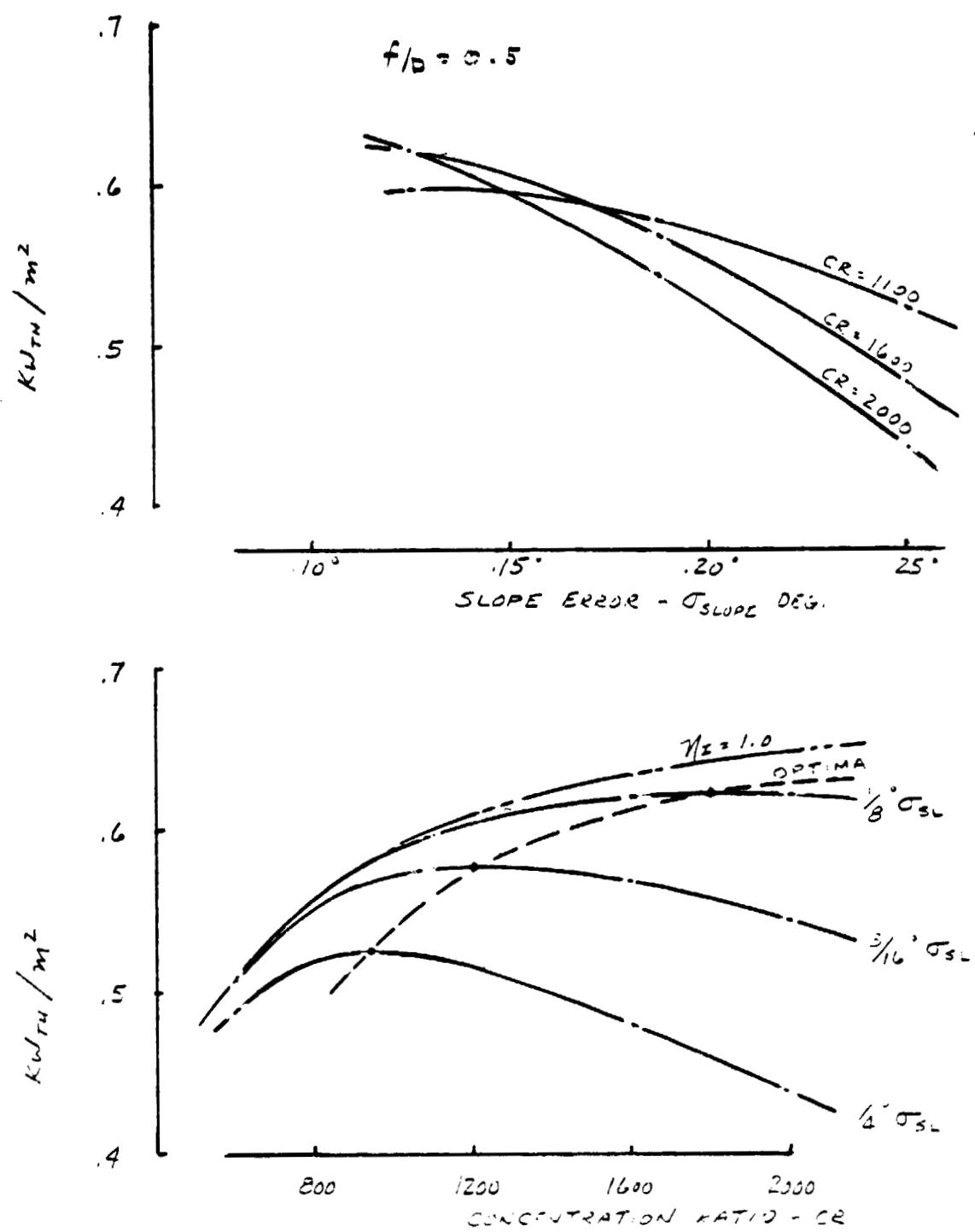
Figure 3-6. Variation in Thermal Performance with CR, σ_{SL}
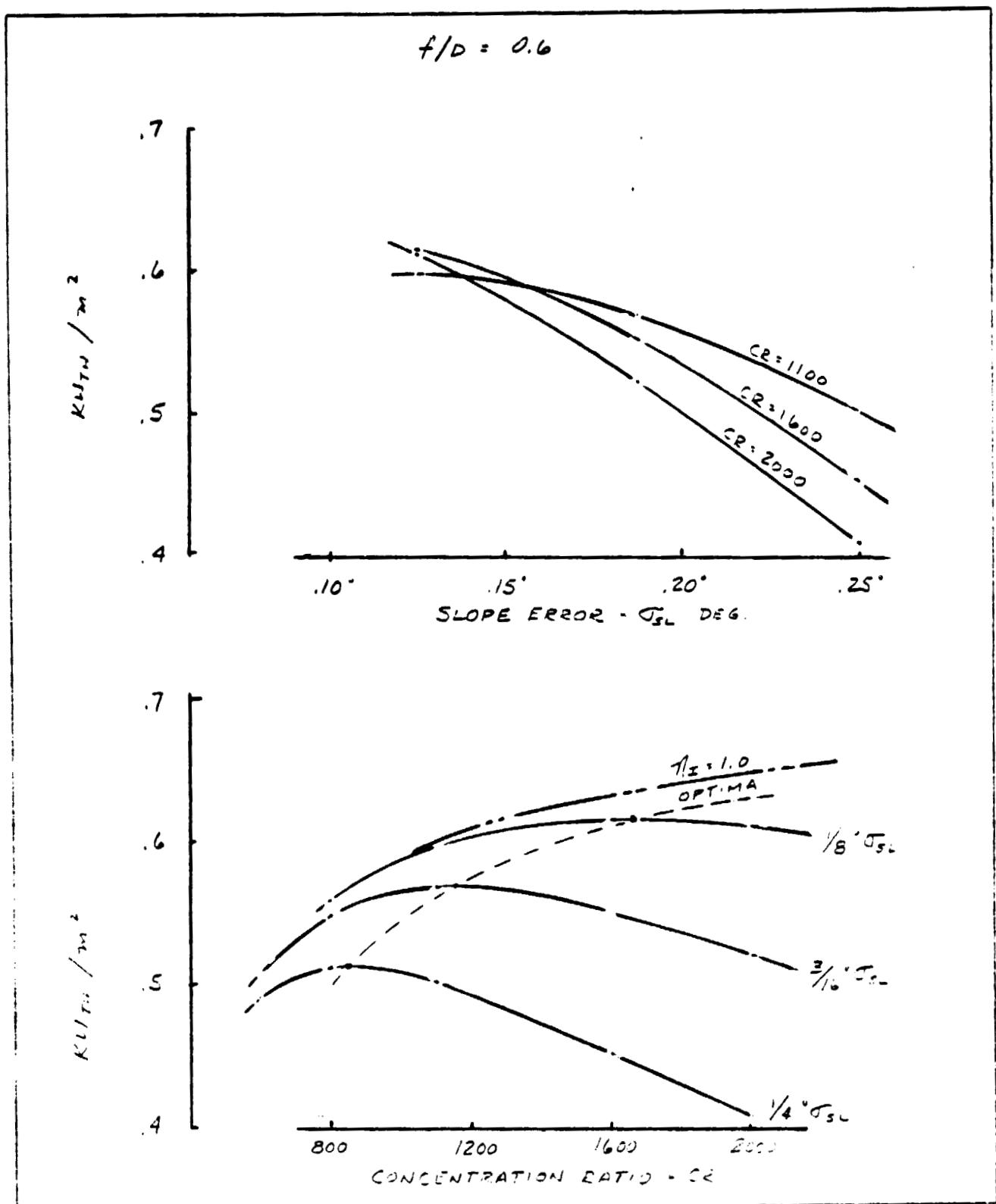
Figure 3-7. Variation in Thermal Performance with CR, σ_{SL}
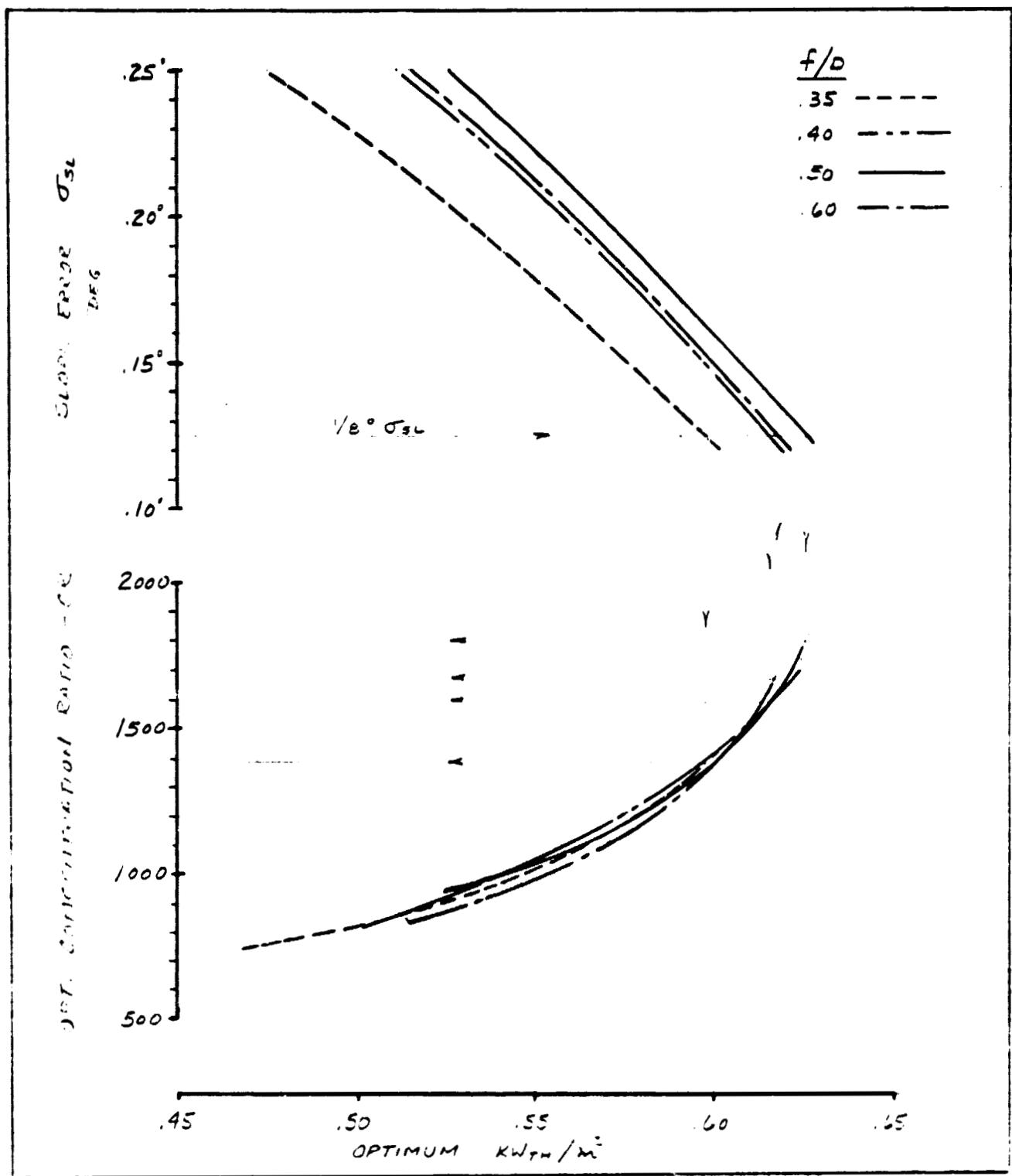
Figure 3-8. Optimum KW_{TH}, CR As A Function of σ_{SL}, _f/D
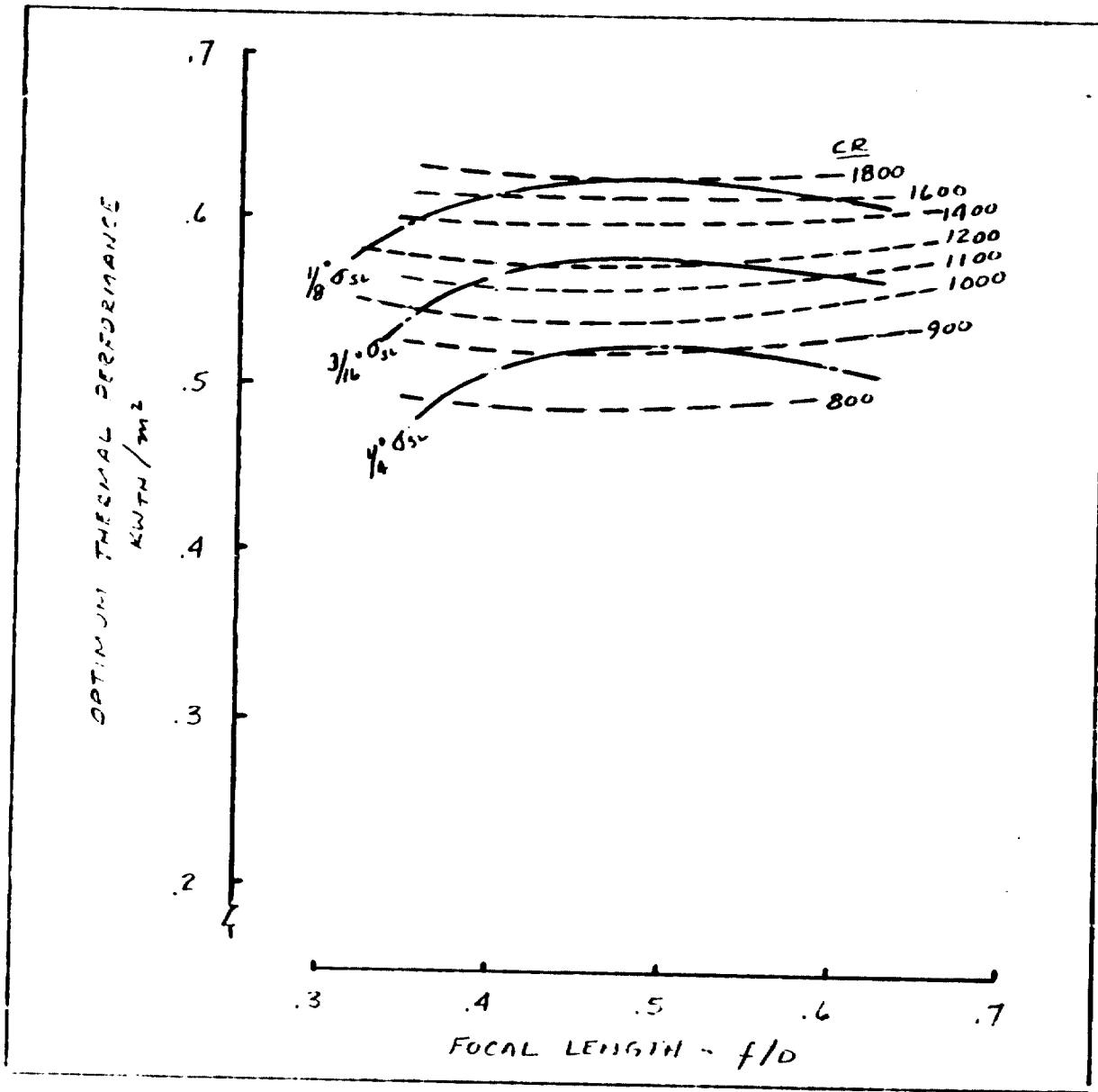
Figure 3-9.   Optimum Thermal Performance - f (σ_{SL}, CR, f/D)

surface optical quality. The appropriate conclusion is that the concentration ratio, not the focal length, should vary with surface optical quality for maximum thermal performance, as indicated in Figure 3-8. The optimum focal length, in terms of optical and thermal performance (KW_{TH}) is shown to be approximately f/D = 0.5.

3.6 Effect of Tracking and Deflection Bias Errors

The system analysis and sensitivities that were discussed above were conducted assuming that the concentrator was aligned with the sun. Two primary sources of bias errors have been considered and which must be factored into the subsystem requirements determination, the tracking bias and the dish gore deflection under wind loads. Figure 3-10 presents the sensitivity of the intercept factor to the tracking bias error. As can be seen, a bias error of ± 0.125 degrees results in little loss of intercepted receiver energy. This value is also consistent with achievable position sensing accuracies and drive system stiffness. The second key bias parameters that was studied is the gore deflection. This parameter is a measure of the bending of the dish gore away from the paraboloid shape due to wind and gravity loading. It is a measure of how much stiffness is required of the dish structure and thus directly influence cost. A detailed discussion of the analysis is presented in Appendix A-2 and the results are presented in Figure 3-11. As can be seen, deflections of an individual gore can be as high as 0.25° with only an additional 1% loss in intercept factor. By designing the gore stiffness for this amount of deflection at maximum operational wind loading, weight of the dish gores can be kept to a minimum. The implications of this analysis will be discussed in Section 4.
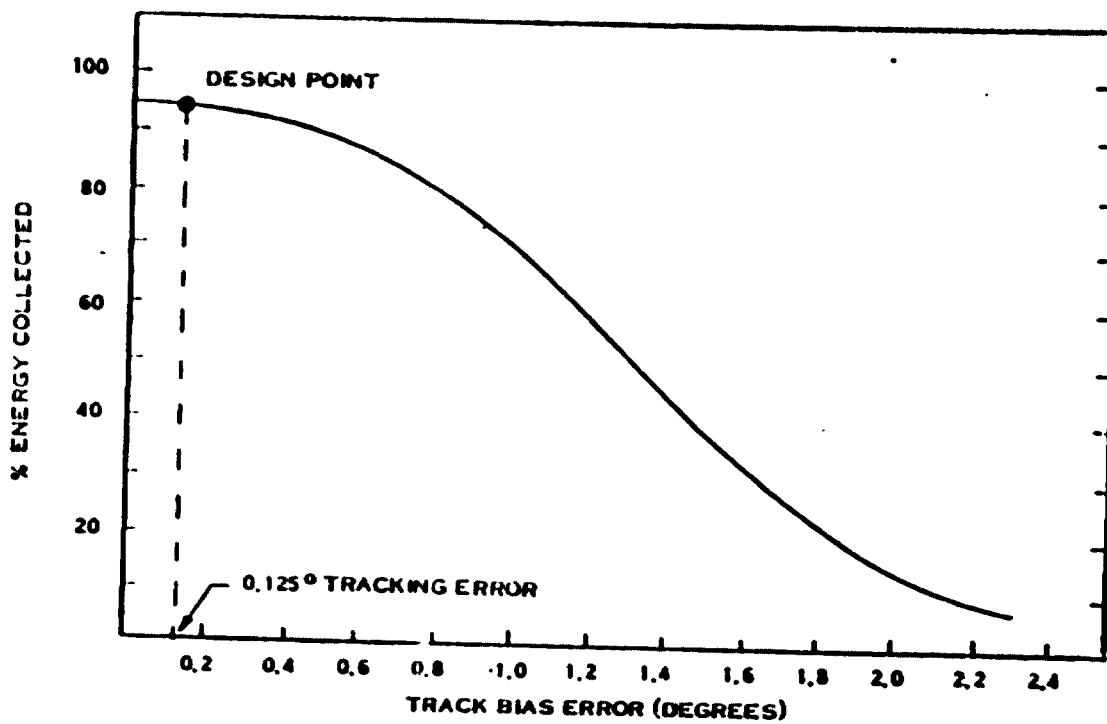
Figure 3-10.   Optical Trades -- Effect of Tracking Error
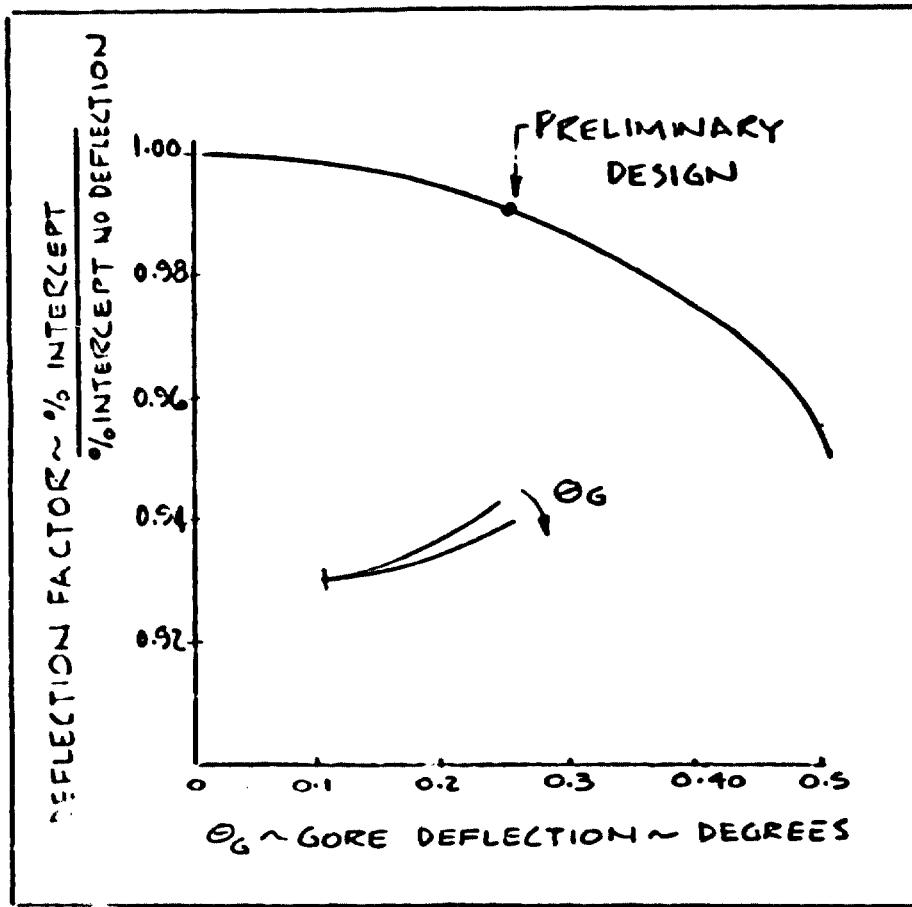
Figure 3-11.   Optical Trades -- Effect of Gore Deflection

3.7 Subsystem Requirements

As a result of the concentrator parametric analysis, a set of subsystem parameters were specified which will serve as the design requirements for the subsystem preliminary design detailed in the following sections. The following conclusions can be drawn:

1) The optical model indicated a strong dependence of performance on slope error. The value of 0.125° RMS slope error is specified as the dish gore manufacturing accuracy.

2) The analysis indicated an optimum focal length of f/D = 0.5 with a weak dependence of performance on f'D between 0.4 and 0.6.

3) The thermal model indicated that the optimum performance is a strong function of slope error and a weak function of focal length and that the optimum concentration ratio will vary with slope error. The following values were specified:

$$\sigma_{SL} = 1/8"$$
$$f/D = 0.5$$
$$CR = 1800$$

4) Tracking and gore deflection bias errors were determined to be $\pm$ 1/8° and 1/4° respectively.

5) No significant performance trends existed with diameter. Diameter will primarily affect cost and is treated in a later section.

SECTION 4.0

DISH SUBSYSTEM

4.0 DISH SUBSYSTEM

4.1 Dish Material Selection

The dish subsystem is represented by a structural substrate and metallic reflector material. This section describes only the dish substrate, and the materials that have been considered and selected for the manufacture of these dish structures.

Prime considerations for the selection of materials for this application were cost, modulus, design and process flexibility, and use history. Based on these considerations, material type and composition was then established to provide the structural properties and characteristics to meet performance requirements.

Glass reinforced plastic was selected as the prime material because it provides a system with good mechanical and thermal properties and low cost. Typical reinforced and unreinforced plastic properties are shown in Table 4-1. Reinforced property data shown were obtained by the use of 30-40 percent continuous strand glass mat.

Significant features of glass reinforced plastics are given in Table 4-2. Parts consolidation in the dish structure refers to incorporation of ribs and the in-situ molding of the reflector in a single co-cure operation. Lower part finishing costs are possible because the part is molded net. Edge trimming and sealing is the only post-mold finishing required. Because of excellent weathering and structural integrity, GRP provides longer life and lower main-tenance. Occasional reflector replacement and painting or sealing should be the only maintenance required. With increased volume requirements, the part cost should be reduced.

Table 4-1. Typical GRP Material Properties

PROPERTY/CHARACTERISTIC	TYPICAL UN-REINFORCED	TYPICAL REINFORCED
• FLEXURAL MODULUS, X 10^6 psi	0.3-0.5	1.5-2.0
• FLEXURAL STRENGTH, X 10^3 psi	4-13	18-30
• COEFF. OF LINEAR THERMAL EXP., IN/IN/°F x 10^{-6}	40-55	8-12
• CREEP RUPTURE, X 10^3 psi (UP TO 1000 HOURS)	0.8-2	4-6
• PROCESS REQUIREMENTS	MODERATE TO HIGH	LOW MODERATE
• MATERIAL COSTS	HIGH	LOW

GRP SELECTED FOR

THIS APPLICATION

Table 4-3. Recommended Material System

COMPONENT	RECOMMENDATION	REASONS
RESIN	EPOXY	GOOD BALANCE OF PROPERTIES
FILLER	IMSIL, WOLLASTONITE	LOW COST
REINFORCEMENT	CONTINUOUS GLASS MAT	UNIFORMITY OF PROPERTIES
GEL COAT	PARENT MATERIAL	BONDING AND OPTICAL QUALITY
CURING	PROCESS DEPENDENT	

The recommended material system is shown in Table 4-3 and consists of basic-
ally an epoxy resin, fillers and continuous glass strand mat reinforcement.
Exact amounts of each ingredient will be established for each process used. A
low temperature initiated catalyst system will be used to cure the material
system in the mold. The proprietary catalyst was developed by General Electric,
and provides a 2-3 minute cure system at 150-200°F.

Resins

The resins systems evaluated were epoxy and polyester, both thermosetting
resins. Both systems provide design and processing flexibility. They can be
cured either by room temperature reactive catalysts or temperature initiated
catalysts. This allows them to be cured by most any available process. The
key requirements used in the resin selection process are shown in Table 4-4.
Epoxy resin provides the best potential for long life because it is character-
ized principally by good dimensional stability. Polyesters must be filled with
additives (styrene) to reduce shrinkage. When filled with particulates, a low
cost material system is possible. Glass reinforced epoxy has been used exten-
sively in aircraft and Naval ship-board radome and radar applications for over
fifteen years as well as extensive use in the pleasure boat industry. Field
repairs are easily and quickly made with epoxies.

Fillers

Fillers are used for several reasons: to reduce shrinkage and subsequent
cracking in resin rich areas, improve surface quality, improve stiffness and,
principally, to reduce cost of the epoxy system selected. Table 4-5 provides
a list of candidate fillers that can be used in this application. The most common-
ly used fillers are calcium carbonate and clays; however, calcium metasilicates
is now being used to replace part of the glass fiber in glass-filled systems

for Reaction Injection Molding. Either Calcium Carbonate or Calcium Metasilicate will be used in the dish structure composition.

Table 4-2. GRP Features

```
Lower Component cost by parts consolidation as demonstrated
    in automotive industry (Grille opening panels)
Design Flexibility
Lower Finishing Cost
Lower Maintenance Cost
Longer Life
Corrosion Resistant
Lower Cost in High Volume
Dimensional Stability
```

Reinforcements

Glass mat reinforcements provide the improved mechanical porperties shown in Table 4-1. This is the principal reinforcing material in the system, supplemented by interstitial improvements provided by fillers. Continuous strand glass mat, as shown in Table 4-6 will be used in the dish substrate because of its good formability over the curved mold surface, fiber wash resistance, high bulk factor and uniform part fill-out. These characteristics are particularly important for the Resin Transfer Molding (RTM) and Liquid Reaction Injection Molding (LRIM) processes selected for low and high volume dish production. Continuous mat is amenable to most any molding process; whereas, the other forms listed in Table 4-6 are process limited.

Table 4-4.   Resin Types

MATERIAL KEY REQUIREMENTS	EPOXY	POLYESTER
LONG LIFE	BEST	GOOD
DIMENSIONAL STABILITY	GOOD	FAIR
STRUCTURAL INTEGRITY	GOOD	FAIR
FATIGUE	BEST	GOOD
STIFFNESS	BEST	GOOD

EPOXY SELECTED FOR
GORE MATERIAL

Table 4-5. Use of Fillers

WHY FILLERS	Surface Finish Good Moldability Low Cost Low Shrinkage
CANDIDATE FILLERS	Calcium Carbonate Silicas Silicates Clays Oxides

Gel Coats

Table 4-7 indicates why gel coats are used and the types considered for use in dishes.

First of all, gel coats are used in this application to provide a high quality reflecting surface. In experiments conducted in our laboratory with veil/surface mats versus unreinforced gels, it was found that the latter provided the smoothest surface finish and prevented fiber show-thru on the reflector surface. And, this is primarily why such systems will be used in the dish application.

It is preferable to use the parent or prime resin primarily from a compatibility and stability standpoint. Polyesters with a slight amount of silica filler would be the second choice, because of their similarities in properties, and also because of their low cost.

Table 4-6. Reinforcement

WHY REINFORCEMENT	Improved Properties
	Dimensional Stability
	Resistance Microcracking
CANDIDATE REINFORCEMENT	Chopped Strand (Random)
	Continuous Mat
	Oriented Mat
	Woven Fabric

Table 4-7. Gel Coats

WHY GEL COATS	Surface Finish
	Improve Weathering
	Impact/Abrasion Resistance
	Necessary to Eliminate Fiber Show thru on Reflector
CANDIDATE GEL COATS	Parent System
	Urethanes
	Polyesters

4.2 Dish Preliminary Design

Having selected a material system to be used in the fabrication of the gores there remains the task of developing a preliminary design. The methodology used to define the preliminary design parameters is a logical sequence starting with the design requirements shown in Table 4-8. Almost all of these design and operating requirements were given in Exhibit VII of the original JPL Request for Proposal.

The next step in the sequence was to establish credible load case from the requirements and use these, along with representative material properties,

to perform the structural analysis required to determine the gore design geometry. The details of how this was accomplished are explained in the following paragraphs.

Perhaps the most difficult portion of the design task was the establishment of realistic design cases. The optical performance is an important driver for the dish design. Not only are there reflectance and specularity requirements, but also requirements on dish shape change, specifically the .25° of edge slope change or deflection. See Figure 4-2. These requirements combined with the overall program objectives of low cost placed heavy emphasis on establishing realistic load cases lest the thickness and therefore the weight be overestimated. The requirement "30 mph operating x 1.2 gusts" was examined in light of the above. Figure 4-1 shows a compilation of insolation versus wind speed taken from NOAA weather tapes for selected sights. This figure clearly indicates that over 92% of the yearly available energy is received while wind speeds are less than 20 mph.

Table 4-8. Dish Requirements Summary

1. 30 mph Operate x 1.2 Gusts
2. 100 mph Survival (Stowed) Stow through 60 mph
3. 1 in. Ice/12 in. Snow with $\mathcal{C}$ = .1 water
4. -20°F to 140°F
5. .75 inch Diameter Hail
6. Sand, Rain, Fog, 100% RH, Dew, Frost
7. Seismic: 1 g Vertical .25 g Lateral Simultaneously
8. 30 Year Life
9. Freezing and Thawing
10. Ocean Shore Environment
11. .25° Rim Deflection
12. .125° Slope Error

WIND SPEED vs INSOLATION
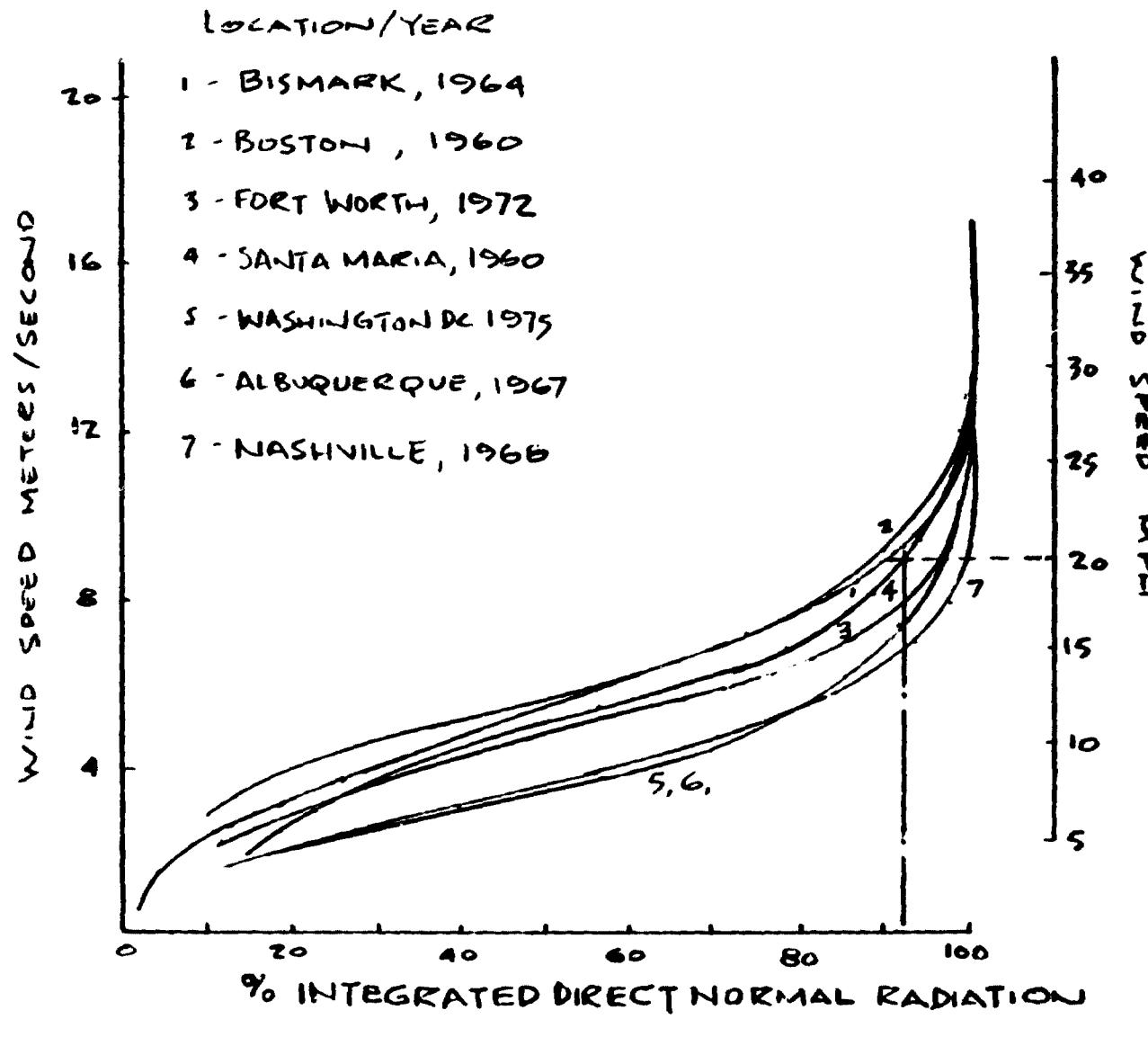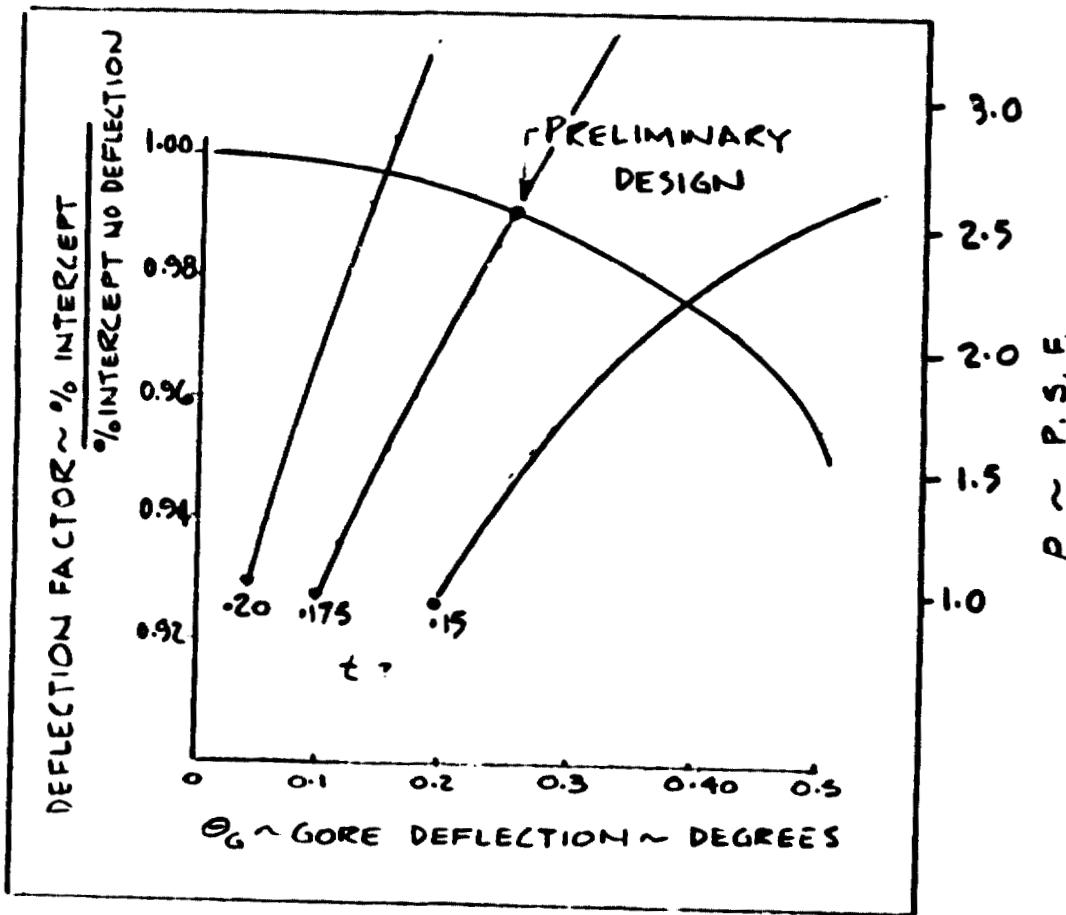
FIGURE 4-1

Figure 4-2.   Effect of Gore Deflection

If the design pressure loading corresponding to 20 mph is used with .25° edge deflection the resulting dish structure will be lighter than that designed for 30 mph and .25°. From Figure 4-2 it can be seen that if we assume the shape change to be linear with pressure (most shell solution are) then with a design point of 2.5 psf and .25°, the deflection at 5 psf should be .5° for the same thickness. Thus the slope intercept factor from 20 mph to 30 mph goes from .99 to .95 but only for 8% of the year.

The design pressure load was therefore set at the vector sum of the 20 mph wind load and an assumed 2 lbs/ft^2 dish structure weight. The validation for the above assumptions will be justified in the results of the dish structural analysis. The dish is therefore designed for deflection and checked for maximum stress. In addition, gusts were not used as a primary design criteria since historically they are short time phenomena about a steady state value. Thus, stresses were checked at 30 mph x 1.2. The remainder of the design requirements had no major impact on the structural design.

Table 4-9 shows a typical set of material properties for glass reinforced plastics GRP. For the structural design and weight calculations it was assumed that the material had a room temperature modulus of 2 x 10^6 psi and a SpGr of 1.7.

Structural Analysis

The design configuration analyzed in this section evolved from consideration of receiver/engine mount concept and drive concepts. Figure 4-3 shows the curciform structured formed by the intersection of the mount internal rib and the drive internal rib. Due to the concentrated loads at the receive/engine support and the dish mount, it was decided that metal structure should be used for the internal rib since metals have higher stiffness and strength to provide

MOUNT INTERNAL
RIB
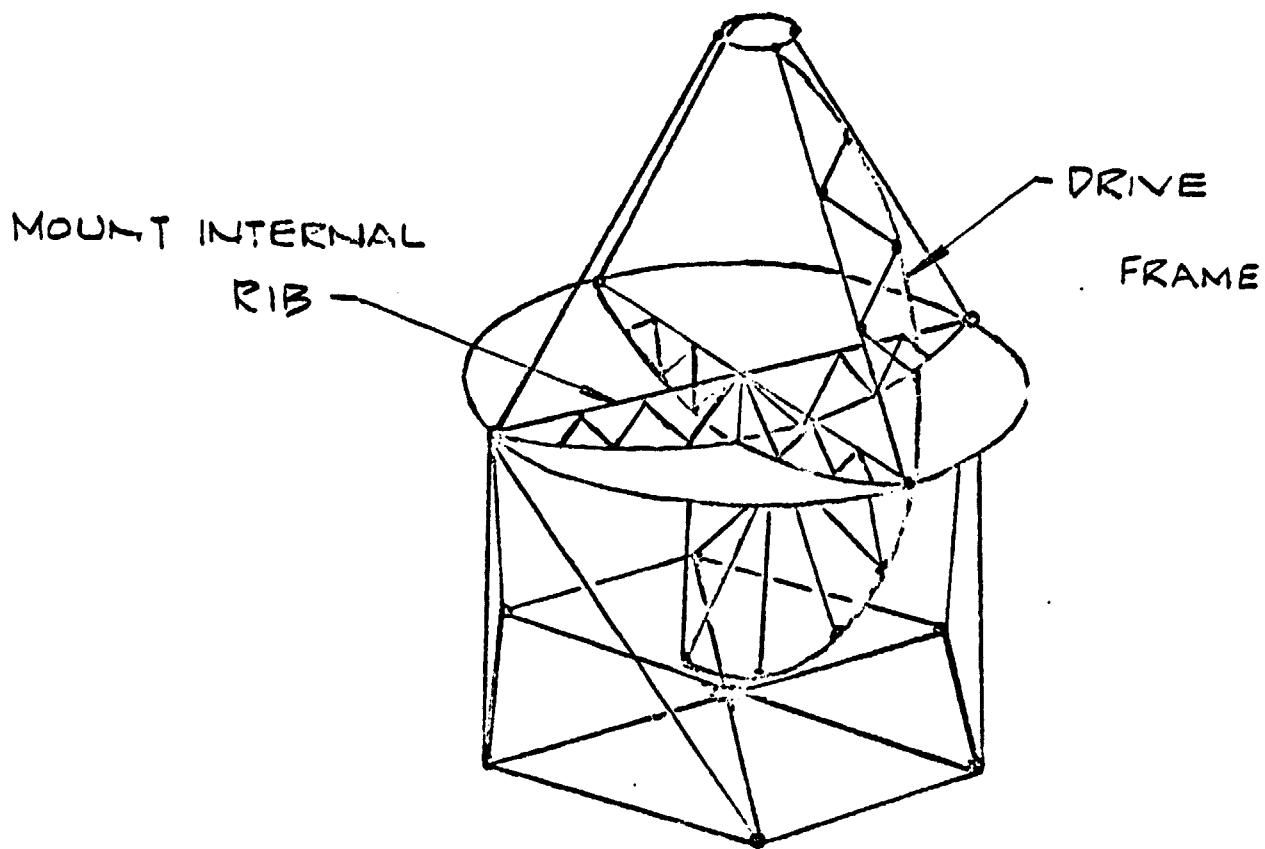
DRIVE

FRAME

Figure 4-3. Preliminary Mount and Drive Frame Configuration

adequate load paths in the area of load concentration. Aluminum was chosen for its light weight. To minimize thermal stress problems, the plastic would be tailored in coefficient of thermal expansion to match the value for aluminum ($13 \times 10^{-6} \frac{in}{inF}$). The plastic gore segments carry their own weight plus the aero and seismic loads only. The internal ribs are then designed to take the receiver weight _plus_ gore loading and weight and distribute these loads to the mount structure and into the foundation.

The initial design interface was then four 90° parabolic sectors attached to four aluminum internal ribs. For the purpose of the plastic structural analysis, it was assumed that the internal ribs can be made sufficiently stiff so as to be considered fixed for deflection in our load range. Thus to estimate the thickness of the plastic gore under uniform weight and aerodynamic pressure loading, the analytical solution for deflection and slope to a uniformly loaded parabolic sector was required. A closed form solution to this problem was not available, so as approximate relationship was developed.

The edge deflection and rotation for a uniformly loaded plate clamped at the inner edge is given in Roark as;

$$y_p = \frac{k_1 w r^4}{E t^3}$$

$$\theta_p = \frac{k_2 w r^3}{E t^3}$$

Table 4-9. Material Properties

CONDITION PARAMETER	ROOM TEMP 68°F	ELEVATED TEMP 140°F
Specific Gravity	1.5-2.0	
Expansion Coefficient	$(8-20)\times10^{-6}$	---
Poission Ratio	.25	---
Modulus x 10^6	1.5-2.5	1.0-1.5
Tensile Strength	10,000-30,000	? -12,000
Compressive Strength	15,000-35,000	---
Fatique 10^6 PSI	5,000-15,000	
Creep Rupture	4,000 @ 10^6 Hrs	---
% Glass Full	20-30	

For a uniformly loaded sector with radial edges clamped and outer edge free, only the equation for maximum edge deflection was given:

$$y_s = \frac{k_s w\, r^4}{E t^3}$$

To develop an approximate relationship for the edge slope of a flat plate sector it was assumed that the ratio of slope equalled the deflection ratio.

$$\theta_s = \theta_p \left(\frac{k_s}{k_2}\right)$$

However, this approximate relationship for the rim slope change does not account for the structural differences between a plate and a shell of revolution. Shells of revolution are inherently stiffer,the plates under uniformly distributed loading due to the membrane action. To estimate a correction for this added shell stiffness over a flat plate, the edge slope relationships were obtained for the cases shown in Figures 4-4 and 4-5. The equation for edge rotation of the flat plate is given by;
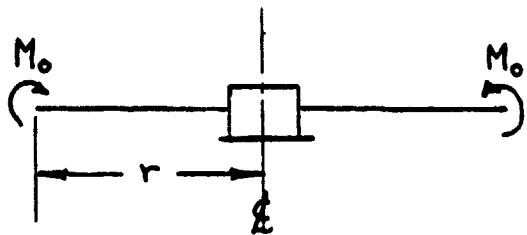
Figure 4-4

$$\theta_p = \frac{\lambda M_o r}{E t^3}$$

and for the shallow sperical shell by

Figure 4-5

$$\theta_{ss} = \frac{M_o \left(4\beta^3 / R_2 C_1\right)}{E t}$$
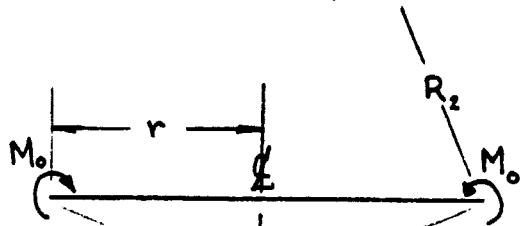
The ratio of the edge slopes for these two cases provides a correction for the shell stiffness. If the slope correction for the plate sector is now applied, an approximate relationship for the slope of a parabolic sector is given by;

$$\theta_{ps} = \theta_p \left(\frac{k_s}{k_2}\right)\left(\frac{4\beta^3 t^2}{\lambda r R_2 C_1}\right)$$

Estimates of gore thickness obtained using the .25° rim rotation and 2.5 lbs/ft load results in high gore weight because the material was not being used effectively. An alternate design approach was to use a thin shell with grid reinforcing ribs as shown in Figure 4-6.
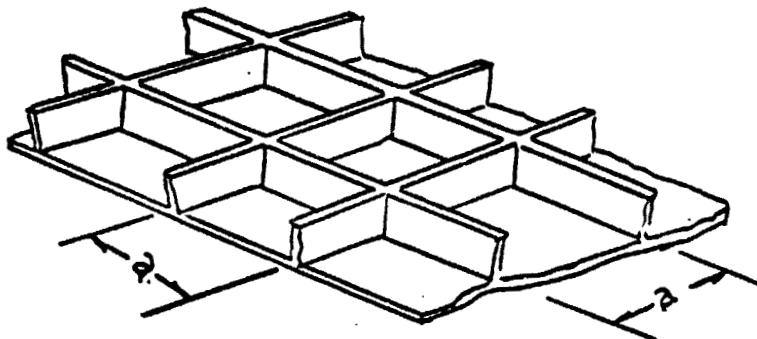
Figure 4-6

Thus an equivalent thickness was used for the stiffness of the sheet/rib pattern with that stiffness being given by the equation

$$\frac{E\,t_{eqv}^3}{12(1-\nu^2)} = \frac{E\,t_{act.}^3}{12(1-\nu^2)} + \frac{E\,I_{act.}}{a}$$

Where I_{act} is calculated about the N.A. of the section shown in Figure 4-7.
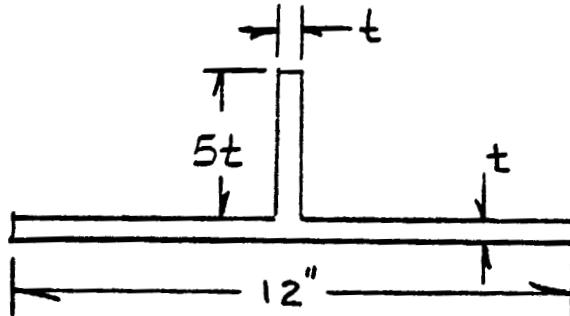
Figure 4-7

Further t_{eqv} is calculated as a function of the pressure loading W and the gore rim rotation θps from

$$\theta_{ps} = \left(\frac{k_s W\, r^3}{E\,t_{eqv.}^3}\right)\left(\frac{4\beta^3 t_{eqv.}^2}{\lambda r\, R_2 C_1}\right)$$

then t_{act} is determined from the stiffness relationship given above. The results of these calculations for an elastic modulus of 2×10^6 and two internal rib configurations are plotted in Figure 4-8 for the given shell reinforcement

4-17
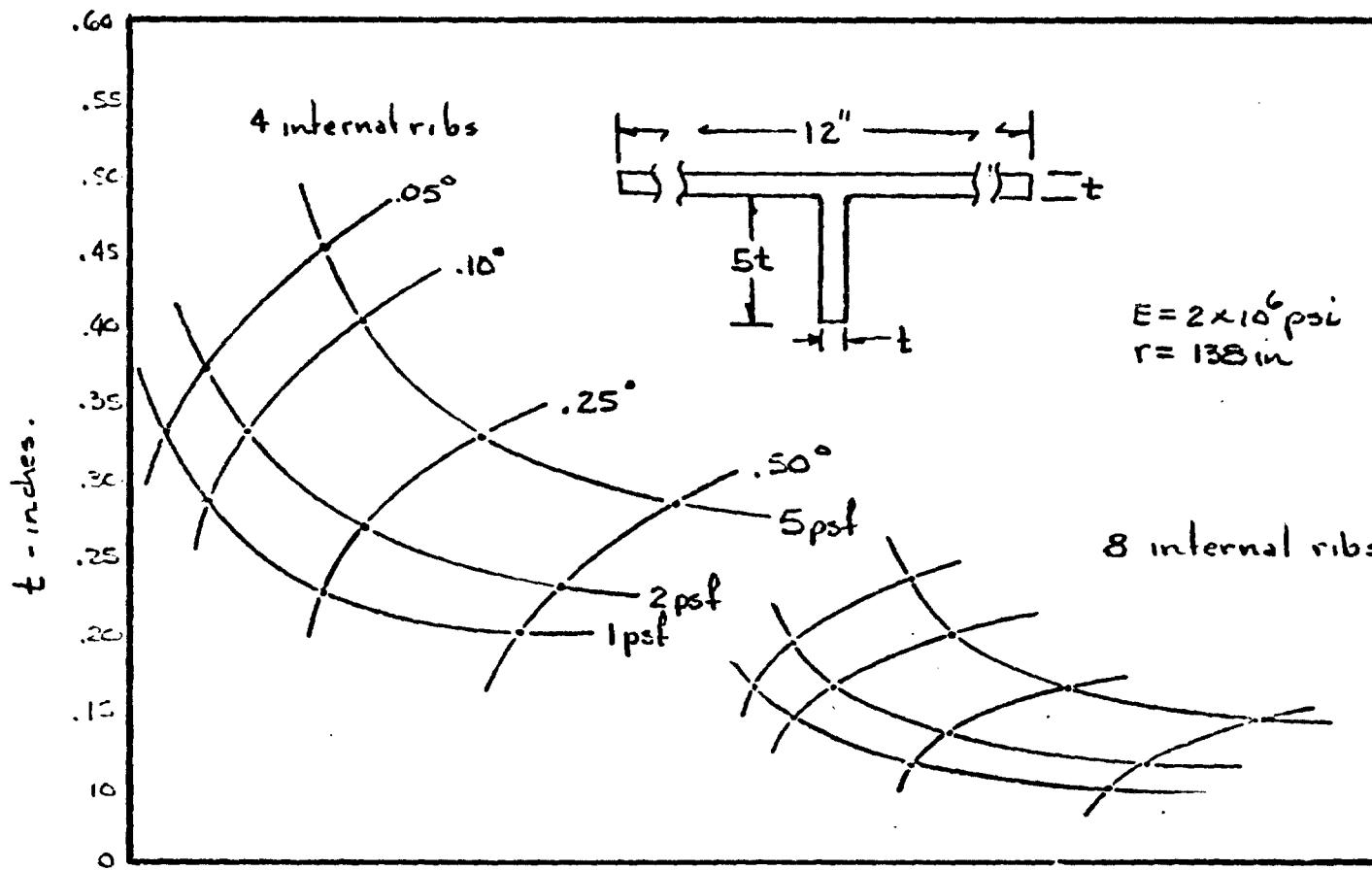
Figure 4-8.   Effect of Pressure loading and
              Angular Deflection on Shell Thickness

geometry. This ~~carpet~~ plot provides parametric data on actual shell thickness as a function of gore rim rotation and uniform pressure load. The implication is quite clear, that eight internal metal ribs result in approximately half the required plastic shell thickness for the same .25° rim angular deflection and 2.5 psf. This results in a more efficient use of the comparatively expensive plastic ($1.25/lbs) while trading this against an increase in the cost and weight of the aluminum internal trusses (about $1.00/lb). Figure 4-9 shows essentially the same data except that an allowance has been made for the potential effects of a lower modulus plastic rib. With the same design requirements, the eight internal rib case requires an actual shell thickness of .175 inches with a reinforcing rib height of .875 inches.

A cursory examination of the shell stresses as a function of loading and thickness is shown in Figure 4-10. Under the assumed shell weight of 2 lbs/ft^2 acting alone, the tangential edge stresses are about 1500 psi. The addition of a 20 mph wind pressure increases σ_T to 2000 psi. For the 1 inch ice and 12 inch of snow at 0 mph, the 12 inch of snow is most severe at a pressure loading of 6.2 lbs/ft^2 or about 4000 psi. The design criteria for this non-operating case is that the tensile strength ($\approx$ 10,000) of the material not be exceeded.

Other areas of concern, structurally, are panel buckling, local panel bending stress and hail impact. Figure 4-11 shows the results of a shallow spherical shell buckling analysis using the method given in Reference Bruhn. For the 7^m dish geometry and a 12 inch reinforcing rib pattens, a shell thickness of .175 inch gives a buckling pressure of 1.5 psi. 100 mph is a pressure loading of .1736 psi, resulting in a large margin. Local panel bending stress occurs in the unsupported shells portion between the reinforcing ribs,
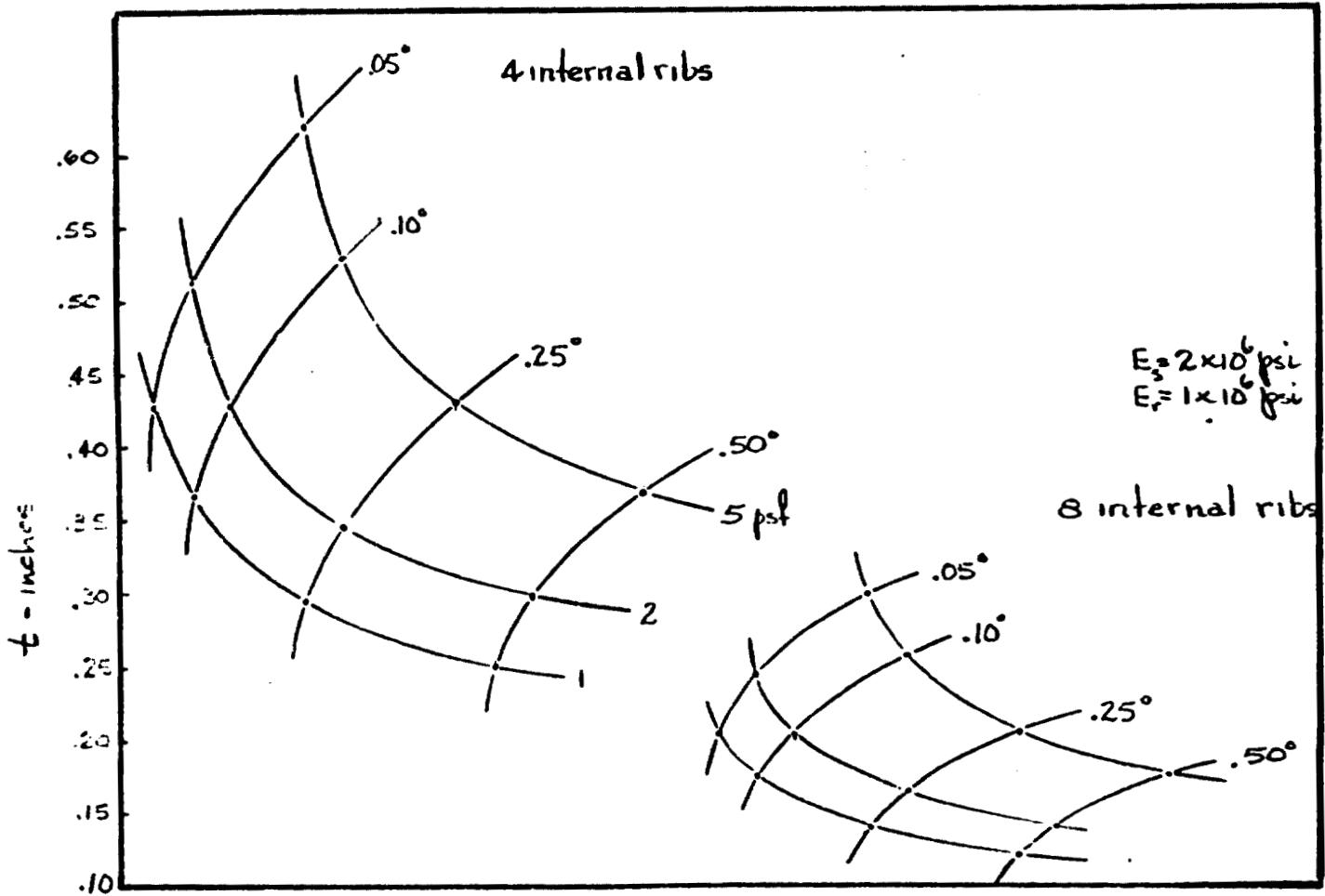
Figure 4-9. Effect of Pressure Loading and Angular Deflection on Shell Thickness
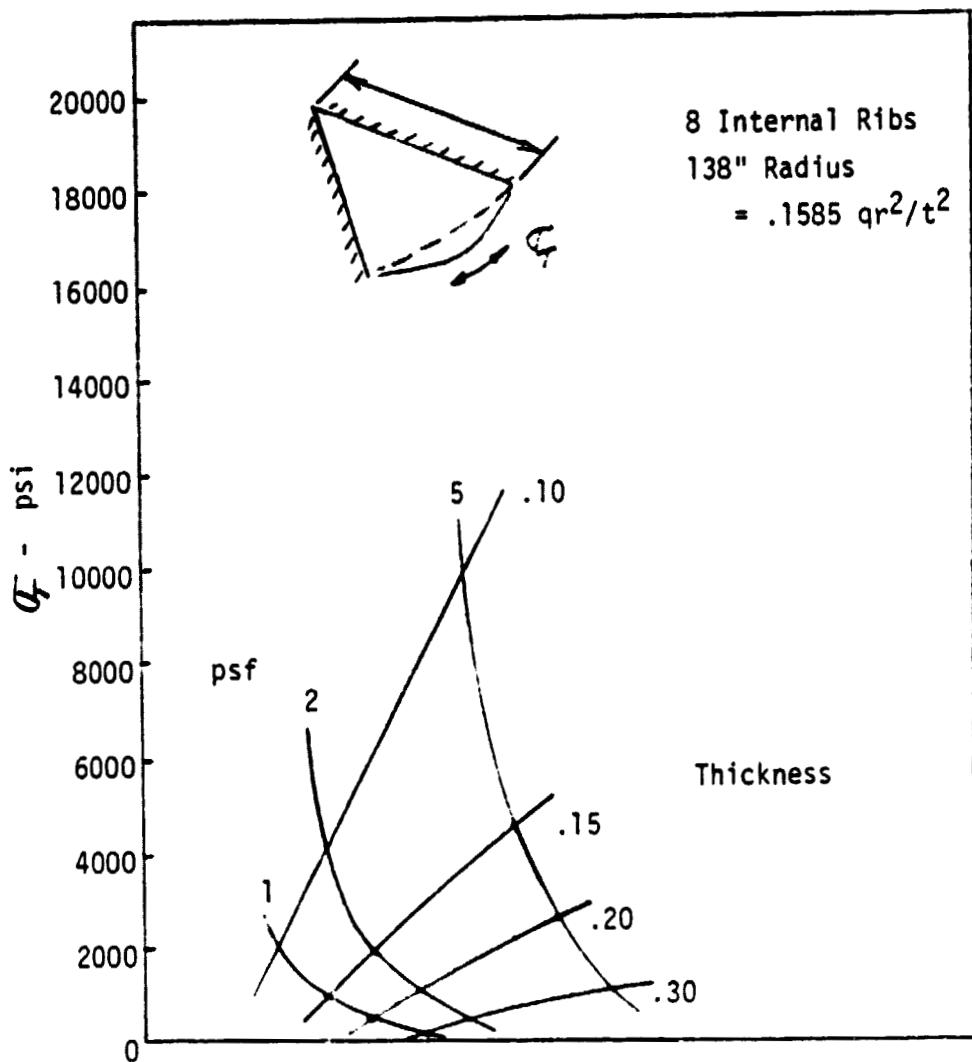
Figure 4-10. Gore Tangential Stresses
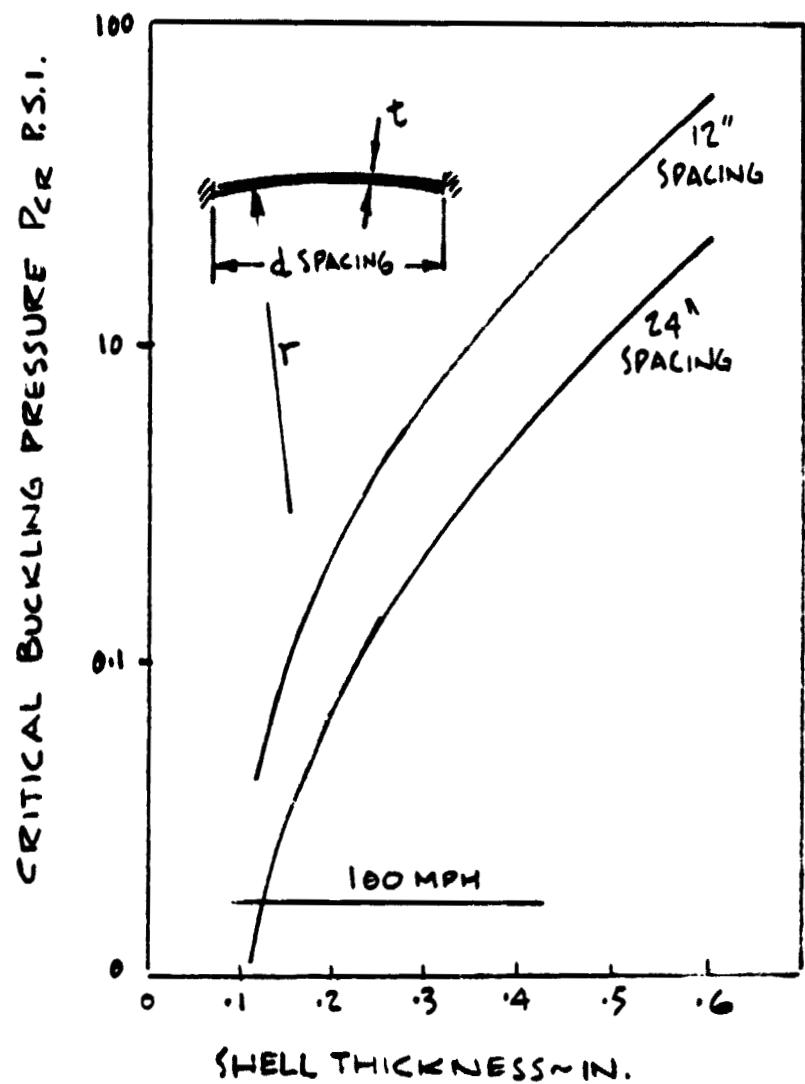
Figure 4.11. Shallow Spherical Shell Buckling Analysis

however, even at 100 mph, this stress adds about 250 psi to the general shell bending stresses.

Finally, hail impact was examined as a 3/4 inch diameter ball impacting the plastic at terminal velocity of V_t = 120 mph. The kinetic energy in the hail particle at the instant of impact is about 3.8 ft-lbs. The available IZOD data for GRP shows values greater than 5 ft-lbs at 68°F. While this is not a large spread between applied and allowable, it is nonetheless positive.

The structural analysis conducted during this study examined gross effects and did not attempt to predict a final stress picture for the gore segment, particularly the metal/plastic interface or the details of the plastic/plastic joints. While edge thicknesses were estimated (.40 inches), only a finite element computer analysis of this shell structure would allow us to do final sizing and detailed joint design. It is felt that the estimates of shell thickness, rib spacing and height have been examined in enough depth so that the weight estimates used for costing and dish subsystem are reasonable.

SECTION 5.0

REFLECTOR

5.0 REFLECTOR

5.1 Introduction

The baseline 7 meter point focus dish requires 435 ft^2 of reflector surface formed as a paraboloid with an f/D of .5. The design divides the reflector into eight separate segments and each segment into two equal area gores. The area of each gore is ≈30 square feet. This section discusses the optical and reliability requirements of the reflector; the candidates which satisfied these requirements; the testing program through which the candidates were placed; and finally, the reflector selection for the prototype concentrators. Maintenance of the reflector choice is also discussed. Note that the reflector choice is based on state-of-the-art technology and presently available cost estimates. As volumes increase the availability of such reflector candidates as silver and protective systems such as glass will undoubtedly increase while their costs decrease. The design allows such candidates to be integrated with the substrate as they become available and cost effective.

5.2 Requirements

Major determinants in the cost effectiveness of a solar collector are the optical characteristics, reliability, and cost of the reflector. The major optical characteristics are the total solar reflectivity, ρ, and the specularity. Specularity is given in milliradians as σ, where σ represents the cone angle through which one standard deviation (63%) of the reflected energy passes. Higher specularity thus implies smaller values of σ. Collector efficiency has been quantified as a function of ρ and σ. The cost effectiveness of a solar reflector is determined by ρ and σ in combination with reliability and cost.

As an example, the increase in performance obtained by changing from an aluminum reflector (ρ = .82) to a silver reflector (ρ = .92) is cost effective only

5-1

If the increase in cost is less than $.65/ft^2. To bound the problem, however, the following set of baseline requirements was established.

The optical and cost requirements of the reflector are that the total solar reflectivity be greater than .8, the beam spread be less than 3 milliradians, and the cost be less than $.50/ft^2. A reliability goal of 30 years was set. Reliability is treated as a goal since solar reflector service data of such duration is unavailable. Reflector life must be inferred from accelerated outdoor tests and carefully controlled indoor bench tests. Finally, the reflector must take the paraboloidal shape and be compatible with a glass reinforced epoxy substrate. The paraboloidal shape can be achieved by using a reflector which has that shape or using the substrate to hold an otherwise flat sheet in the required shape.

5.3 Reflector Candidates

Initial reflector approaches can be grouped as metalized films, glass mirrors, and direct part metalization. The latter category will be discussed first. This approach minimizes the integration of the reflector with the substrate. The gore is first molded to the proper optical shape. After molding, a thin metalized layer is applied to the gore surface. This requires that the surface of the molded piece be specular. This requirement is separate from slope error considerations. Specularity is required since the gore is defining the smoothness of the reflective layer. In this approach, the gore serves the same specularity function as does the glass in a silvered mirror.

A potentially promising silver deposition approach is the silver precipitate method. The silver precipitate approach is a quick and inexpensive process of spraying genuine silver on virtually any substrate. This technique differs significantly from the vacuum metalizing and electroplating methods in both the method of deposition and equipment required. In the spray plating method, the silver plating is deposited by chemical reactions of water based solutions on

the substrate. The solutions are sprayed on with specially designed spray guns and, therefore, there is no large capital expense associated with this method as compared with other methods of plating.

Another aspect of this process is the speed with which a silver plating can be deposited on the substrate. Objects can be plated in this manner in literally seconds compared to the 10-20 minutes or more for an electroplating or vacuum metalizing cycle. Specifically, the spray plating method of metalizing consists of first, a brief rinse with the first gun with activator solution which prepares the surface to receive the metal, followed by a brief rinse with the demineralized water gun. The object is then ready to receive the silver solutions from the third gun followed by a quick rinse with demineralized water.

Perhaps the most important aspect of this method is its versatility and low equipment and material cost. These features combine to make the process well suited for the present prototype design and material development phase the solar industry is in. Combined with this is the added feature that the process can be adapted to an automatic conveyorized spray coating line making it potentially suitable for large production.

The process described above generates a front surface silver mirror which must then be environmentally protected. A cost effective and reliable protective system which could be sprayed on the silvered part has not yet been developed. Thus, the direct part metalization approach shows high potential but requires substantial development in the area of a protective coating. Glass mirrors may also be integrated with the GRP substrate approach. Glass is produced in high volume as flat sheet. After silvering such sheets must be formed into the re-quired paraboloidal shape. Two techniques are available. Sagging glass is equivalent to thermally forming it into the proper shape. The mirror would then be bonded to the gore substrate or the gore would be molded behind the

mirror. With zero external load on the reflector, there would be no loading on the bond surface between the glass and substrate. If the thermal coefficients are matched between the glass and substrate, thermal stresses will not develop.

A second technique is available to generate a paraboloid from an initially flat glass surface. In this approach the glass is elastically deformed into the required shape and held in this position by a bond between the glass and substrate. Note that the bond in this case is stressed continually -- independent of whether the reflector is externally loaded. Furthermore, the glass is elastically stressed in this design. The stresses generated by the deflection into the paraboloidal shape must, of course, not exceed the strength of the glass. The stress generated by deforming a flat piece of glass is proportional to the maximum deflection and glass thickness. The required deflection is reduced as smaller mirror segments are used. Chemical strengthening of the glass may be used to achieve large deflections without glass breakage. In this process the outer surfaces of the glass are put in compression ($\sim$40,000 psi) through a chemical diffusion technique commercially available through Corning Glass Works. Such preloading allows tensile loading at the surface to approach 40,000 psi before the glass is truly put in tension and is near its fracture point.

This glass may be deformed into the required shape by the proper control of segment size, glass thickness and chemical strengthening. The latter may not be required if a proper balance can be achieved with the first two design parameters.

The glass itself should have no problem achieving a thirty-year life goal. The highly reactive silver layer, however, must be well protected in order to claim such a predicted life. At the present, however, cost is a more serious consideration than protection of the silver layer. Fifty mil chemically strengthened glass was quoted by Corning Glass Works at $5.00/ft^2 for a 50,000 square foot order. This cost does not include silvering or protection of the silvered layer.

Without chemical strengthening glass cost for Corning 0317 50 mil glass is $1.59 in quantity. Again, silvering is not included. Corning is presently studying the producibility of 20 mil glass. Costs are as yet unavailable. The major point, however, is that at the present, glass mirror costs, whether sagged, elastically deformed, or chemically strengthened, exceed the cost bogie of $.50/ft^2. As higher volumes reduce glass costs to a cost effective range, glass mirrors can be integrated into the substrate design. The major requirement will be that the thermal coefficient of expansion, α, of the substrate match that of the glass. The range of α for epoxy resin GRP spans that of glass and such a match is therefore feasible.

The third reflector class considered for integration with the GRP substrate was metalized films. As with glass mirrors, two techniques are available to generate the paraboloid shape. The film may either be thermally formed into the required shape or elastically held in shape by the substrate. Figure 5-1 shows the metalized film candidates considered for the point focus concentrator. Note that in each case the film is metalized by a coil process in a vacuum chamber. Coil speeds are on the order of 150 ft/min. During a single blow down of the vacuum chamber as much as 50,000 ft^2 of reflective film may be metalized. The cost of commercial metalizing is on the order of $.05/ft^2 when high volume coil processes are used. Also note that reflective films in general are characterized by high specularity (due to film smoothness). The first four candidates of Figure 5-1 have less than 3 milliradians beam spread (σ <3 milliradians).

The first film listed in Figure 5-1 is available from the 3M Company and has substantial field service data. The protective coating is clear acrylic. The film is commercially sold with a pressure sensitive adhesive on the reverse side. This allows convenient lamination of the film by hand. The second reflector is a composite film available commercially from Martin Processing. The upper layer

FILM	COST/FT^2	DESCRIPTION
3M SCOTCH CAL	.50	ACRYLIC VACUUM METALLIZED PRESSURE SENSITIVE ADHESIVE
MARTIN UV STABLE POLYESTER	.20	UV STABLE POLYESTER (DYED) VACUUM METALLIZED POLYESTER
ICI UV STABLE POLYESTER	.20	UV STABLE POLYESTER (BATCH) VACUUM METALLIZED
SHELDAHL	1.20	TEFLON VACUUM METALLIZED POLYESTER
KURZ HASTINGS	.15	CLEAR COAT METALLIZING ABS
KURZ HASTINGS	.50	UV STABLE POLYESTER METALLIZING PVC

Figure 5-1. Film Candidates

is a high clarity 3 mil UV stable film sold under the tradename LLUMAR. UV absorbers are added to the film in a dying process. This film is currently in use as a glazing on commercial flat-plate solar collectors and has been in use for 15 years as a greenhouse glazing. The lower film is a 1-mil clear polyester film. The upper film is vacuum metalized to a thickness having a resistance of less than one ohm per square. The two films are laminated with the metalizing sealed in between. ICI (third film candidate of Figure 5-1) also sells a UV stable polyester. In this case the stabilizer is added as the film is first polymerized. An advantage of this approach is that the distribution of absorber is constant across the thickness of the film. While a dying process results in a diffusion profile of absorber from each surface of the film, ICI's product is in the developmental stage. It will be marketed as a polyester film alone. The user must metalize and perform any further lamination. The fourth candidate of Figure 5-1 is the commercially available Sheldahl film. Its main difference from the Martin composite is that the upper layer is Teflon rather than UV stable polyester. This choice for the protective coating substantially affects the price. The first four films of Figure 5-1 would be stretched over a mandrel of the proper shape. The GRP gore would then be molded behind the stretched film. The bond between the molded gore and film would then maintain the film in proper optical shape. The stretching of the candidate film and its integration with the substrate is discussed in a separate section. The last two reflectors of Figure 5-1 would be thermoformed into the correct shape before mating with the GRP substrate. Candidate five utilizes foil hot stamping. Kurz-Hastings manufactures wood grain and other decorative foils which are hot stamped to the surface of plastics such as ABS. One of the foils is an aluminum reflective foil presently used for interior automotive trim. The first candidate, also from Kurz-Hastings, is a composite film marketed for exterior automotive trim.

5.4 Reflector Testing

As part of the reflector surface development task of the low cost concentrator program, four of the reflector films listed in Figure 5-1 were subjected to a battery of screening tests. These tests were designed to evaluate the durability of the candidate reflector materials to severe accelerated environmental conditions. The reflector materials investigated were:

1) Scotch Cal 5400

2) Martin UV Stable Polyester

3) Kurz-Hastings Metalized ABS

4) Kurz-Hastings Metalized PVC

The assessment of a reflector's environmental stability was based on optical performance before and after testing. Results of this testing has led to the selection of a leading candidate for the reflector.

The optical property characterization of reflector materials consists of three tests: 1) Total Hemispherical Reflectance, 2) Diffuse Reflectance, and 3) Specular Reflectance.

Total Hemispherical Reflectance - This measurement is obtained with a Beckman DK-IL spectroreflectometer. The measurement consists of determining the reflectance characteristics of each reflector material, based on a Ba_2SO_4 reference standard, as a function of wavelength from 350 to 1750 μM weighted against the solar spectrum and summed.

Diffuse Reflectance - This measurement is also obtained with the Beckman spectroreflectometer. The measurement consists of determining the non-specular or diffuse component of the reflectance characteristics of each reflector material. Also, the data is referenced to a Ba_2SO_4 standard over the wavelength range of 350 to 1750 μM weighted against the solar spectrum and summed. This measurement is not designed to give specular reflectance information, but is used only as an in-

dication of how a samples' diffuse reflectance component may change after exposure to environmental tests.

Specular Reflectance - In order to complete the characterization of a reflecting surface, the reflected beam profile of the specular reflected component over the wavelength range 350-1750μM must be determined. As a first approximation to this measurement, and as a tool to obtain preliminary data, this measurement is obtained at one wavelength (.6328μ). This is accomplished with the aid of a laser specular reflectometer. The instrument consists of source optics and detector optics. The source optics consist of a Helium-Neon laser, a beam expander and a beam-defining aperture. The detector optics consist of a variable collecting aperture and a silicon detector mounted inside an integrating chamber.

Each of the reflector samples was tested according to test procedures designed to simulate long-term exposure to outdoor conditions that would be encountered by a solar collector. Unfortunately, no uniform set of test standards has been established in the industry for testing solar reflector surfaces. Therefore, these tests are the most appropriate ones developed by the Materials Engineering Department of GE to suitably obtain simulations of 10-20 year reflector surface exposure by short-term acceleration tests.

The following are the environmental tests to which the reflector samples were exposed:

Preconditioning - All test samples were conditioned for 24 hours at 45 $\pm$ 5 percent relative humidity and 21 $\pm$ 1°C immediately prior to and after environmental tests for the purpose of measuring physical or optical performance. Prior history is maintained.

Salt Spray (Fog) Test - This test is to determine the relative corrosion resistance of coated reflector samples. The test is conducted in a standard salt spray chamber in accordance with ASTM-B117-64 for 15 days.

<u>Temperature Cycle Stability</u> - The purpose of this test is to determine reflector sample thermal stability to freeze-thaw-dry cycles. Samples are exposed to 25 cycles of the following: 20 minutes + 70°F, 2 hours - 65°F, 20 minutes + 70°F, 2 hours + 150°F, 20 minutes 70°F, etc. This test was not designed to examine the structural integrity of substrate materials, but only to determine if any optical parameters would be affected by a freeze-thaw-dry cycle.

<u>Abrasion</u> - This test is designed to determine the relative resistance of film and coating systems to abrasion by falling sand and dirt. Natural silica sand and dirt are allowed to fall on a 3 cm^2 area of a sample at a rate of 15-20 gms/min. in increments of 3ι gms. (FED-STD-141A, Method 6191 Equivalent). This is a comparative test, where the optical results of the samples were compared to those of glass micro-sheet exposed to identical abrasion tests. (Sand - natural silica of a grade, which passes through a No. 100 sieve; Dirt - local variety of a grade which also passes through a No. 100 sieve).

<u>Accelerated Weathering</u> - The purpose of this test is to determine the effects of a given set of heat, moisture and UV exposure cycles on the reflector samples. Based on ASTM-G53-77, the test consists of exposing the samples to 16 to 20 hours of condensation produced by exposing the test surface to a heated, 110°F, saturated mixture of air and water vapor (93 $\pm$ 3 percent relative humidity), while the samples' reverse side is exposed to cooling room air. The samples are then exposed to simulated solar UV (20 sun equivalent) at a temperature of 150°F for four hours. The test is for 15 cycles.

<u>Cleaning Maintenance</u> - Concentrating solar energy collectors are required to maintain their specular reflecting quality in order to achieve effective energy transfer. Since these concentrators are located in an outdoor environment, they will be exposed to dust, dirt and rain deposits over long periods with consequent

residue build-up. In order to continually maintain the reflectance quality of the concentrator in this environment, periodic removal of these residue deposits is required in such a way as not to damage the surface of the reflector.

The intent of this test was to determine the washability of soiled reflector samples when exposed to a cleaning technique.

The cleaning method consisted of a relatively low pressure detergent spray and rinse. Visual appearance was noted and reflectance measurements were taken prior to and following contaminating exposure and cleaning operations. A "Porto-Blast" washer operated at 75 psi at a flow rate of 3 liters per minute with a nozzle velocity of 31 m/s was used. The cleaning solution consisted of a two percent solution by volume of "Hurri-Clear" SH No. F1-42 biodegradable detergent and warm tap water.

The mirror samples were contaminated with local dry drit that was ground fine and dumped on the reflector samples with the excess removed. A fine tap water spray was allowed to fall on dirty reflector samples, and then the samples were placed in an oven and baked at 175°F for 20 minutes. Each reflector sample underwent 10 contamination and cleaning cycles.

The results of this testing program are shown in Figure 5-2. In general the most severe test was the weathering cycle. Scotch Cal and the metalized ABS completely failed this test. After this test essentially all reflectance was diffuse. The film which showed the least degradation was the Martin composite. Also note that the salt resistance and cleanability of the Martin film are equivalent to that of Scotch Cal. As shown by Figure 5-2 the Martin film is the most environmentally stable film tested by the GE Materials Department. It also compares favorably with surface conversion aluminum reflectors such as Kingslux when run through the same bench test cycle.

	MATERIAL	SOURCE	AS REC'D		SALT		WEATHERING		ABRASION		CLEANING 1		CLEANING 2		REMARKS
			T*	D*	T	D	T	D	T	D	T	D	T	C	
1	SCOTCHEAL-5400	3M COMPANY	.873	.025	.865	.136	.650	.625	NO TEST		.858	.058	.848	.070	FAILED WEATHERING TEST
2	LLUMAR	MARTIN PROCESSING, INC.	.813	.032	.784	.161	.802	.076	.789	.076	.800	.067	.795	.088	DECREASED PERFORMANCE AFTER ABRASION AND CLEANING TESTS
3	METALIZED POLYESTER ON POLYVINYL	KURZ-HASTINGS	.800	.165	.783	.162	.780	.250	NO TEST		NO TEST		NO TEST		DIFFUSE COMPONENT TOO HIGH
4	METALIZED ABS PLASTIC	KURZ-HASTINGS	.829	.076	.822	.167	.612	.517	NO TEST		NO TEST		NO TEST		FAILED WEATHERING TEST
	TEST DESCRIPTION				ASTM-B117-64 FOR 15 DAYS		ASTM-G53-77 FOR 15 CYCLES		FEC-STD-141A METHOD 6191		LOW PRESSURE DETERGENT SPRAY & RINSE		LOW PRESSURE DETERGENT SPRAY & RINSE		

*T: TOTAL HEMISPHERICAL REFLECTANCE
*D: DIFFUSE REFLECTANCE (3° APERTURE)

Figure 5-2. Reflector Bench Test Results

Scaling from bench tests to reliable field life predictions is difficult.
Therefore, the literature was searched for carefully controlled outdoor tests of
reflective films. Reference A describes a test of eight reflectors, one of which
was Scotch Cal, a reflector tested in the GE bench test program. Samples were
exposed at eight times normal solar intensity (by using concentrating mirrors).
Distilled water was sprayed onto the samples for eight minutes of each sunny hour.
Tests were conducted at Desert Sunshine Test Labs and lasted a total of 2 1/2
years. At the test's conclusion the amount of radiation which falls in 20 years
fell on each sample. Listed below is the test history of the Scotch Cal sample.

MATERIAL	ρ_0	t-WEEKS	ρ CLEAN
3M Scotch Cal	.85	52	.81
		97	.73
		129	.69

After 129 weeks at eight suns, the authors report that the reflector was
still specular with a total reflectance of 69%. The same sample completely failed
the GE accelerated weathering test and thus, helps calibrate the severity of this
test. Scaling from this test to predictions of field life remains difficult.
However, test results lead to the conclusion that the Martin film is substantially
more environmentally stable than Scotch Cal and should have a greater field life
(on the order of 15 years greater). In addition the major component of the
Martin film, the LLUMAR upper layer, has been in the field for over 15 years with
satisfactory service as a greenhouse glazing. The above, in combination, with the
low cost of the Martin film, has led to its choice as the near-term reflector for
low cost concentrator dish. Other reflectors of higher total reflectivity will
replace the Martin film when their costs make such a change cost effective.

SUMMARY OF DEGRADATION RATE
DATA FOR SUMMER AND WINTER

Ranking (In Order of Increasing Rate)	Degradation Rate (% Per Day)	
	Glass (ASG Laminate and 2nd Surface	Sheldahl Acrylic
1. Permanent face-down	0.06 ± 0.04	0.03
2. Sensor face-up/face-down	0.12 ± 0.14	0.23 ± 0.16
3. Astronomical timer face-up/face-down	0.20 ± 0.16	0.283 ± 0.12
4. Astronomical timer/near vertical stow	0.315 ± 0.11	0.32 ± 0.28
5. Permanent face-up	0.45 ± 0.20	0.40 ± 0.24

PROCEDURE

-- MEDIUM PRESSURE (75 PSI) SPRAY WASH

--- 2% DETERGENT SOLUTION

FREQUENCY

-- TBD - INVERTED STOWAGE

Figure 5-3.   Recommended Cleaning Procedure

Periodic cleaning of the reflector, whether a film or glass mirror, will be required to maintain peak performance. The cleaning test cycle has shown the Martin film to be cleanable. Twenty spray-type cleanups of a complete layer of baked-on dirt had a minor effect on reflectivity. During a 15 year life only 90 cleanings (of a small amount of dirt) would be required with a bi-monthly maintenance schedule. Note that dirt build-up is a strong function of reflector stowage orientation. Reference A contains a study of dust build-up rates. The data is shown in Figure 5-3 (expressed as degradation in reflectivity) for five separate stowage orientations. The present design is comparable to the orientation 2; i.e., the reflector is face down when the sun is not shining. This orientation minimizes dust build-up and will therefore reduce cleaning requirements.

5.5 Test Samples

The reflector must be physically integrated with the GRP substrate. The substrate must hold the reflector in the proper optical orientation. Specularity of the reflector must be maintained. Thermal loading of the reflector must not distort the optics. Several reflector-substrate composites were manufactured to demonstrate the compatibility of the film reflector and GRP substrate. These samples were used to identify acceptable process and manufacturing techniques.

The Martin reflective film was first stretched in a frame under bi-axial tension. The frame was then pressed over a piece of glass such that the film was intimately in contact with the glass surface. An epoxy fiberglass substrate was then layed up behind the film. After curing, the composite was inspected for optical properties (reflectivity, specularity, and smoothness) and for adhesion between the film and plastic.

This test program identified several key manufacturing and process considerations. For the first samples, a continuous strand cloth was placed behind the film and a layup of the design epoxy resin was made. A vacuum bag was used during curing. This process resulted in an unacceptable reflector. Fibers from the mat deformed the film surface. Local unacceptable slope errors resulted. This problem is identified as fiber show through in the discussion below.

The next reflector samples were manufactured with a veil (surfacing mat) located between the film and reinforcing mat. However, even the relatively fine texture of the veil distorted the film surface and was considered unacceptable.

The fiber show-through problem was ultimately solved by using a gelcoat of epoxy on the film surface. A gelcoat is a layer of resin which is allowed to cure before the molding process is continued. After the gelcoat has cured, the reinforcing mat was properly placed and a hand layup of the epoxy resin was made. This technique solved the fiber show-through problem. Figures 5-4 through 5-7 depict a sequence of steps leading to a small plastic parabolic dish. A smooth fiber-free film surface was obtained. Note that the slope error of the resulting dish is quite visable. This resulted from the fact that the mold was a spun aluminum dish. The spinning marks were replicated very accurately and reinforce the fact that the accuracy of the molded part lies in the accuracy of the mold.

Several manufacturing processes were studied to maximize the adhesion between the film and gelcoat. With no surface preparation, peel strength between the film and substrate was minimal. Etching of the film surface was therefore investigated. Experiments were conducted with two etching agents: Ecco prime (available from Emerson and Cuming, Inc.) and chromic acid. The latter agent proved to be more effective. It was determined that adequate peel strength was achieved when the composite Martin film separated before the bond between the lower film and gelcoat failed. A chromic acid etch, allowed to sit for

approximately one hour, satisfied this requirement.

Reflectivity of the composite reflectors was measured and compared to that of the unstretched film. No decrease in reflectance was measured. The test samples proved the feasibility of molding a GRP substrate behind a film stretched to the proper shape. Important considerations are the smoothness of the mold surface (glass in the case of the test samples), the need for a gelcoat, and proper preparation of the film surface.

REFERENCES

REFERENCE A: Exposure Test Results for Reflective Films
                    Rauch, Gupta
                    Institute of Environmental Sciences
                    Seminar on Testing Solar Energy Materials and Systems, 1978.
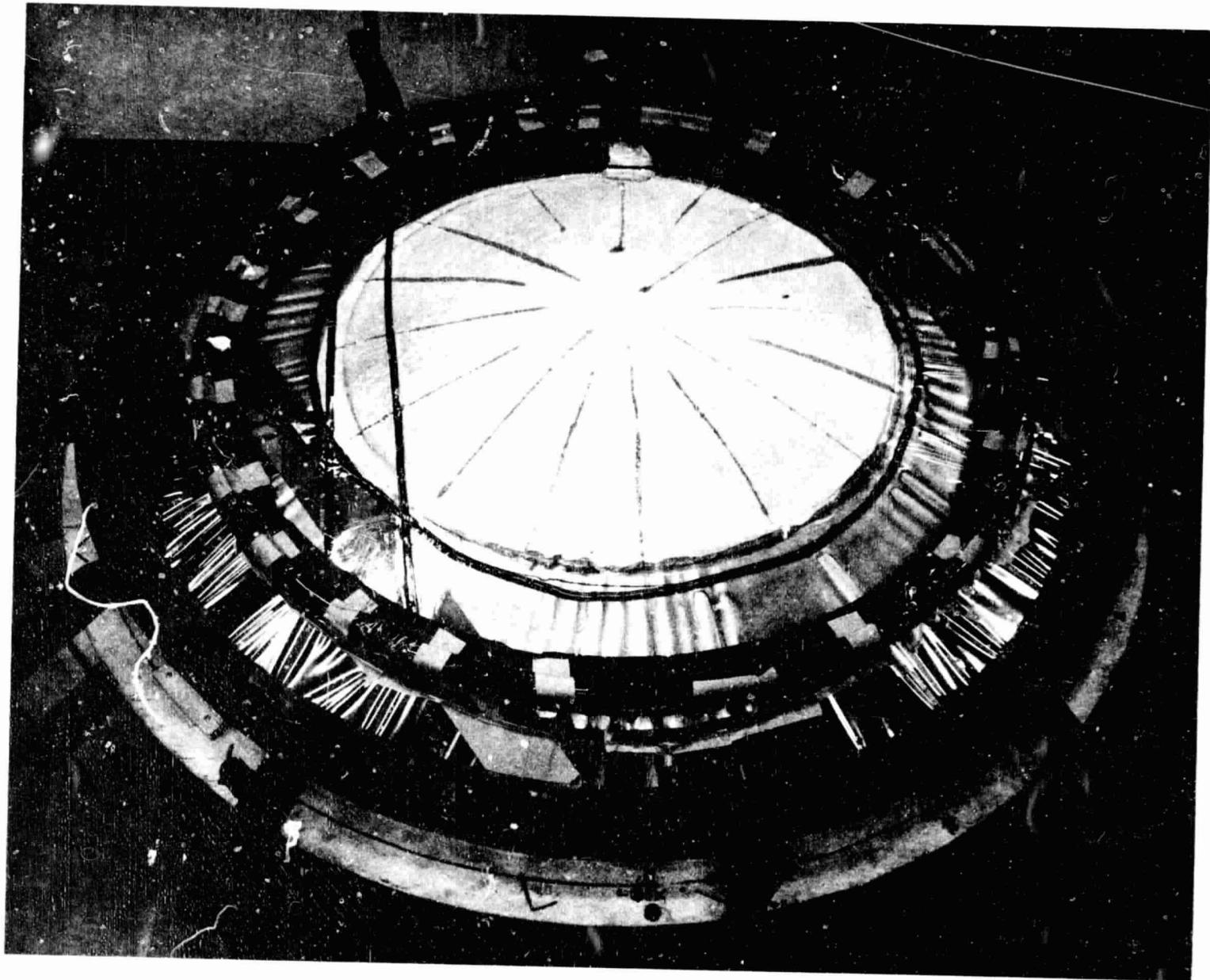
Figure 5-4. Film Stretched Over Mandrel (79-145-C)
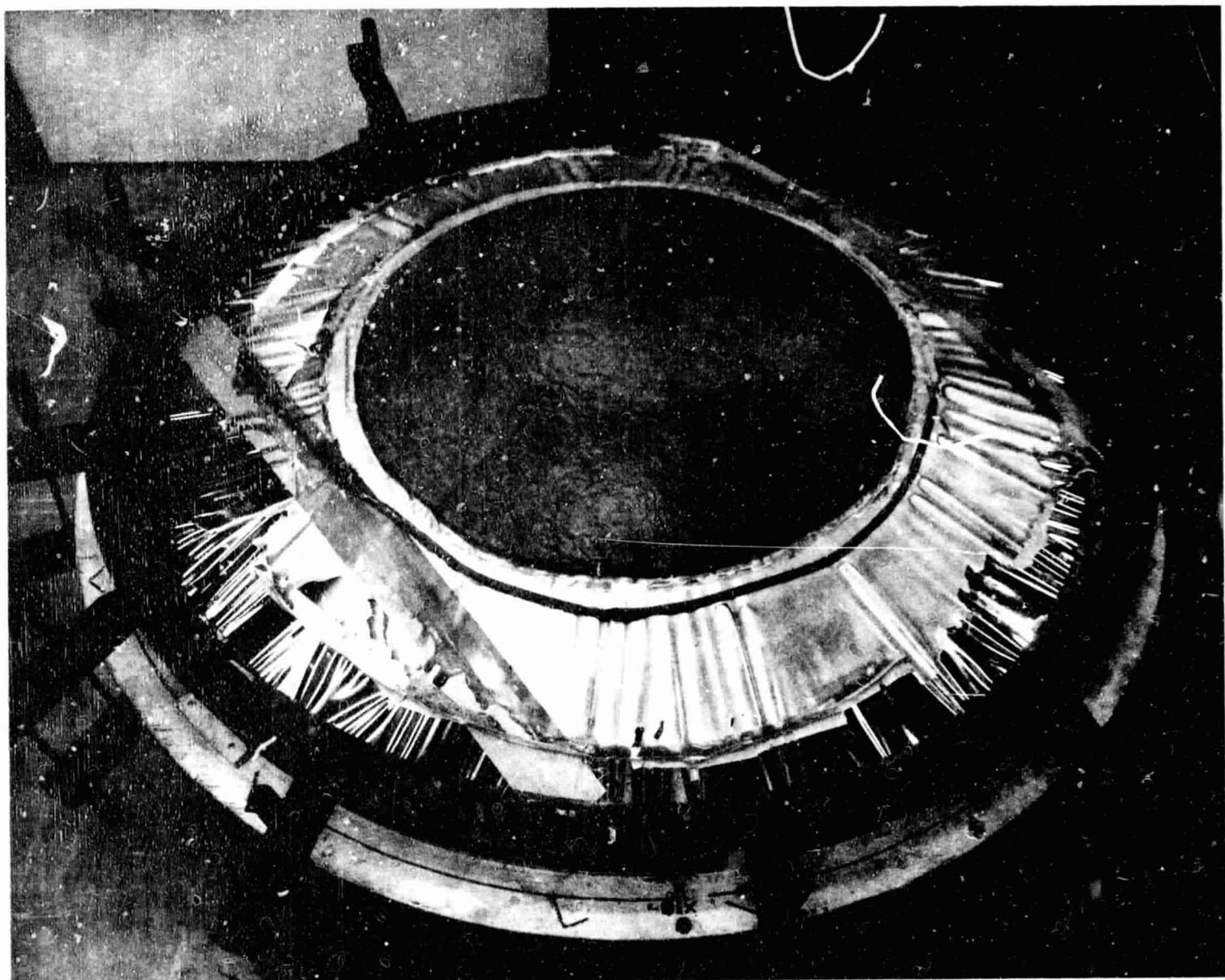
Figure 5-5. Plastic Lay-Up (79-145-E)
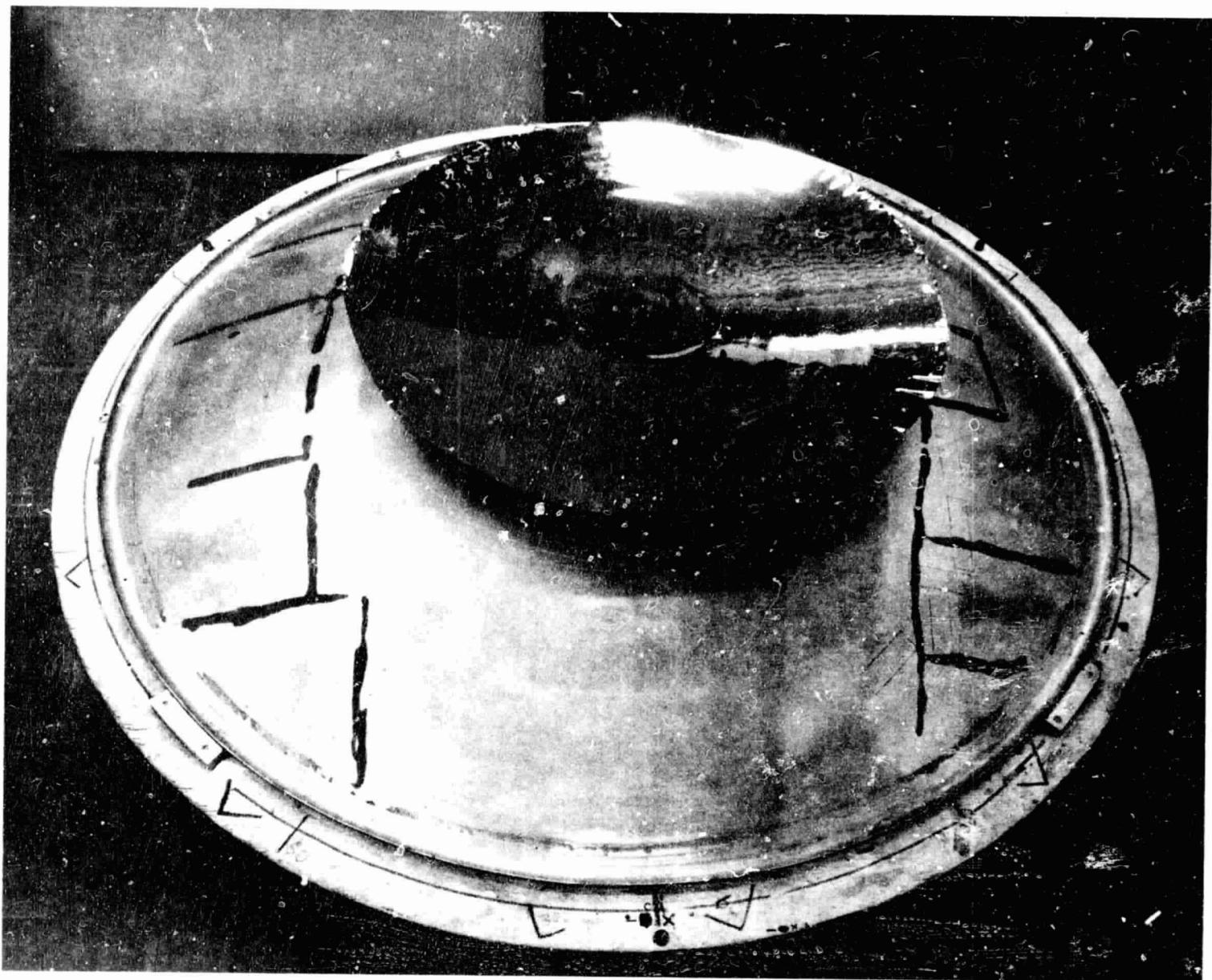
Figure 5-6.   Completed Small Dish (79-145-B)
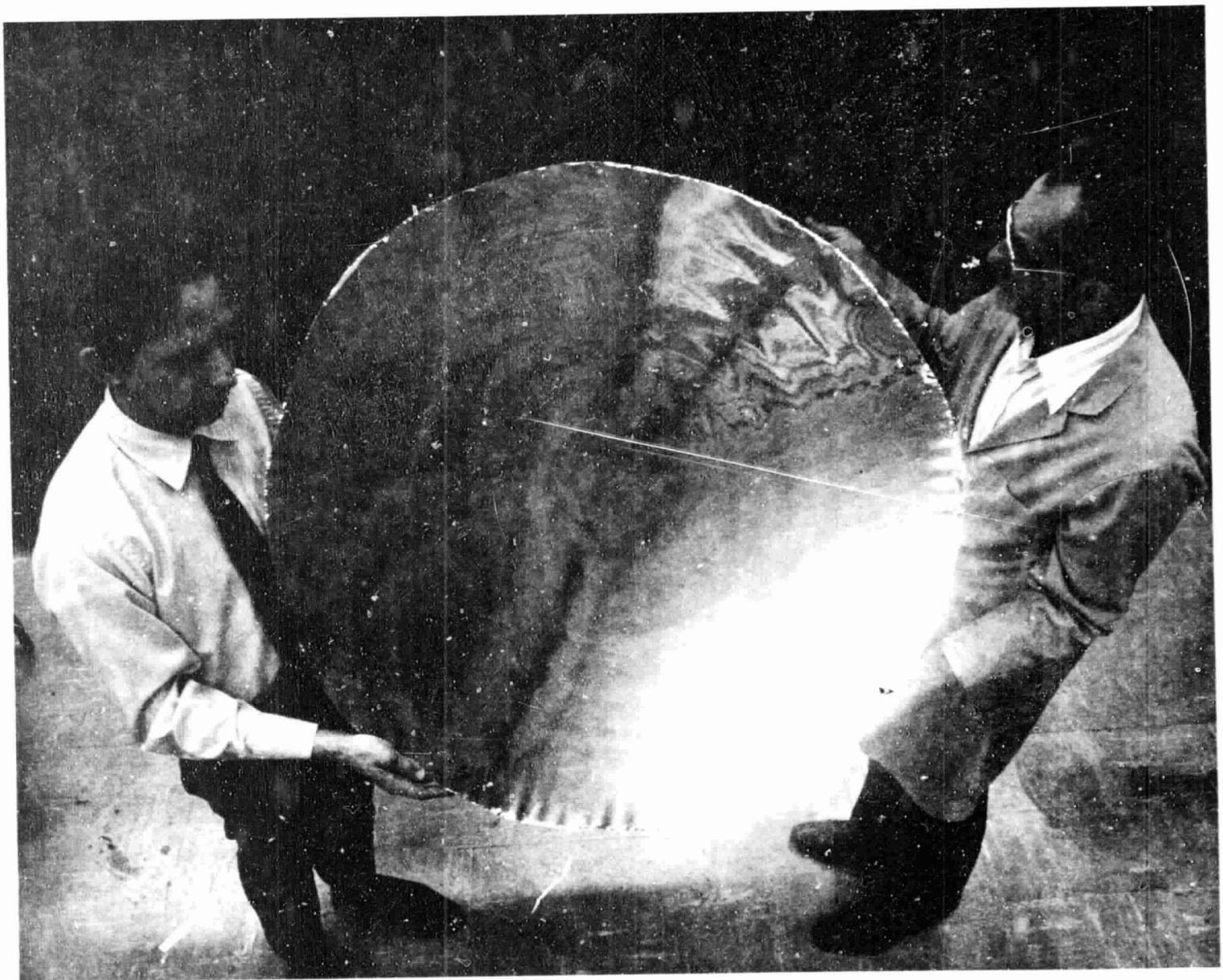
Figure 5-7. Completed Small Dish (79-145-A)

SECTION 6.0

MOUNT SUBSYSTEM

6.0 MOUNT SUBSYSTEM

The mount subsystem shown in Figure 6-1 is the result of an early configuration trade-off between a single pedestal polar (equatorial) mount and the AZEL configuration. The configuration allows the receiver/engine to be stowed vertically down which is one of the requirements given in Table 6-1. Further, this configuration allows the loads to be distributed over a wide base rather than a single pedestal, resulting in lower loads into the foundations and lighter mount members, as will be seen.

The next phase in the mount design is to determine which loading case resulted in the most severe loads into the foundation and mount members. The number of loading cases considered is shown in Figure 6-2.

A simplified model (as shown in Case I), was used to determine the magnitude of the forces P_1 and P_2. The results of this analysis showed Case VI to give the highest loads (Table 6-2). However, Case VI was considered as too improbable to become a design case so Case II was selected as the next most realistic case based on the simplified model.

Another brief analysis conducted prior to the final member sizing was the Mount Attachment Trade-Off shown in Table 6-3. In this study, it was assumed that the receiver/engine weight was 1000 lbs. and the dish and internal rib weight was 1000 lbs. Further, the dish was in the 6 A.M. position with the wind at 30 mph from the west with 1g vertical and 1/4g lateral. In addition to gravity loading, note also that in Case I, all base spoke members, 3-9-6, 4-9-7, and 5-9-2 had I_0 (inertia) values of 1.0 in^4 in Cases II, III, and IV. I_0 was 100 in^4. The results shown under "Deflections" were obtained by running a simplified version of a computer program called FEAST.

MOUNT INTERNAL RIB
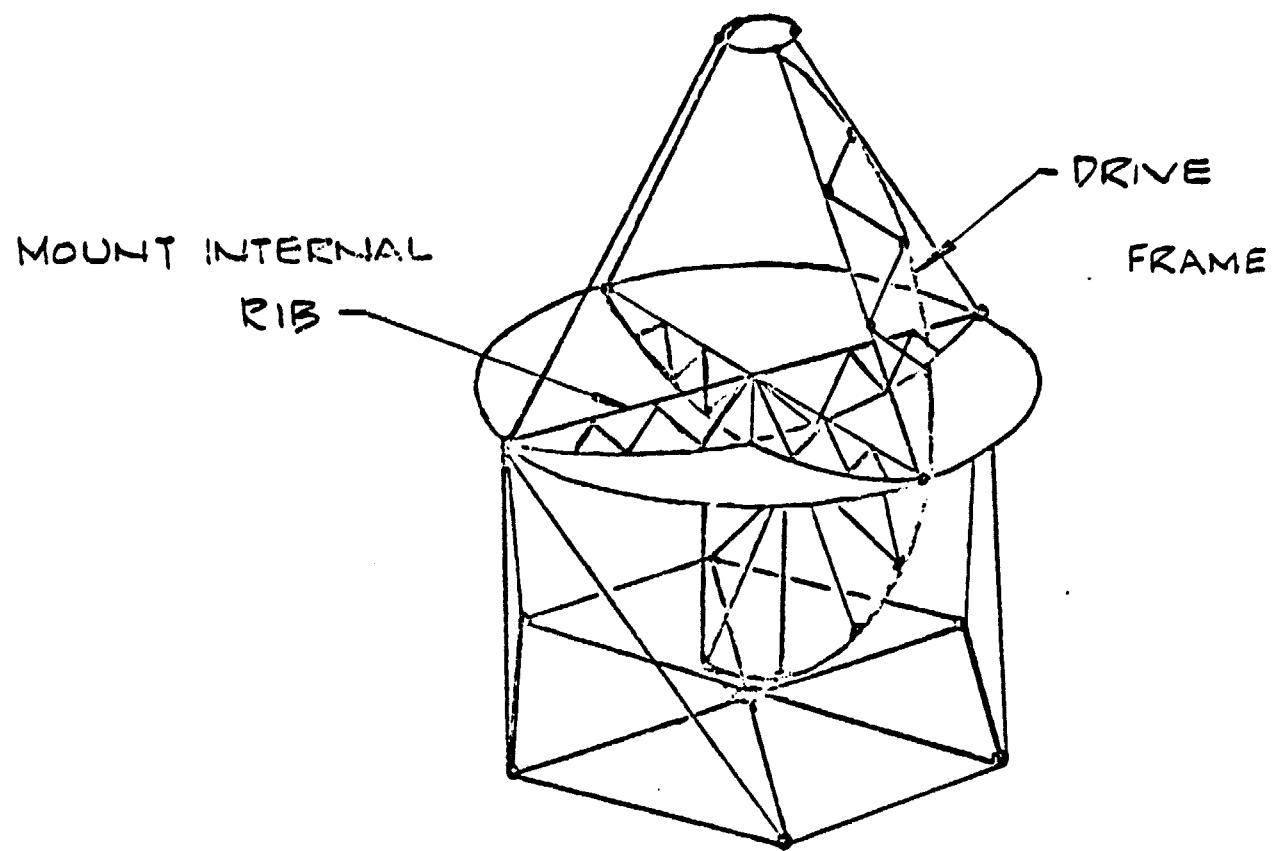
DRIVE FRAME

Figure 6-1. Preliminary Mount and Drive Frame Configuration

6-2

Table 6-1. Mount Requirements Summary

1.	Allow 210° Azimuth
2.	Allow 180° Elevation
3.	Carry, without Yielding or Buckling, the Weight and Aero Loads of Receiver/Engine and Dish Structure
4.	Use Commercially Available Hardware
5.	Provide for Stow Capability with Receiver/Engine Vertically Down
6.	Provide Load Paths into Foundation
7.	Field Assembly without Welding

This code required that member geometry and end coordinates definition be entered, along with boundary conditions and the above loading, to obtain a solution. The solution clearly shows that for Cases II, III, and IV, large member sizes (120 lbs/ft, 18-20 in. diameter) are required and deflections are still 30 times too large. From this analysis, Case I was chosen for further study. Case I has six symmetric attachment points that can take only vertical tension or compression, but no side load. Only the pintle can take side loading.

At the time the initial attachment trade-off was being conducted, it was noticed that the unsymetrical geometry and weight distribution of the dish about the mount elevation axis was resulting in high X-component loads. Further, the stiffness of the internal rib between mount bearings 1 and 2 coupled with a Z restraint boundary condition, resulted in large Z-forces. These two conditions caused the frame or mount member sizes to be about seven inches in diameter and very heavy, even with .109 inch wall thicknesses. By placing a counterweight symmerically opposite the receiver/engine and by designing the joints 1 and 2 to take x and y loads only, the member sizes and hence weights, could be reduced.

I

II

III

30MPH

30MPH

90MPH

P_2 P_1

1G VERTICAL
1/4G LATERAL

IV

V

VI

90MPH

12" SNOW
0MPH

1" ICE
90MPH
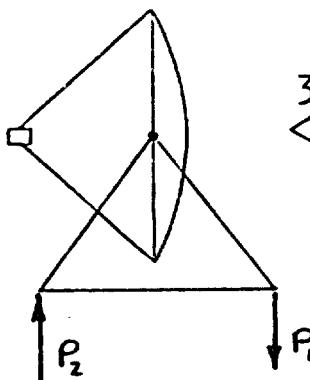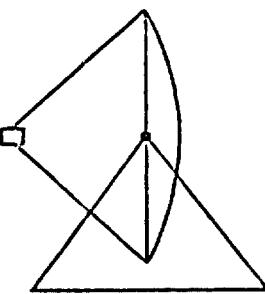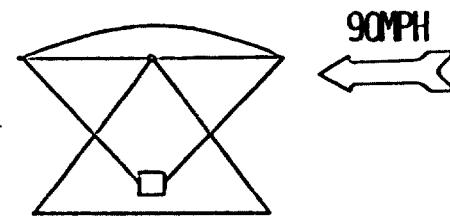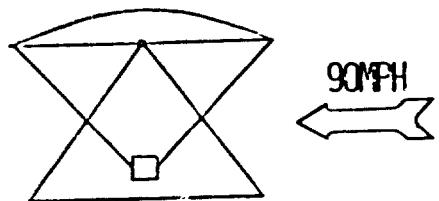
1G VERTICAL
1/4G LATERAL
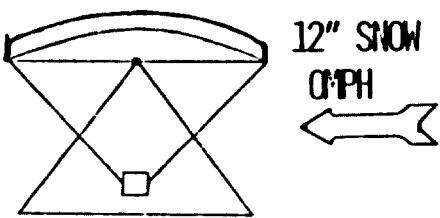
1G VERTICAL
1/4G LATERAL
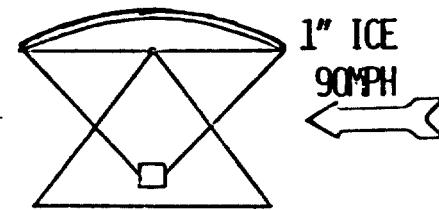
1G VERTICAL
1/4G LATERAL

Figure 6-2. Mount Load Case Configurations

Table 6-2. Load Case Table

PARAMETER \ CASE	I	II	III	IV	V	VI
ORIENTATION	0°	0°	90°	-90°	-90°	-90°
WIND VEL	30MPH	30MPH	30MPH	100MPH	0MPH	100MPH
SEISMIC	---	1g VERT/ 1/4g L	---	1g VERT/ 1/4g L	1g VERT/ 1/4g L	1g VERT/ 1/4g L
DEAD LOAD	---	---	---	---	12" SNOW	1" ICE
P_1	456	286	-1425	-501	---	-2312
P_2	2456	4285	+2574	3498	---	6159

Table 6-3. Mount Attachment Trade-off

LOADS TO BASE FRAME

JOINT	FX	FY	FZ	MX	MY	MZ
1	-1531	-2000	3391			
2	-1531	-2000	-3391			
5	+1584	0	0			

DEFLECTIONS

CASE	JOINT	DEFLECTIONS		
		X	Y	Z
I 6 Wheels (Tens & Comp)	1	-.026	+.052	.190
	2	-.026	-.052	-.190
II Wheels 5, 8 Compression Only	1	-.447	-.161	1.725
	2	-.447	-.161	-1.725
III 3 WHEELS 8,4,6 (Tens & Comp)	1	-.440	-.160	1.725
	2	-.022	-2.351	-4.26
IV Pintle Only	1	-.447	-2.389	6.089
	2	-.447	-2.389	-6.089
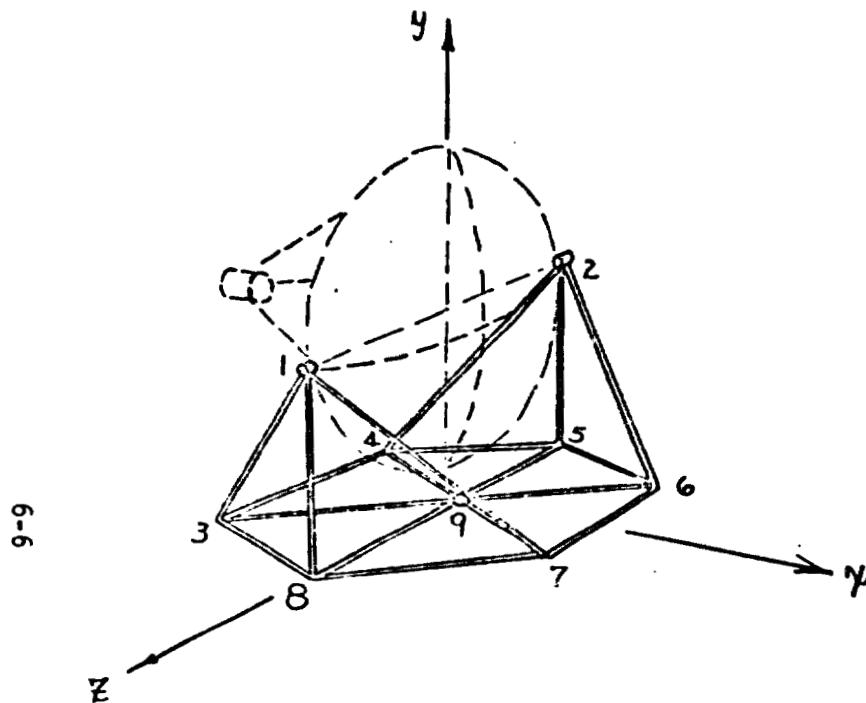
CASE I $I = in^4$

CASES II, III & IV $I = 100 \ in^4$

The above design boundary conditions were inputs to the FEAST code with members having an I_o of 1.0 in^4. The load and component weight were as follows:

- Receiver/Engine wt. - 600 lbs.

- Counter wt. - 600 lbs.

- Aerodynamic drag - 1407 lbs.

- Dish subsystem wt. - 870 lbs.

- Applied 1g vertical 1/4g lateral, simultaneously

The results of the FEAST run are shown in Tables 6-4, 6-5, 6-6 for deflection of member joints, axial loads and vertical attachment forces, respectively. From Table 6-5 the member axial loads were used in conjunction with the AISC code to determine the pipe geometry required to prevent column buckling for fixed end columns under the given loads. Figure 6-3 is an excerpt from the AISC Handbook, seventh edition, and shows that for fixed end conditions, the fixity coefficient is .65. This coefficient was used to calculate $\frac{kl}{r}$ during the member sizing. Members were sized such that $\frac{kl}{r}$ (r is radius of gyration and l is the actual length) ≤ 120. Knowing $\frac{kl}{r}$, the value of F_a is determined by table look-up for $F_y = 36$ksi. For example: with $\frac{kl}{r}$ equal to 110, $F_a = 11.67$ksi.

The allowable buckling load is obtained by multiplying F_a by the pipe metal area corresponding to the r value of the pipe used to calculate (kl/r). F_a is calculated from the formula given in Figure 6-3, item 1.5.1.3.2. This is the Euler column formula corrected for variations in pipe manufacturing tolerances such as pipe or tube bow, variations in wall thickness and pipe concentricity. The AISC code is a conservative design method and therefore other design criteria were studied to understand their effect of pipe size and total weight.

1.5.1.3.2
Compression on the gross section of
axially loaded compression members
when Kl/r exceeds C_c:
Formula (1.5-2)

$$F_a = \frac{12\pi^2 E}{23(Kl/r)^2}$$

Table 1-36

TABLE C 1.8.1

Buckled shape of column is shown by dashed line	(a)	(b)	(c)	(d)	(e)	(f)
Theoretical K value	0.5	0.7	1.0	1.0	2.0	2.0
Recommended design value when ideal conditions are approximated	0.65	0.80	1.2	1.0	2.10	2.0
End condition code	Rotation fixed and translation fixed	Rotation free and translation fixed	Rotation fixed and translation free	Rotation free and translation free		

Figure 6-3. AISC Code Design

Main and Secondary Members
Kl/r not over 120

$\frac{Kl}{r}$	F_a (ksi)	$\frac{Kl}{r}$	F_a (ksi)	$\frac{Kl}{r}$	F_a (ksi)
1	21.56	41	19.11	81	15.24
2	21.52	42	19.03	82	15.13
3	21.48	43	18.95	83	15.02
4	21.44	44	18.86	84	14.90
5	21.39	45	18.78	85	14.79
6	21.35	46	18.70	86	14.67
7	21.30	47	18.61	87	14.56
8	21.25	48	18.53	88	14.44
9	21.21	49	18.44	89	14.32
10	21.16	50	18.35	90	14.20
11	21.10	51	18.26	91	14.09
12	21.05	52	18.17	92	13.97
13	21.00	53	18.08	93	13.84
14	20.95	54	17.99	94	13.72
15	20.89	55	17.90	95	13.60
16	20.83	56	17.81	96	13.48
17	20.78	57	17.71	97	13.35
18	20.72	58	17.62	98	13.23
19	20.66	59	17.53	99	13.10
20	20.60	60	17.43	100	12.98
21	20.54	61	17.33	101	12.85
22	20.48	62	17.24	102	12.72
23	20.41	63	17.14	103	12.59
24	20.35	64	17.04	104	12.47
25	20.28	65	16.94	105	12.33
26	20.22	66	16.84	106	12.20
27	20.15	67	16.74	107	12.07
28	20.08	68	16.64	108	11.94
29	20.01	69	16.53	109	11.81
30	19.94	70	16.43	110	11.67
31	19.87	71	16.33	111	11.54
32	19.80	72	16.22	112	11.40
33	19.73	73	16.12	113	11.26
34	19.65	74	16.01	114	11.13
35	19.58	75	15.90	115	10.99
36	19.50	76	15.79	116	10.85
37	19.42	77	15.69	117	10.71
38	19.35	78	15.58	118	10.57
39	19.27	79	15.47	119	10.43
40	19.19	80	15.36	120	10.28

$F_y = 36$ ksi

Table 6.4

F E A S T

11/1/77

Finite Element Analysis of Structures

Collector Base: .6 Wheels
Bandwidth - 53   0 Passes Required

Results of Load Case I

DEFLECTIONS

JOINT NO.	X (IN)	Y (IN)	Z (IN)	OX (RAD)	OY (RAD)	OZ (RAD)
1	-1.487E-02	-1.608E-02	3.795E-02	3.026E-04	-2.768E-05	6.748E-05
3	-3.081E-03	0.	-1.123E-03	5.652E-05	-2.188E-05	1.057E-05
8	-4.104E-03	0.	-3.148E-04	6.696E-05	-2.093E-05	1.942E-05
7	-3.682E-03	0.	1.379E-03	4.753E-05	-9.514E-06	-2.866E-06
4	-3.018E-03	0.	1.123E-03	-5.652E-05	2.188E-05	1.057E-05
9	0.	0.	0.	0.	0.	0.
6	-3.682E-03	0.	-1.379E-03	-4.753E-05	9.514E-06	-2.865E-06
2	-1.487E-02	-1.608E-02	-3.795E-02	-3.026E-04	2.768E-05	6.748E-05
5	-4.104E-03	0.	3.148E-04	-6696E-05	2.093E-05	1.942E-05
10	6.138E-03	-1.490E-02	0.	0.	0.	-8.975E-04

Table 6-5. Member Axial Loads

	MEMBER	AXIAL LOAD-LBS		MEMBER	AXIAL LOAD-LBS
FRAME 1	1-3	557	FRAME 2	2-4	557
	1-8	2394		2-5	2394
	1-7	1021		2-6	1021
	3-4	485		3-9	455
	4-5	104		4-9	455
	5-6	104		5-9	63
	6-7	595		6-9	539
	7-8	104		7-9	539
	8-3	104		8-9	68

Table 6-6. Forces of Attachments

JOINT NO.	FX (LB)	FY (LB)	FZ (LB)	MX (IN-LB)	MY (IN-LB)	MZ (IN-LB)
1	-8.615E-02	-2.039E 03	-7.629E-06	-5.603E-06	1.192E-06	-3.010E-06
3	-1.144E-05	4.193E 02	7.629E-06	-7.379E-04	-3.445E-04	9.537E-04
8	-4.753E-06	2.390E 03	5.722E-06	4.268E-04	-4.945E-04	1.490E-07
7	3.815E-05	-7.687E 02	1.1442E-05	6.969E-04	1.446E-03	-1.219E-03
4	0.	4.193E 02	1.907E-06	-1.919E-04	7.713E-05	-1.419E-03
9	1.523E 03	-2.434E 00	-4.768E-06	6.773E-04	3.324E-04	2.003E-03
6	0.	-7.687E 02	3.815E-06	2.308E-04	-3.428E-04	1.151E-03
2	-8.615E 02	-2.039E 03	-7.629E-06	7.749E-06	-4.768E-07	-1.818E-06
5	3.353E-08	2.390E 03	-6.676E-06	-4.268E-04	7.701E-05	1.192E-07
10	2.000E 02	-2.809E-06	0.	0.	0.	6.886E-05

Table 6-7 is a structural weight summary showing the effect of different design criteria. The first column shows member weights based on code requirements $\frac{kl}{r} < 120$ and $F_a = \frac{12 \; \pi^2 E}{23 \left(\frac{kl}{r}\right)^2}$ with the load determined from the simultaneous applicaton of wind, weight, and seismic. The second column shows member weights obtained by using a higher F_a. The larger F_a was justified based on fabricating tube from steel sheet and drawing them over a mandrel in the projects own pipe factory. In this way, there is better control over the manufacturing tolerance and a higher F_a based on tighter tolerances, is justified. It appears that a maximum of about 220 lbs. could be removed from the member weights depending on the design criteria and loading requirements. For the purpose of this study, the members sized in column one are recommended and shown in Figures 6-4 and 6-5.

During the detailed design phase, it will be important to reassess some of the decisions made during this preliminary design in the areas of mount member configuration, internal rib geometry, dish support span and the number of mount-foundation attachment points. While this additional work may result in more members and a slightly different mount configuration, the results could be a lighter more efficient structure with more stable sections.

Table 6-7. Structural Weight Summary

MEMBER	DESIGN CRITERIA			
	AISC 1g VERT 1/4g LAT	CLOSE TOLER 1g VERT 1/4gLAT	AISC NO SEISMIC	CLOSE TOLER NO SEISMIC
1. TRUSS	318.4	265	266	162
2. RING	111.0	88.8	111.5	76.9
3. SPOKES	111.0	88.8	111.5	76.9
	540.4	442.6	489.0	315.8
4. INTERNAL RIBS (ALUM)	156.0	---	---	---
5. ELEVATION DRIVE FRAME	130.0	---	---	---
6. RECEIVER SUPPORT MEMBERS	243.7	---	---	---
	529.7			
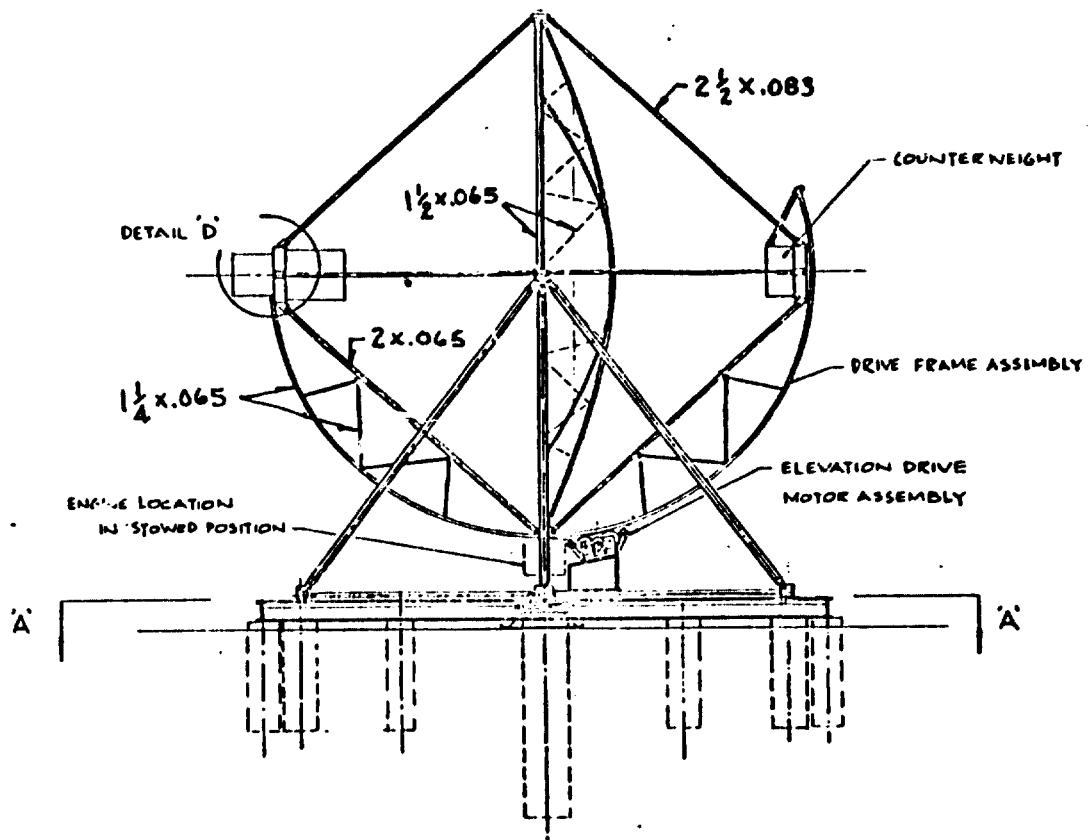
Figure 6-4. Frame Member Sizes

DETAIL 'E'

3.5x.083

3x.083

SEE DETAIL C

'B'

MOUNT

AZIMUTH DR
MOTOR ASSEI

SEE SHEET 2

'B'

AZIMUTH POSITION
SENSOR

PINTLE BEARING
ASSEMBLY

ELEVATION DRIVE
MOTOR (REF)

AZIMUTH DRIVE
MOTOR (REF)

2x.065

VIEW 'B-B'

SHOWING LATERAL MOUNT
MEMBERS & PINTLE BEARING HOUSING.
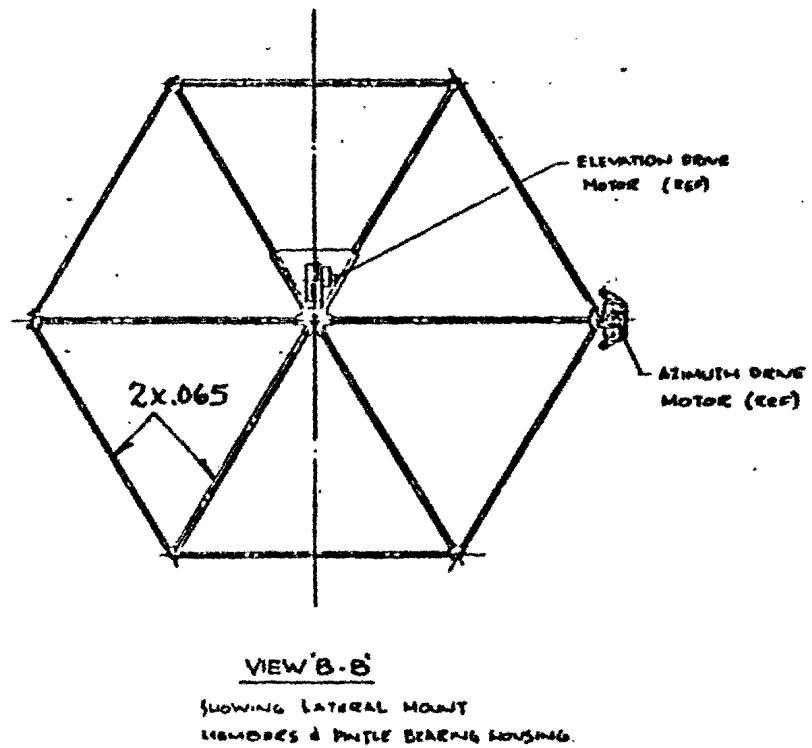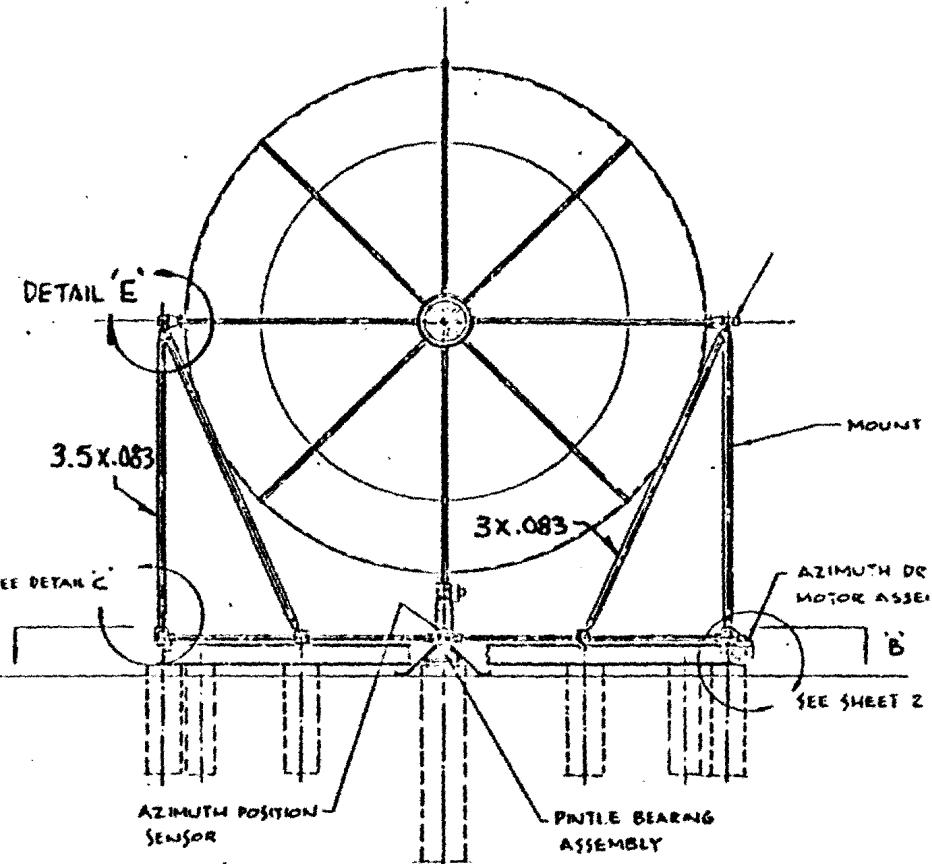
Figure 6-5.   Mount Member Sizes

SECTION 7.0

DRIVE SUBSYSTEM

7.0 DRIVE SUBSYSTEM

7.1 Drive Requirements

The drive subsystem serves to maintain the collector in proper alignment for maximum energy collection. As such, it must have provision for sun tracking in azimuth and elevation, with an error of $\pm$ 1/8° max. The drive must accomplish two other functions - return the dish to the starting position after sunset and per- form a rapid defocusing at the rate of 1/2 deg/sec. Tracking rates in elevation are .002-.02 degrees per second and .00417 degrees per second (max) in azimuth. Additionally, the drive must exhibit a sufficiently high stiffness and driving torque to meet the accuracy requirements under gust load conditions.

Drive cost was set at $1.0/ft^2 as a goal.

7.2 Drive Options Studied

From a variety of past and current studies, GE gained an insight into the suitability of a range of drives in specific solar collector applications. These range from direct drives through a large diameter sector gear about the elevation and azimuth axes to clock drives mounted directly on the axis driven. Consistent with the goal of a low-cost drive, the choice was narrowed down to three candidate systems: Motorized Screw Jack, Friction Drive, and Cable and Drum. Table 7-1 summarizes the salient features of the three drives. The motorized screw jack is driven by an electric motor whose output speed was reduced by means of a worm and pinion gear box. The linear motion of the jack screw is converted to angular motion by means of a bell crank. This limits the angle to far less than the 180° required for the azimuth. To extend the angular range, a second screw jack is added in series with the first. Although in all other respects the motorized screw jack meets design requirements, the complexity and high cost of a tandem arrangement make this drive unattractive.

Table 7-1. Drive Options Studied

APPROACH	ADVANTAGES	DISADVANTAGES	COST
MOTORIZED SCREW JACK	• OFF-THE-SHELF • TC-600 EXPERIENCE • PROVEN ENVIRONMENTAL OPERATION	• PRECISION MECHANISM • TRAVEL LIMITATIONS • COST	$600/AXIS
FRICTION DRIVE	• SIMPLE DESIGN WITH MINIMUM PARTS	• REQUIRES STIFF ACCURATE STRUCTURE AND LARGE CONTACT FORCES TO MEET STIFFNESS REQUIREMENTS	$300/AXIS
CABLE AND DRUM	• COMPATIBLE WITH MOUNT • UNSOPHISTICATED COMPONENTS • PROVEN DESIGN • ALLOWS LOOSE TOLERANCES • HIGH STIFFNESS	ENVIRONMENTAL OPERATION TO BE DETERMINED IN THIS APPLICATION	$206/AXIS

CABLE AND DRUM DRIVE SELECTED FOR PRELIMINARY DESIGN

An alternate approach was to use geared down electric motors whose output shafts drive friction wheels that ride on circular tracks running about the perimeter of the dish azimuth and elevation axes, respectively; this is a gear drive without the expense of cutting gears on the driving and driven gears. As the table shows, this approach is much more cost effective than the screw jack but requires high strength track surfaces to maintain high tangential force without slipping. This structure and drive mounts accordingly have to be stiffened leading to increased cost.

The selected drive uses an aircraft cable wrapped about a gear motor-driven capstan to provide the driving force. The cables are attached at either end to the circular drive structure. As the motor-driven capstan (on the stationary frame) rotates, the cable pulls the collector frame along as it passes over the capstan. Tensioning pulleys on either side of the capstan assure that proper friction forces are maintained between the cable and capstan to provide the required driving torque.

7.3 Drive Subsystem Description

The primary drive motor is a Von Weise Gear Company Model VW47 geared down to yield 2 RPM at the output shaft. The motor, in turn, drives a pair of capstans arranged as shown in Figure 7-1 Drive Subsystem Mechanism. The need for two capstans arose from the fact that a cable wrapped 360° about a single capstan tends to ride up on the adjoining strands and jam the drive. By using two capstans, the cable can be so wrapped that no physical contact between the adjoining strands occurs. Since both capstans are motor driven, the torque produced is sufficient to meet drive requirements. Bearings, cables, sprockets, shafts and chains are all off-the-shelf hardware. The only non-commercial elements are the capstan and support structure - both simple and cheap to design and
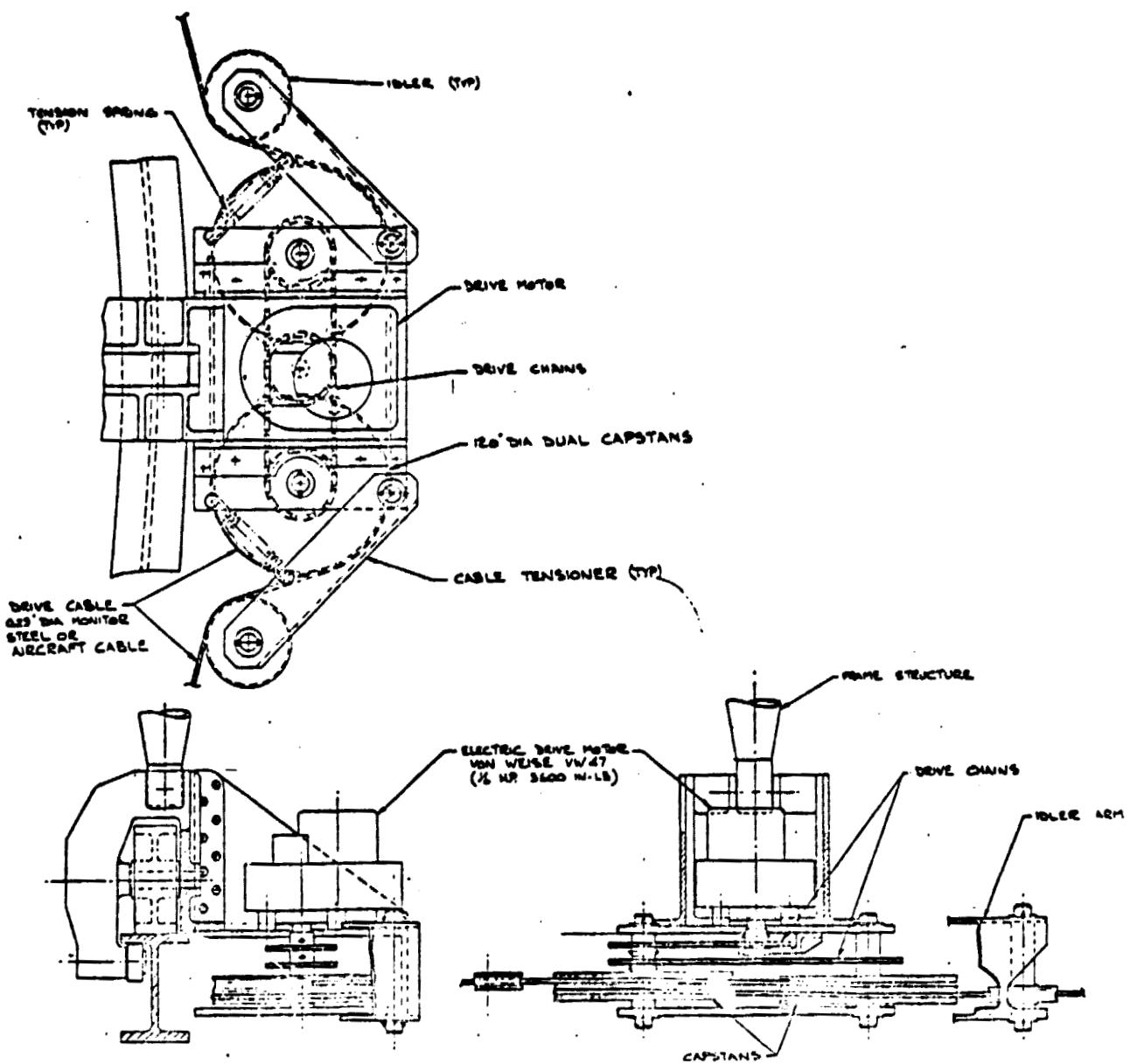
Figure 7-1. Drive Subsystem Mechanism

manufacture. To prevent back-driving, the drive motor contains a solenoid operated friction brake. The driving motor is 1/6 HP, permanent split capacitor, yielding 6000 in-lbs of torque at the output shaft. The driving rate at the dish will be 1/2°/second, dictated by the defocusing requirement. In the tracking mode where rates vary between .002 and .02 degrees/second, but the driving rate is 1/2 degree/second, the motor will be pulsed at a duty cycle consistent with pointing error requirements. With an error band of 2 x .1 degrees, a power pulse of $\frac{.2 \text{ degrees}}{.5 \text{ deg/sec.}}$ = .4 seconds will drive the dish through the width of the error band. At a sun rate of .002 degrees per second, it will take 100 seconds "off" time before the next pulse needs to be applied. At sun rates of .02 degrees/second, the "off" time will be 10 seconds. In any event, this is a low duty cycle and very well suited for the selected motor. During return to the morning position, the motor will be run continuously for $\frac{180 \text{ degrees}}{0.5 \text{ deg/sec.}}$ = 360 seconds or six minutes. To promote heat dissipation in the contiguous drive mode, the motor is fan cooled. Bearings, chains and sprockets have been selected for 20 year life under one daily back and forth excursion cycle. The cable selected is aircraft quality capable of 100,000 bending cycles over the capstan diameter. This offers a large margin compared with the expected bending cycles due to daily operation. Similarly, the cable diameter of 0.29 inches assures a drive angular stiffness which is three times higher than that required for pointing accuracy. Under worst case gust condition, the cable strength offers a safety factor of 5:1. It should be noted that only inertia, friction and aerodynamic forces need to be overcome by the drive, since the dish will be counter-balanced to avoid any unbalanced torques.

7.4 Drive Subsystem Specification

Table 7-2 summarizes the salient performance requirements based on dynamic, environmental, and cost considerations.

Table 7-2. Specification Summary

- Two-Axis Drive -- 1/2 Deg/Sec Continuous
- Drip Proof Enclosure, Fan-Cooled Motor
- Brake on Motor to Prevent Back-Driving
- Permanently Lubricated Bearings
- Commercially Available Hardware
- Unattended Operation - Minimum Maintenance
- 2 RPM, 3600 In-Lbs Torque at Motor
- System Stiffness 0.35×10^6 Ft-Lb/Rad
- 4:1 Safety Factor
- 20 Year Life
- Typical Duty Cycle Tracking 1/2 Sec "On" - 50 Sec "Off"
- Power Consumption Not to Exceed 0.2 KWHR/Day/Axis

7.5 Drive Subsystem Cost Summary

The low cost drive design concept benefits from the 20:1 gear reduction in-herent in the arrangement of the drive frame for the elevation drive and the foundation rail which serves also as the drive frame for the azimuth drive. This allows the use of a low-cost "off-the-shelf" gear motor with a 900:1 ratio. The drum mechanism is a fabricated steel weldment fitted with simple capstans, pulleys, shafts, springs, sleeve bearings, sprockets and chain which are stock items and available in mass-produced quantities. The cable is also a stock item available pre-stretched to the required specification at low cost. For a summary of drive subsystem costs (both drives identical), see Table 7-3.

Table 7-3. Drive Subsystem Cost Summary

- Cable $ 5.00
- Drum Mechanism   96.00
- Sprockets   15.00
- Gear Motor   65.00 (See Appendix B for Estimate from Von Wiese Gear Company)
- Track   __25.00__
                 $206.C0/Axis ⟹ $0.50/Ft^2/Axis

SECTION 8.0

CONTROL SUBSYSTEM

8.0 CONTROL SUBSYSTEM

The principal function of the control subsystem is to point the concentrator at the sun as accurately as possible. The requirements placed on the control subsystem are outlined in Table 8-1, and the major subsystem components are shown in Figure 8-1.

Under a central computer control, the system operates totally automatically utilizing potentiometers for coarse tracking and a fiber-optic closed-loop system for fine positioning, also, on-site manual control has been provided to override the computer control.

An emergency power system for defocus of the concentrator under a condition of a power failure has been incorporated into the design. The source for the defocus power comes from the receiver/engine assembly. A thermal log capacity which would completely remove the focused image from the receiver is the necessary requirement to enable its use in this mode.

In the design of the subsystem, special attention has been focused on lightning protection. Special devices and circuitry have been incorporated to achieve a degree of lightning protection.

8.1 Sun-Tracking Mode

Algorithms are built into the central computer which are used to calculate ephemeris data. The concentrator is pointed toward the sun via a closed-loop control system which utilizes potentiometer position sensors. Ephemeris data indicates where the sun should be at each instant in time and the position potentiometers indicate where the concentrator is actually pointing. Control logic will compare the ephemeris data with the position sensor data and generate the appropriate motor control signals to keep the dish pointing at the sun with an accuracy of ± 1 degree in both azimuth and elevation.
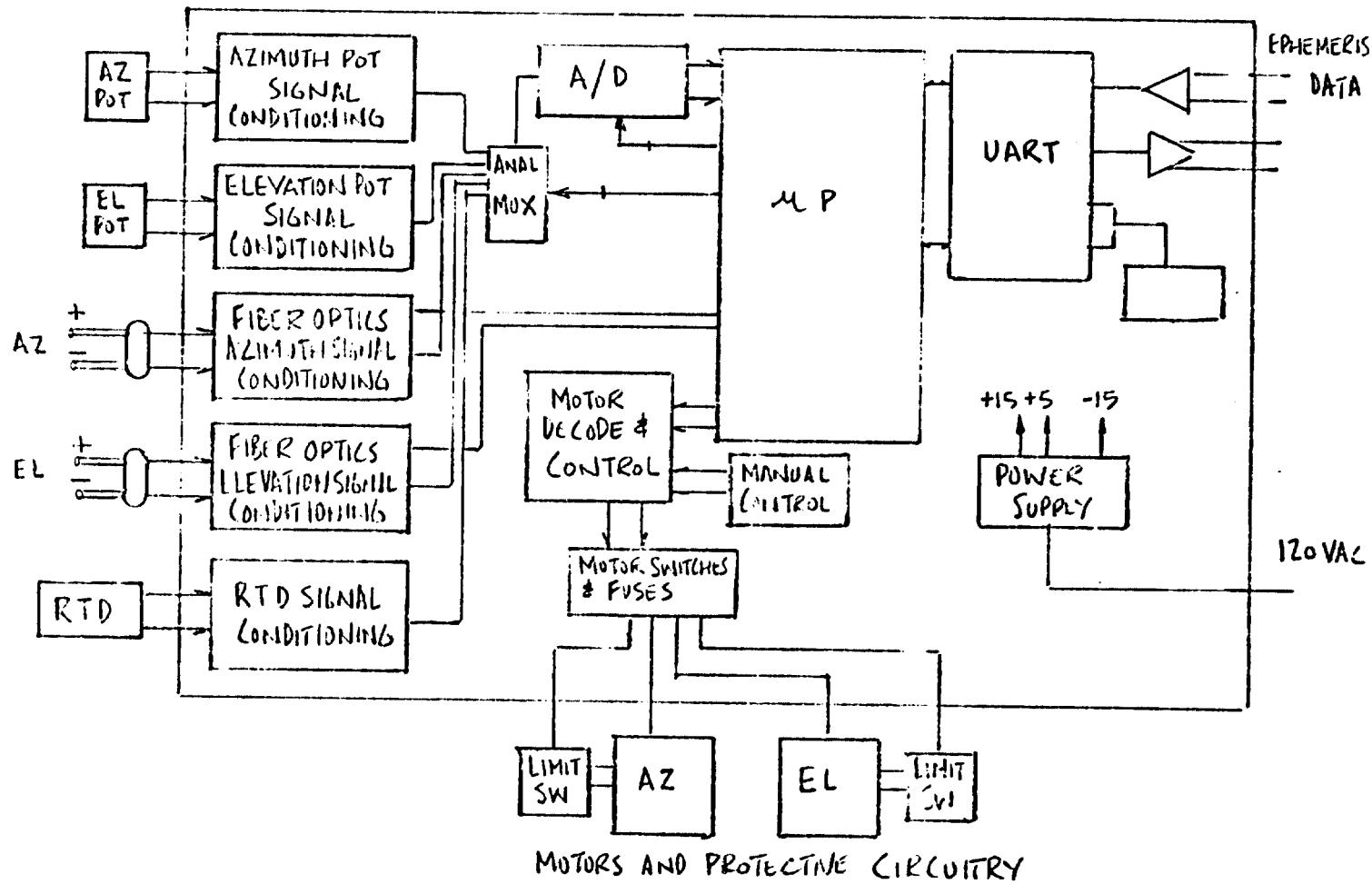
Figure 8-1. Control Description

Table 8-1. Controls/Electrical Subsystem Requirements

Sun Tracking - Coarse	Achieve coarse sun tracking of ± 1° in both azimuth and elevation Absolute sun position using programmed ephemeris data Feedback: Potentiometer Control: Azimuth and elevation drive motors
Sun Tracking - Fine	Achieve fine sun tracking of ± 1/8° accuracy in both azimuth and elevation Absolute focused sun image using fiber optics Feedback: Optical sensor Controls: Drive motors
Non-Tracking	Provide for stowing concentrator for: Night time, Maintenance, inclement weather Provide high speed defocus on overtemperature using receiver mounted RTD

Additional accuracy is required to properly focus the system and this control is implemented through sun sensors. Two pairs of fiber optics operate as the sun sensors so that for any misalignment differential signals representing azimuth or elevation are provided to the conditioning electronics. These signals are processed by the microprocessor to affect the appropriate motor control.

In the morning, the concentrator begins to track the sun via ephemeris start-up data. When sufficient solar insolation is available, an automatic switch from potentiometer to optical tracking will occur. At sunset, the concentrator will be returned to a stow position.

This hybrid control system was chosen because it is a cost-effective system which provides the high degree of tracking accuracy required. Potentiometers are in standard use in servo-position controls but

cannot supply the accuracy required. Fiber optics were chosen for fine tuning on the basis of prototype development on the GE TC-600 collector. Tables 8-2 through 8-4 present a summary of the sun-tracking mode.

8.2 Central Computer

The central computer handles a minimal amount of signal processing due to the capabilities of the local microprocessor. The control functions performed by the central computer are shown in Table 8-5. All concentrator/computer command signals will be processed via command protocol at RS-422 signal levels. This scheme greatly minimizes the complexity of the electronics and the wiring between the central computer and the concentrator.

This scheme of local microprosessor/control computer allows a great deal of flexibility to be built into the system. It frees the central computer from excessive data processing while allowing for localized control of a series of concentrators.

Table 8-2. Sun Tracker Sensor

```
Dual Mode
      - Coarse point computer data
      - Fine point optical sensing
Acquisition by computer data
      - Accuracy ± .125°
Automatic switch on acquisition (computer to tracker mode)
Supervisory control available thru ephemeris data
Local control through mount electronics box
```

Table 8-3. Computer Data Mode

- Command Signals Generated by Central Computer
- Command Signal sent to Concentrator
- Feedback Pots on Azimuth and Elevation Axis
- Pot Position Digitized and Compared to Command Signal
- Error Signal Generated for Appropriate Axis and Direction
- Update Command Sequenced at Microprocessor Level

Table 8-4. Optical Sensing Mode

- Silicon Photo Diodes used as Detectors Aligned with Axes
- View Wings of Reflected Image at Focal Plane
- Sense Image Shift thru Imbalance of Flux Level
- Generate Error Signal from Difference Signal
- Update Command Sequenced at Microprocessor Level
- Fiber Optics Coupling/Electronics Box Mounted on Receiver

Table 8-5. Functions of the Central Computer

- Generate Ephemeris Data
- Generate Start-up and Nighttime Stow Data
- Provide Emergency Stow Signal
- Process Over-Temperature Defocus Notification Signal

Table 8-6. Functions of Local Microprocessor

- Process and Compare Ephemeris Data with Potentiometer Data
- Process Fiber Optic Data
- Effect Proper Motor Control Signals
- Process Start-up and Stow Signals
- Defocus Concentrator on Over-Temperature Condition
- Process Emergency Stow Signal

8.3 Control Electronics

The electronics for an operational concentrator are shown in Figure 8-2. The system incorporates inexpensive integrated circuits and discrete logic for signal conditioning. Signal processing is implemented through a microprocessor which was chosen for the reason that it represents an excellent compromise between minimum cost and maximum flexibility. It frees the central computer from excessive data processing; it allows the experimental flexibilities to be built into the prototype system; and finally, the technology in this area is developing so rapidly that implementation on such a large scale with the specialized microprocessor unit appears to be very cost effective. The control functions performed by the microprocessor are shown in Table 8-6.

Coarse positioning control of the concentrator is actuated through axes-mounted potentiometers. A conditioned voltage signal corresponding to the position of the axis will be converted through an A/D converter before being processed by the microprocessor. A comparison will be made with the ephemeris data sent to the microprocessor from the central computer. Appropriate motor control signals will then be generated. Automatic switchover to optical tracking will occur whenever a determined threshold level is achieved. Similarly, a drop below this level will turn control back over to the servo-loop.

8-6
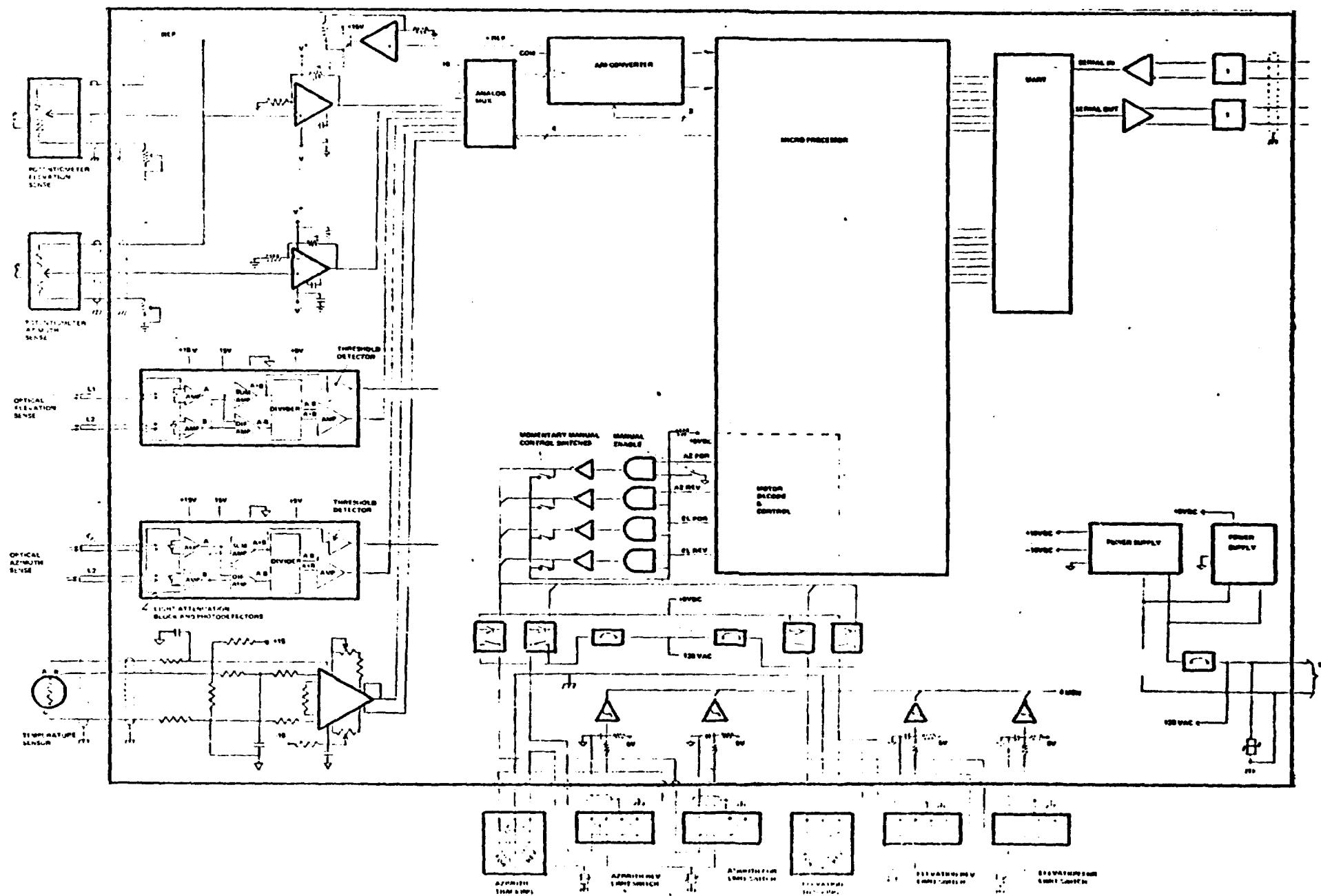
Figure 8-2. Concentrator Electronics

Fine position control will be achieved through fiber optic light sensing. Two fiber optic pairs will be aligned with the axes of rotation of the system such that a differential signal will arise when an imbalance in the energy intensity distribution exists. The signal will be received through fiber-optic channels and properly attenuated previous to diode sensing and conversion to an electrical signal. The detected signal will be amplified and processed through summation and difference amplifiers incorporated with a divider network. This will enable flux sensing independent of solar intensity. As long as the minimal threshold level of detection is achieved, the control electronics will operate in the sun sensing mode with the output voltage proportional to the error angle. This signal will then undergo A/D conversion before being processed by the microprocessor. Appropriate motor control signals will then be generated. There are two pairs of fiber optic position sensors; one for azimuth and one pair for elevation. They will be mounted at the focal plane perpendicular to the axis they will control. At levels below the threshold, the potentiometers will actuate control.

The receiver will have an RTD located in it to sense for an over-temperature condition. Threshold detection will occur when the over-temperature state is reached. This signal will be processed through the microprocessor and the elevation motor will be activated to effect an emergency defocus. Simultaneously, the control computer will be informed of the alarm condition.

The motor decode and control circuitry accepts information from the microprocessor to affect appropriate motor operation. Included in the design are limiting switches to sense the end of the motors traversal for automatic shutoff. Lightning protection has been incorporated into the wiring for the motors. Manual control has been designed into the motor control circuitry. The manual

signal overrides the microprocessor control signals.

8.4 Controls Cost Summary

Using the circuitry described in Paragraph 8-3, vendor contacts were made and cost estimates were generated for the control subsystems. The production costs presented in Table 8-7 reflect mass production levels where considerable parts consolidation has been achieved by using functional chips. The costs of prototypes would reflect hand wiring of many components.

Table 8-7. Controls/Electronics Cost Summary

FUNCTIONAL BLOCK	MAJOR COMPONENTS	PRODUCTION COST, $
Potentiometer Position OP AMPS Sensing	Potentiometers OP AMPS Circuitry	40
Fiber Optic Position Sensing	Fiber Optic Cables of 5' Length OP AMPS Analog Dividers Threshold Detectors Silicon Photo Diodes Light Attenuation Blocks Circuitry	65

Motor Switching
    Circuitry
    and
    Protection
	Relays
	Microswitches
	Circuitry
		75

Data Transmit and Receiver	Receiver Transmitter Band Rate Generator UART Circuitry	25
Microcomputer System	Example; 8049 - INTEL Complete System	10

Table 8-7. Controls/Electronics Cost Summary (cont.)

FUNCTIONAL BLOCK	MAJOR COMPONENTS	PRODUCTION COST, $
Analog Signal Conversion	A/D Converter MUX Switch	35
Housing	Electronics Box Unit Connectors etc. 2 P.C. Boards Misc.	20
Other	Power Supply	40

Controls/Electronics - $310
Production Cost

SECTION 9.0

FOUNDATION SUBSYSTEM

9.0 FOUNDATION SUBSYSTEM

The foundation subsystem consists of the rail assembly and the rail supports. The concept that has been used throughout the latter portion of this study was that the mount was attached to the rail assembly through a wheel casting capable of both up and down load as shown in Figure 9-1. The design of the rail assembly and subsequent foundations to support it, complied with the requirements listed below:

- Rail assembly must support the weight and live loads of the dish and support structure.
- The foundation members must not fail, pull-out, sink or rotate under applied loading.
- Foundation design must be compatible with 2000 lbs/ft^2 soil bearing allowable.
- Foundation design must penetrate below frost line.
- Rail assembly design per AISC Code.

For the rail assembly, A36 steel was used during the design development. Sizing of the rail also involved picking the number of pilings since that determined the beam span and offset. Figure 9-2 shows a summary of the method of analysis used to size the rail. The worst case loading condition is with the maximum down load of 2390 lbs. applied to midspan between supports.

Beam stresses in both torsion and bending were determined using the equations shown and the geometry for a 6 pile design and a 12 pile design.

With a 4 inch wide flange beam required, the 6 pile design has shear stresses in excess of the allowables set forth in the AISC Code for A36 steel. However, the 12 pile design yielded a 12W22 as meeting the requirements and was chosen along with 12 supports as the preliminary design for the rail assembly.
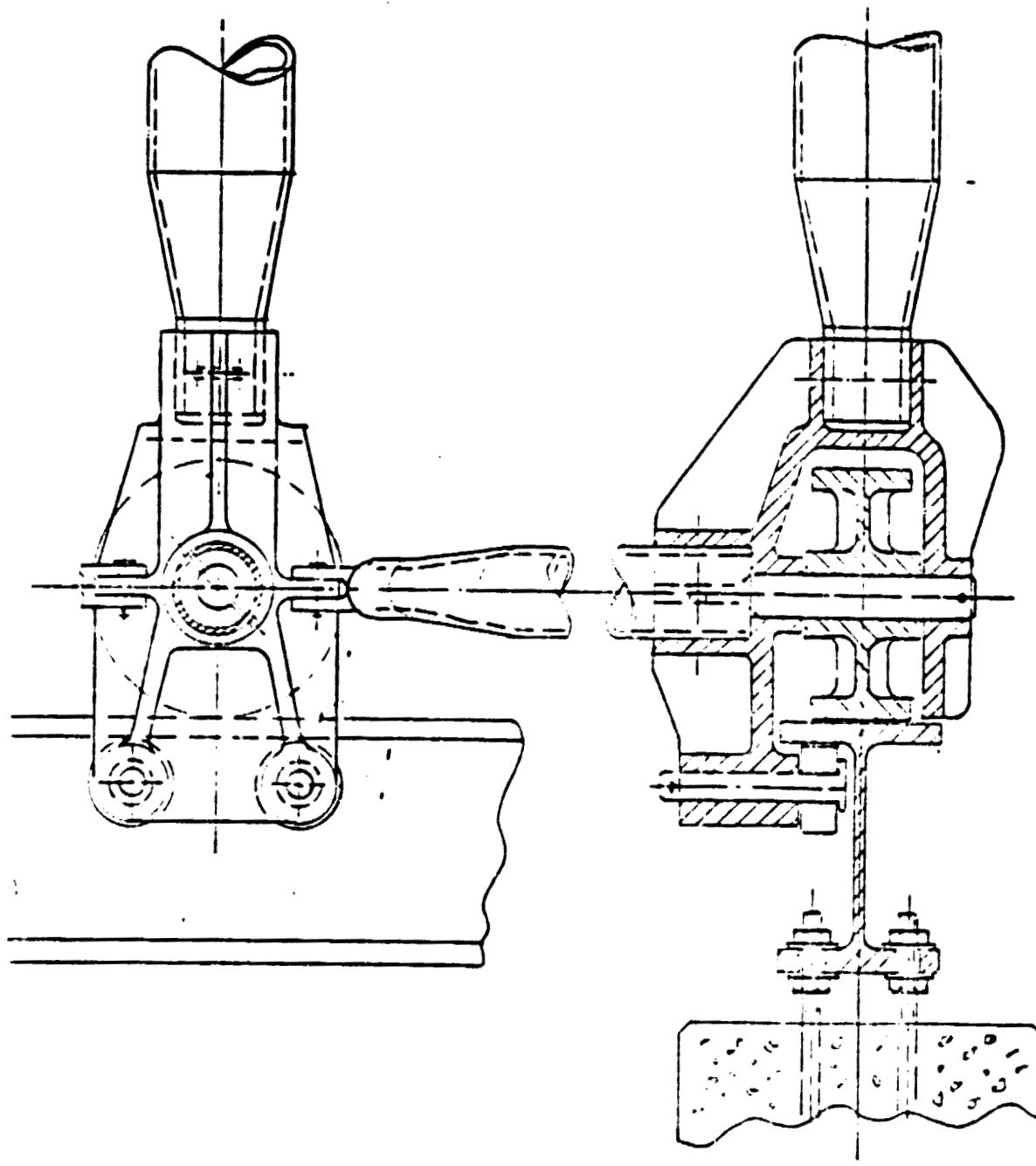
Figure 9-1. Detail C - Wheel Fitting

P=2390 lbs.

18.4"

60°

6 Piles (139" span)

P=2390 lbs.

4.7"=L

30°
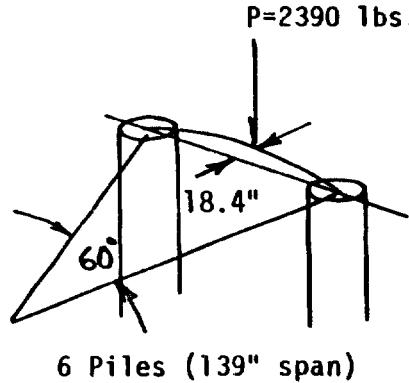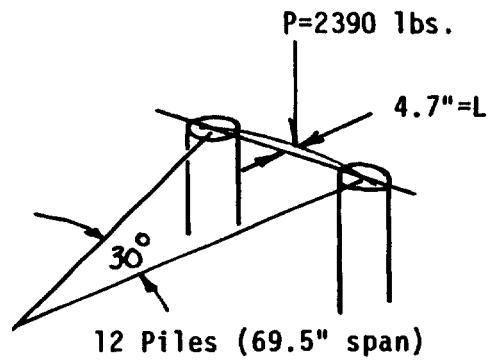
12 Piles (69.5" span)

4" Flange Desired

4"

SHEAR

$$f_s = \frac{3T}{dt^2}$$

BENDING

$$f_b = \frac{M}{S}$$

Design: 12W22 with 12 Piles
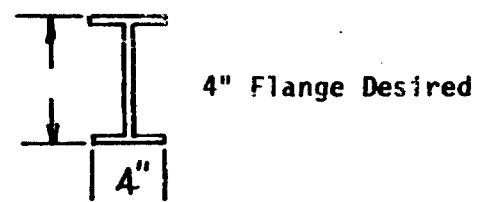
Total Rail Weight = 1601 lbs.

$$T = \frac{2390\ H}{2}\ (\text{in lbs})$$

$$M = \frac{2390 \times \text{Span}}{2}$$

6 Pile Design $\quad f_s > .6\ f_y\Big/F_v \quad$ All Sections

12 Pile Design $\quad f_s = .365\ f_y\Big/F_v \quad$ 12W22

Figure 9-2. Rail Assembly Design

12 PILE CONFIGURATION

1.5'

3/4"

6' ABOVE
GRADE

L = 4.25'

UNDISTURBED
9" SOIL LINE

L_A
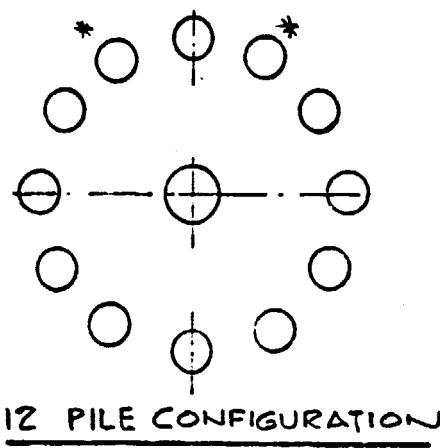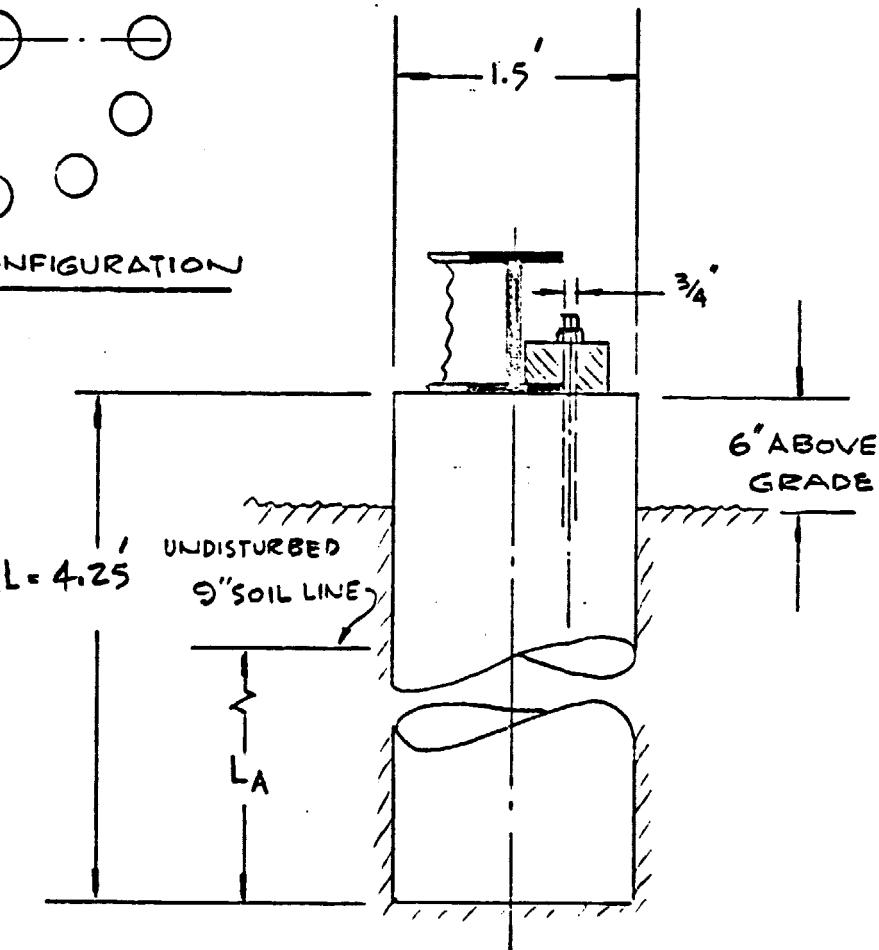
Figure 9-3. Pile Geometry

Next, the pilings were sized to meet both down and upload capability. As it turned out, the down load or soil bearing sized the piling diameter while the depth was determined by frost line, rotation or pullout requirements. For instance, the 12 pilings that support the rail assembly have a diameter of 1.5 feet. This was determined by equating the down load to the soil bearing capacity for a piling of diameter, D, as follows:

Down load - 2390 lbs.

Soil bearing pressure - 2000 lbs/ft^2

Soil bearing capacity = 2000 $\frac{lbs}{ft^2}$ x $\frac{\pi}{4}$ D^2

Equating capacity to applied load and solving for D is:

$$D = \left(\frac{2390}{200} \frac{4}{\pi}\right)^{1/2} = 1.23' \implies 1.5'$$

Pullout of the pilings for the rail assembly supports determine their length. The active pullout length was assumed to start 9.0 inches below undisturbed soil. The soil pullout shear value was assumed to be 125 lbs/ft^2* for soil bearing of 2000 lbs/ft^2. Further, the total pullout load was calculated as the sum of the pile weight and skin friction.

Considering an active piling below each of two wheels shown in Figure 9-3.

Pile Shear = π D L$_A$ x 125 lbs/ft^2

D = 1.5'   Assume L$_A$ = 3 ft. min.

Total Pullout = wt$_{pile}$ + Shear

$$= \frac{\pi}{4} D^2 L \mathcal{C}_c + \pi D L_A \times 125 \text{ lbs/ft}^2$$

P = 2968 lbs.

---

*Estimated from known soil analysis for Shenandoah of 4000 lb/ft^2 soil bearing and shear of 250 lb/ft^2.

The pintle is designed to support its own weight without sinking and not rotate under the applied loads. Sizing of the pintle is an iterative process started by calculating a soil bearing diameter based on an assumed length. Next, using the analysis proposed by Czernick, Figures 9-4 and 9-5, calculate the required pile length to resist the applied moment of 2003 in-lbs and a shear of 1583 lbs denoted by M and H, respectively in Figure 9-4. Having determined the length, recalculate the pile weight and see if it is consistent with the soil bearing diameter. If it is, then L is a solution. For D = 2 feet, H = 1583 lbs., M = 2003 in-lbs, it was determined that the required length was 10 feet for the pintle.

An alternate foundation design approach examined briefly was the driven piling. However, beside the pile driver, a cut-off torch or saw would be required to remove the excess length allowed for deformation. Further, driven pilings would require greater length to compensate for lost soil bearing in the cross-section. This concept was discarded on cost, but may have future application advantages that would require it to be reconsidered.

Finally, the extrapolation of the 12 pile design to a continuous foundation was examined on cost. Table 9-1 summarizes the results of this comparison. Based on an assumption that the minimum depth of a foundation is three feet below grade for frost line protection, the continuous foundation, with a lightweight 4 inch flange section 8W10, is more expensive than the 12 pile concept.

The pilings as determined in this study would, of course, be reinforced concrete pilings with tied-in anchor bolts for attaching the rail assembly.

D
M
H

VARIES*

FINISHED GRADS

RESISTING SURFACE

SOIL PRESSURE

DEFLECTED
SHAPE

R #/FT^2/FT
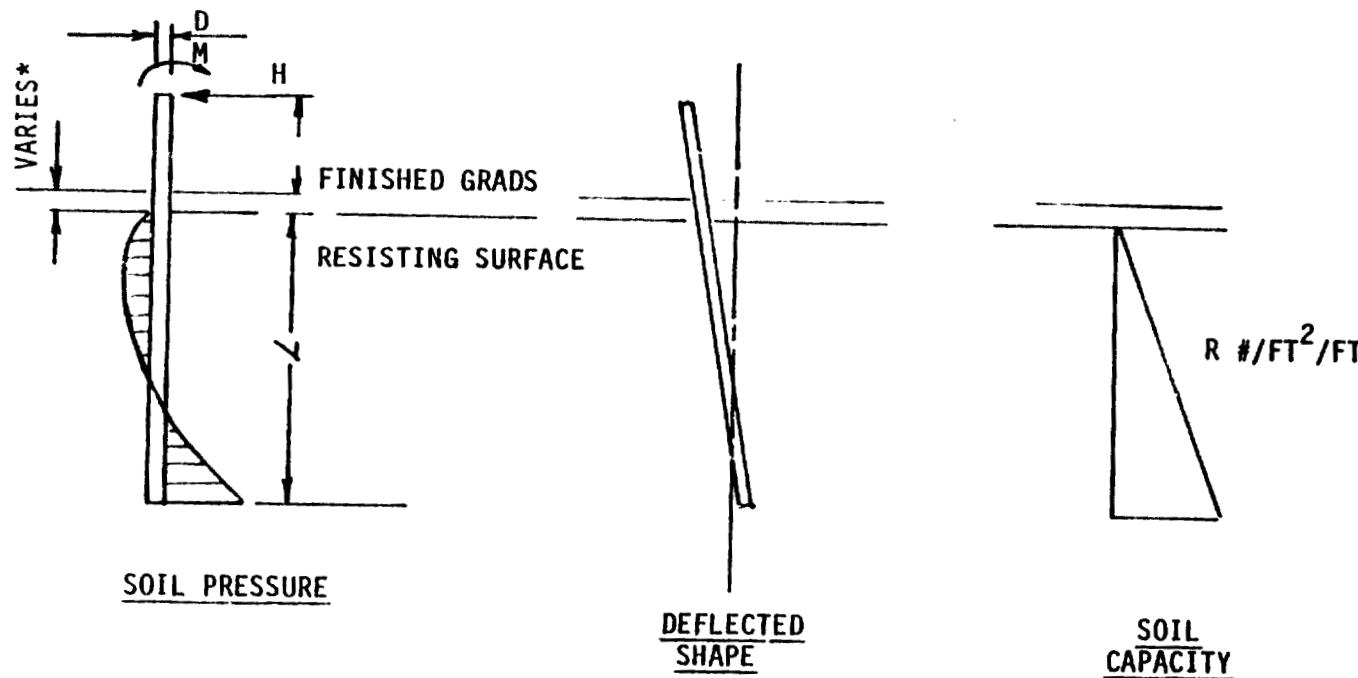
SOIL
CAPACITY

* Czerniak Suggests 1 - 2 Feet

Figure 9-4. Pintle Foundation Analysis

EMBEDDED LENGTH (L)

$$L^3 - 9\frac{H_oL}{R} - 12\frac{M_o}{R} = 0 \quad \left|\text{Square Pile}\right|$$

Where $\quad H_o = \frac{H}{D} \; ; \; M_o = \frac{H \times E^1}{D} \quad$ R = Soil Capacity
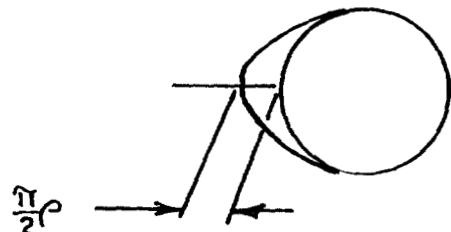
SHAPE FACTOR

Soil Pressure assumed Cosine Distributed
Function Results in Soil Pressure
Times Average Soil Pressure

$$L^3 - 14.14\frac{H_oL}{R} - 18.85\frac{M_o}{R} = 0 \quad \left|\text{Round Pile}\right|$$

$E^1 = \frac{ExH \pm M}{H} \quad$ Where M - Applied Moment at Top of Pile

Figure 9-5. Pintle Foundation Analysis

Table 9-1. Foundation Cost Trade-Off

- CONTINUOUS RING FOUNDATION 3.5' x DX1' with 8W10

  <u>CONCRETE</u>

$$\text{COST} = \text{Volume} \times \$/\text{Yd}^3 = \frac{\varPi DLt}{27} \times \$100/\text{yd}^3 = \qquad 943$$

  <u>RAIL</u>

$$\text{COST} = \text{Lbs/Ft} \times \text{Ft} \times \$/\text{Lb} = 10\pi D \times .30 \ \$/\text{lb} = \frac{218}{1161}$$

- 12 PILES + RAIL ASSEMBLY

  <u>CONCRETE</u>

$$\text{COST} = \text{Volume} \times \$/\text{Yd}^3 = \frac{12}{27} \times \frac{\varPi D^2}{4} L \times \$100/\text{yd}^3 = \quad 333$$

  <u>RAIL</u>

$$\text{COST} = \text{Lbs/Ft} \times \text{Ft} \times \$/\text{Lb} = 22 \times \varPi D \times .30 \ \$/\text{lb} = \frac{480}{813}$$

SECTION 10.0

ASSEMBLY/MAINTENANCE

10.0 ASSEMBLY/MAINTENANCE

10.1 Assembly Requirements

The impracticality of shipping factory assembled collectors leads to the requirement for field assembly; because this will be labor intensive, it is necessary to provide for an assembly technique requiring minimum time and skills in the field. Therefore, the major elements of the collector, namely, the dish. assembly, mount, and foundation have been broken down into piece parts and sub-assemblies which meet the combined requirements of factory mass production and field assembly techniques. These requirements include:

- Handling and shipping limitations for size and weight
- Minimized number of parts consistent with above
- Maximized factory assembly of components combining as many features as practical
- Modularized assemblies
- Maximum utilization of automated machinery for component production and assembly
- Minimized labor requirements both in factory and field, particularly skilled.

These requirements have been met in the design; additional features implementing low-cost assembly include:

- Self-jigging assemblies requiring minimum fixturing
- Simple quick assembly fastening systems - no field welding required
- Color coded parts - idiot proof assembly
- Factory assembled electrical harness
- Foundation design allows for minimized site preparation and grading compatible with soil characteristics.

10.2 Factory Part Production and Assembly

The major collector components and subassembly production is described below.

10.2.1 Gores

The process for the production of the GRP gores is discussed in Section 11.

10.2.2 Ribs

The aluminum alloy rib truss subassembly has stretch-formed extruded lower cap members providing the accurate dish contour. The complete rib subassembly is built in a fixture providing accurate location and flatness after assembly of the members and end fittings. This is a typical high production aircraft factory assembly technique.

10.2.3 Mount

The production quantity requirement for the tubular steel members (350,000 lbs/day) justify the investment in dedicated tube mills to produce these parts. The members will be made from sheet stock, rolled and seam welded, nosed and trimmed to exact length and painted. The daily production requirement for the 2400 caster fittings, 800 receiver support/rib fittings, 800 rib gimbal fittings, 800 mount gimbal fittings, and 400 each of foundation and mount pintle fittings likewise justifies the investment of multi-headed automated welding equipment. Again, this is a proven high-production technique typical in the motorcycle industry.

10.2.4 Drives

The azimuth and elevation drive assemblies are identical; therefore, the daily production output is 800 units. These are factory assembled with purchased parts (gear motor, sprockets, chain bearings, capstans, etc.). This is typical of automotive-type production assembly.

10.2.5 Foundation

The foundation rail is made from steel I-beam pre-rolled to the required radius; it is made in segments to facilitate handling and field assembly by two men. The foundation bolts are attached to the concrete reinforcing steel structures which are pre-fabricated in the factory.

10.2.6 Pallet

The functions of part storage in both factory, field and shipping are combined in specially designed reusable pallets which house a complete kit of parts for individual collectors.

10.3 Site Assembly

Table 10-1 and Figure 10-1 show the site assembly task sequence, labor, and equipment costs. It is evident from Table 10-1 that the foundation is a major contributor to the site assembly cost; the foundation approach selected using mechanized hole drilling, simple concrete forms, alignment and levelling features, and preformed rails clamped in place, has greatly reduced the cost relative to conventional foundation methods.

10.3.1 Detailed Description of Site Assembly

The pallets are unloaded at the site and loaded onto a specialized parts truck which is provided with an air compressor, light crane, hand tools, and storage for fixtures required for the collector assembly. Rough grading only is required for the site preparation as the foundation design is tolerant to ground level variations within approximately ± 6". The centers of the collectors are marked out and foundation holes are bored with a specialized power earth auger. The prefabricated concrete reinforcing with foundation bolts attached are lowered into the holes and attached to the positioning fixture and levelled after disposable circular cardboard forms are put in position.

Table 10-1. Site Assembly - Labor, Tooling, Plant and Equipment

OPERATION	LABOR			TOOLING	EQUIPMENT REQMTS.	ALIGNMENTS OR CRITICAL OPERATION
	ELAPSED TIME	NO.OF PERSONNEL	MAN-HOURS			
1. Parts Unloaded at Site in Reusable Pallet (Included in Shipping Cost)						
2. Site Preparation, Clear Scrub, Rough Grade, Mark Out Foundation Centers	.25	3	.75		Bulldozer, Front Loader, Dump Truck Surveying Equipment. (Local Contractor)	Grade Level to ± 0.5' 30' x 30' Area
3. Bore Foundation Holes	2.00	1	2.00		Specialized Power Earth Auger	
4. Pour Concrete Foundation 12 Pilings & Centre Pintle	.50	1	.50	● Bolt Positioning & Levelling Fixture ● Concrete Forms	Concrete Truck (Transit Mix)	
5. Assemble Foundation Rails (12 Preformed Rails) and Fixed Pintle with Bearing	.50	3	1.50		Specialized Parts Truck & Light Crane (PT/LC)	
6. Assemble Horizontal Frame - Assemble Movable Pintle - Mount Radial Members - 6 Caster Fittings with Caster Wheels - 6 Tie Members - Azimuth & Elevation Drive Assembly Modules	.50	3	1.50		PT/LC	
7. Assemble Elevation Gimbal Fittings Main & Diagonal Members	.35	3	1.00		PT/LC	
8. Assemble Dish - Assemble 8 Ribs with Splice Plates - Assemble 8 Inner Gores - Assemble 8 Outer Gores Fix Gores in Rib Channels Locking Device	.75	2	1.50	● Rib Positioning Fixture	PT/LC	
9. Assemble Dish to Frame - Add Bearings - Bearing Caps	.25	2	.50	● Jury Strut to Prevent Dish Rotation	PT/LC	
10. Finalize Structural Assembly Add Receiver Support & Members Add Counterweight Support & Members Add Drive Frame Add Drive Cables	1.00	3	3.00		PT/LC	
11. Assemble Sensors, Control Box & Wiring Harness	.25	1	.25	● Alignment Fixture		Align Potentiometers. Check Operation
	6.35		12.50 Total @ 60% Efficiency = 20.6 Man-Hours			

10-4
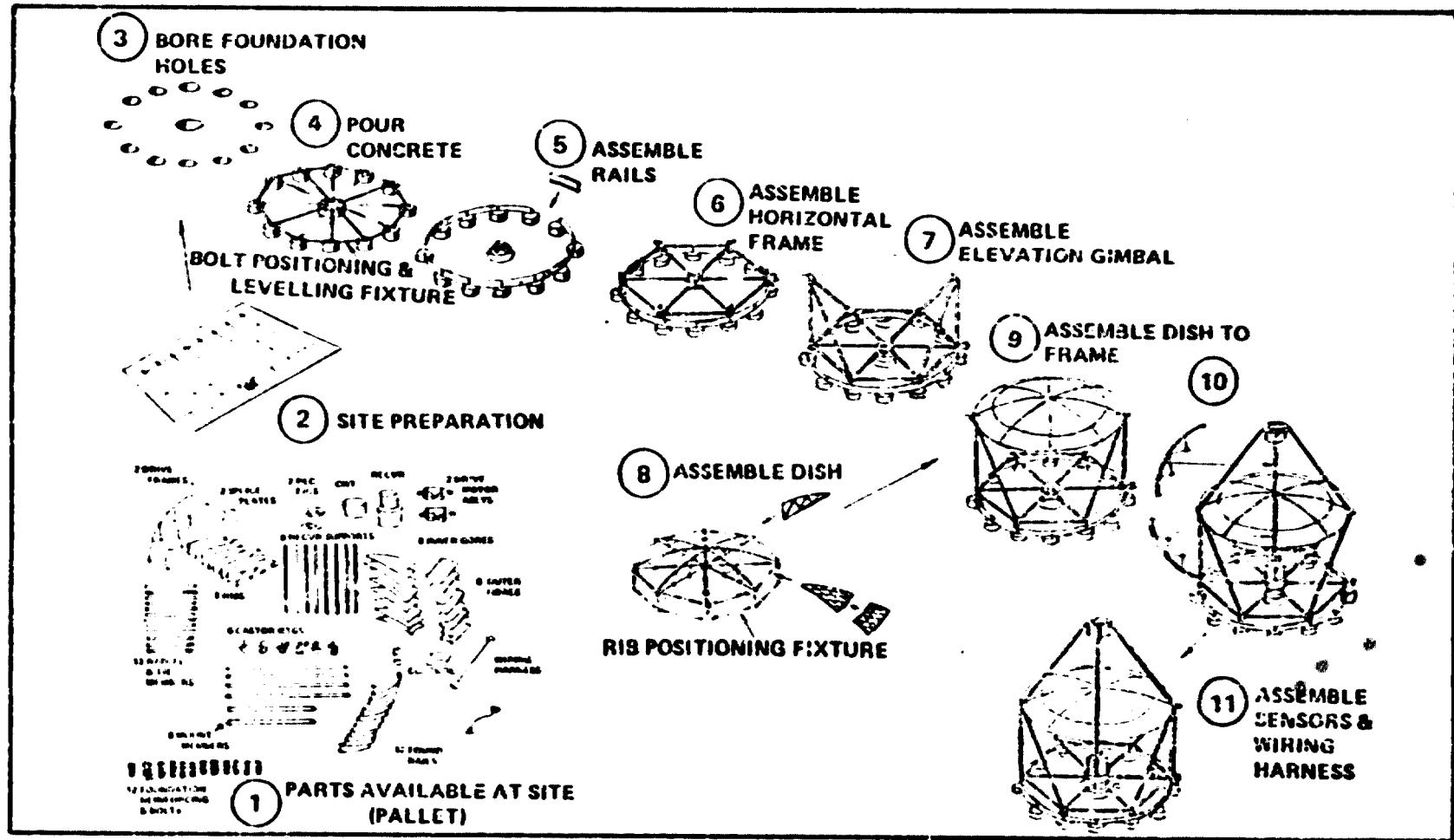
Figure 10-1. Site Assembly Sequence

After the concrete is poured and allowed to set (several done in sequence), the foundation rails (single heaviest part - 138#) are put in position and then the fixture is removed. The foundation pintle fitting is then assembled. The six caster fittings are rolled onto the rail assembly and the horizontal frame is assembled and completed with both the drive assemblies.

The elevation gimbal fittings and mount main and diagonal members are attached to the horizontal frame. No fixture is required as these parts are self-jigging.

The dish is being assembled at another adjacent location on a fixture which may be incorporated with the foundation positioning fixture. This task may be started in parallel with the horizontal frame assembly. The dish rib subassemblies are placed in the fixture and splice plates attached. The inner gores and the outer gores are slid into place and are fixed with quick-locking devices. The entire dish is then lifted by the crane and placed, reflector side down, on the gimbal fittings. The sleeve bearings are slid onto the shafts, and the bearing caps bolted down.

The receiver support attachment, fitting support members and drive frame is then attached (no jigging required), the dish is inverted and the identical procedure repeated for the counterweight assembly. The counterweight is assembled and dish again rotated and receiver is attached. The sensors, controls wiring harness and drive cables are attached, and alignment of the potentiometers complete the job.

10.4 On-Site Assembly Equipment and Costs

The following specialized mobile equipment and fixtures will be required for field assembly:

Specialized Power Earth Auger - $200,000. This machine will be an adaptation of the standard augers used for excavating holes for telephone and light power lines. It will be modified to automatically bore first the pintle hole at a

designated location and then the 12 rail piling holes in a circular, equally spaced pattern at specified radius from the central pintle hole. The machine will be designed to bore holes at maximum rate of 40 per hour, which provides adequate capacity for installing 40 concentrators in a two-shift operation.

Specialized Parts Truck and Light Crane - $100,000. This specialized mobile equipment will dispense parts for each assembly from a kit as needed. It will include a light crane for hoisting and locating heavier parts, assemblies, and fixtures.

Dish Assembly Fixture - $50,000. This will be a mobile work platform with shelter including a fixture for aiding in rapid assembly of the reflector gores and aluminum ribs.

Foundation Bolt Positioning Fixture - $50,000. This fixture will locate the foundation rail and pintle bolts accurately while the concrete is being poured; it is provided with a device to ensure that the foundation is level.

In addition to this unique equipment, other standard items common to modern outdoor steel construction will be included at an estimated cost of $50,000.

Equipment Quotas for High Volume Production and Capital Investment. The elapsed time usage of the various items of equipment were used to establish the quota of each item for a full utilization in high volume field assembly in the range of 10,000-100,000 units/year. See Table 10-2.

Table 10-2. Site Assembly Equipment Cost (8000 Units/Year - 32 Units/Day)

EQUIPMENT	(USE/UNIT) HOURS	USAGE FACTOR	EQUIPMENT QUOTA	CAPITAL COST $
● Specialized Power Earth Auger	2.0	.314	4	800,000
● Specialized Parts Truck/ Crane	3.35	.527	7	700,000
● Foundation Bolt Positioning Fixture	0.5	.078	1	50,000
● Dish Assembly Fixture	0.75	.118	2	100,000
● Standard Outdoor Steel Construction Equipment	----	----	----	50,000
			TOTAL	1,700,000

$$\text{USAGE FACTOR} = \frac{(\text{USE/UNIT})\text{HRS}}{6.35} \qquad \text{FOUND. BOLT FIX. U.F.} = \frac{.5}{6.35} = .078$$

$$\text{EQUIPMENT QUOTA} = \frac{\text{U.F.}}{.078} \qquad \text{FOUND. BOLT FIX. USED} = .5 \text{ HRS} \times 32 \text{ UNITS}$$

$$= 16 \text{ HOURS}$$

Using the foundation bolt fixture as the least denominator, the equipment quota for balanced usage is calculated. The total capital equipment cost of $1,700,000 represents a facility with a maximum capacity of two assemblies per hour or 8000 per year on a two-shift basis.

Site Assembly Costs. Allowing for a labor efficiency of 63%, the costs in Table 10-3 are calculated for 8000 units/year. The capital costs are shown conservatively amortized at 15%/year and this is shown to have a minor effect.

Table 10-3. Site Assembly Costs - 8000/Year

Equipment Amortization:	$255,000 (15%)
+ 166,640 Man Hours @ $20/Hour =	$3,578,000 (Labor and Overhead)
Assembly Cost/Unit =	$447.25 ($1.08/Ft^2)

10.5 Maintenance Assessment

The collector has been designed with minimum maintenance as one of the primary goals. The maintenance requirements for the various components are enumerated in Table 10-4*. Good accessibility for service or replacement is provided for all the components.

---

*These estimates are based on vendor contacts for specific components.

Table 10-4. Maintenance Assessment

ITEM	SERVICE	FREQUENCY	MAN-HOURS/YEAR
Gore Reflector Surface	● Cleaning - 2% Detergent/Water 75 psi Spray Wash	Bi-Monthly	3.0 Estimate - See Section 5
	● Replacement	15 Years	
Drives	● Cable Lubrication	Annual	0.25
	● Cable Tension Check and Adjust	Annual	0.25
Elevation Bearings	● Replacement (unusually severe environmental conditions)	As Required	1.0
Caster Bearings	● Replacement (unusually severe environmental conditions)	As Required	3.0
Pintle Bearing	● Replacement (unusually severe environmental conditions)	As Required	1.0
Control	● Potentiometer Check and Adjust	Annual	0.5
	● Closed Loop Tracking Adjustment	Annual	1.0

SECTION 11.0

PLASTIC PROCESSING ASSESSMENT

11.0 PLASTIC PROCESSING ASSESSMENT

There are numerous processes available to produce dish structures from glass reinforced plastic materials. Compression and transfer molding are the two main methods used to produce molded parts from thermosetting plastics, which has been selected as the dish material.

A number of factors must be considered and understood in any molding process if good moldings are to be obtained. The major factors are the material composition, molds and the parameters affecting the resin polymerization process. In turn, these factors affect the cost of the part.

In our assessment of molding processes for the fabrication of dish structures, consideration was given to low, medium and high volume processes. A process was selected from each of the three categories, with rationale given for each selection.

11.1 Low Volume Production

Low volume production is typified by open and closed mold processing. Table 11-1 shows some of the processes for each type. We used the open mold hand lay-up process for fabricating 1 meter prototype units. This particular process was the least costly for developing in-situ curing and bonding procedures, which could ultimately be used in medium and high volume processes. In the hand lay-up process, vacuum bag pressure was utilized to achieve greater fiber mat compaction, low void content and good part uniformity.

Some of the characteristics of the hand lay-up process are:

1. No shape of size limitation.   6. Output is low.

2. Molds are inexpensive.   7. Labor/unit high.

3. Design is easy to change.

4. Lowest capital investment.

5. Quality of the laminate is dependent upon the operator.

11-1

Table 11-1 Typical Low Volume Processes

PROCESS

● OPEN MOLD PROCESS
 	
   -- HAND LAY-UP
   -- SPRAY-UP
   -- FILAMENT WINDING
   -- VACUUM MOLD
 	
 ● CLOSED MOLD
 	
   -- COLD PRESS MOLDING
   -- RESIN TRANSFER MOLDING

⬅ ● LOWEST COST PROCESS FOR LARGE PROTOTYPE PARTS

● OTHERS SIMILAR BUT SLIGHTLY MORE EXPENSIVE

The general process steps used for hand lay-up vacuum bag cure are as
follows:

1. Continuous glass strand mat and thermosetting resin are laid up on a
   male mold.

2. The materials are then covered with a flexible film diaphragm (vacuum
   bag) and the film is sealed to the mold.

3. Pressure is applied to the laid-up materials by creating a vacuum be-
   tween them and the diaphragm.

Materials can be room temperature cured or cured at elevated temperatures.

11.2 Medium Volume Production

The more significant medium volume processes are shown in Table 11-2. Auto-
clave molding is included in this category because certain shapes and sizes can
be processed in large numbers during a single cure cycle. This could reduce
part cost for large quantity.

However, Resin Transfer Molding (RTM) has been selected for medium dish
volumns for this application because it is at present commercially available for
large part processing. Also, tooling and equipment costs are low. Some character-
istics of the RTM process are as follows:

1. Void content is lowered. Therefore, density and part integrity are
   higher. Structure is higher quality.

2. Process capacity is about 6-8 parts per man hour.

3. Parts can be cured at room temperature as well as low temperature -
   150-200°F.

4. Parts have two smooth sides.

Table 11-2 Typical Medium Volume Processes

PROCESS
● AUTOCLAVE MOLDING ● RESIN TRANSFER MOLDING ● COMPRESSION MOLDING ● DEVELOPMENTAL PROCESSES   -- HOT RESIN TRANSFER MOLDING

COMMERICALLY AVAILABLE LARGE PART

PROCESS

    -- LOW TOOL AND EQUIPMENT COSTS

11.3 High Volume Production

Currently under development within the General Electric Company is the Hot
Resin Transfer Molding process (HRTM). This process is similar to the RTM process
just described, except that the HRTM process is being developed to accommodate a
short cure time, low temperature cure epoxy system. Mentioned earlier in this
section, it is important to understand the resin polymerization process. Epoxy
systems usually provide structures with similar properties regardless of process.
This epoxy system is unique becuase of the short cure cycle and with a combination
of fillers, etc., is low cost. Most of the process development work underway now
is to establish finalized cycles for large parts, and to develop in-situ molding
techniques for the reflector material. This technology will also be usable in
Liquid Injection Reaction Molding (LIRM), which is shown as a high volume process
in Table 11-3. Also indicated as a high volume process in the table is compression
molding. This process is well established, but tooling and equipment costs are
extremely high. These high costs are the drivers toward developing materials for
fast cycle times, and low tooling costs.

Characteristics of the LIRM process are:

1. Process capacity is in the order of 40 parts per hour.

2. Mold costs are low.

3. Capital investment is lower.

4. Higher quality parts are achievable.

5. Lower in-mold and de-mold times.

Table 11-3 Typical High Volume Processes

● COMPRESSION MOLDING

    -- MAT/PREFORM

    -- SHEET MOLDING COMPOUND

    -- BULK MOLDING COMPOUND

● DEVELOPMENTAL PROCESS

    -- LIQUID REACTION

        INJECTION MOLDING

⬅ WIDELY ACCEPTED COMMERICALLY AVAILABLE
MOLDING PROCESS

    — VERY HIGH TOOLING AND EQUIPMENT COSTS

⬅ HIGH POTENTIAL MOLDING PROCESS FOR LARGE PARTS
    — LOW TOOLING COST

    — FAST CYCLE TIMES

In compression molding the resin and reinforcement are premixed to form a molding compound, or the resin and reinforcement are mixed at the press. In LIRM, the reinforcement is placed in the mold, the mold closed and resin injected in a steady stream through a mixing head.

Regardless of the process the glass reinforced plastic properties are similar. This is shown in the properties chart in Table 11-4. It is noted that the resin transfer and LIRM processes produce structures with equal expansion characteristics, assuming everything in the molding material is about the same.

11.4 Summary

Finally, Table 11-5 provides a summary of the various processes available, and those processes selected for near term and mass production. Note that the molding pressures for RTM and LIRM are the same whereas compression molding is extremely high. The lower pressures lead to lower tooling costs. In the case of resin transfer molding, the lower volumes would not require an expensive mold, compared with the high volume LIRM process. Cure time for both processes is low when compared with the other processes. Based upon the potential requirements of 100K units per year, it appears that the most likely long term volume process is LIRM. Resin Transfer Molding is selected for near term until the LIRM process is fully developed two to three years from now.

Table 11-4 GRP Material Properties

PROCESS	FLEX MODULUS PSI	FLEX STRENGTH KPSI	COEFFICIENT OF EXPANSION INCH/INCH-°F
OPEN MOLD	$1.0-1.2 \times 10^6$	16-28	$12-20 \times 10^{-6}$
RESIN TRANSFER	$1.4-2.0 \times 10^5$	20-24	$8-12 \times 10^{-6}$
COMPRESSION	$1.9-2.0 \times 10^6$	18-30	$10-18 \times 10-6$
LIQUID REACTION INJECTION	$1.4-2.0 \times 10^6$	22-26	$8-12 \times 10^{-6}$

MESSAGE

- MATERIAL PROPERTIES OF GRP SIMILAR FOR MANY PROCESSES

Table 11-5 Process Selection

	COMMERCIALLY AVAILABLE PROCESS			DEVELOPMENTAL PROCESS
	OPEN MOLDING	RESIN TRANSFER MOLDING	COMPRESSION MOLDING	LIQUID REACTION INJECTION MOLDING
MOLD CONSTRUCTION	GRP	GRP SPRAY METAL CAST ALUM.	HIGH GRADE STEEL	HIGH GRADE STEEL
MOLD PRESSURE, PSI	ATMOSPHERIC	50-100	1000-2000	50-100
ESTIMATED MOLD COST, $	3-5K	3-25K	250K	150K
MOLD LIFE, PARTS	1000	3-5K	>150K	>150K
CURE TEMP	R.T.	R.T.	275-350°F	150-200°F
CURE TIME	UP TO 8 HRS	10-20 MIN	30-90 MIN	1-3 MIN

```
+-------------------[ MESSAGE ]-------------------+
|                                                 |
|  • PROCESS SELECTION DEPENDS ON PRODUCTION VOLUME
|  • OF TODAYS COMMERCIALLY AVAILABLE PROCESSES, RESIN TRANSFER
|    MOLDING SELECTED FOR NEAR TERM
|  • HIGH POTENTIAL LIRM SELECTED FOR MASS PRODUCTION
|                                                 |
+-------------------------------------------------+
```

SECTION 12.0

FACILITIES ASSESSMENT AND CONCENTRATOR ECONOMIES

12.0 FACILITY REQUIREMENTS AND CONCENTRATOR ECONOMICS

12.1 Introduction

This section presents the results of a study of processes for manufacturing the parabolic reflector concentrator at minimum cost as a function of yearly production rate. Processes for yearly production ranging from prototype quantities to mass production were evaluated for capital investment, materials and labor costs. For each production level, an effort was made to seek out low-cost methods and minimum-cost materials compatible with engineering requirements.

In order to analyze manufacturing costs, five levels of yearly production rates were selected:

```
    1 - 10           - (Prototype temporary tooling)
                       (All components hand assembled)
   10 - 100         -)
                     )
  100 - 1,000       -)  Low cost tooling and standard
                     )   materials used wherever practical
1,000 - 10,000      -)
                     )
10,000 - 100,000     )  (Fully tooled with central parts factory
                        extensively automated).
```

The next step in the analysis was to chose materials procurement methods, parts manufacturing processes, and assembly sequences appropriate to the production rate.

For compiling costs, estimates of materials, labor and equipment costs were obtained from equipment and materials vendors and persons knowledgeable in the appropriate manufacturing areas, both within and outside of the General Electric Company.

Fortunately, most of the concentrator components are fairly standard items which can be procured off-the-shelf, or are very similar to currently manufactured items. The only non-standard items are the plastic gores of the parabolic

reflector. These precision reinforced plastic parts some 2 x 3 meters in size, weighing 30 Kg and having a metallized, specular reflective surface, represent a challenge for low-cost mass production; therefore, the work was divided almost equally between:

1. Endeavors to minimize the in-place cost of the foundation and support frame

2. Researching and evaluating potential low-cost plastic fabrication methods.

The final compilation of costs is believed to be a realistic appraisal of the economics of manufacturing solar concentrators of the approximate size and design performance described herein.

12.2 Selection of Manufacturing and Assembly Methods

The parts which comprise the concentrator were evaluated with emphasis on low cost, reliability and durability. The following is a brief description of the process selection criteria for the principal categories of parts, starting at the ground and working up.

The ratio of factory manufacturing to field construction will be proportional to the yearly production volume. That is, at low production levels <10,000/yr, most components will be purchased from specialized vendors. As production increases beyond the 10,000/yr. level, a greater percentage of the parts will be manufactured in-house. At the 100,000/yr. level, it will be economical to manufacture all the major structural parts at a central factory.

Foundation

For prototypes and low production rates reinforced concrete with the azimuth rail and pintle support bolted on will comprise the foundation.

Details of the foundation structure are discussed in Sections 9 and 10.

It is likely that at levels of production up to 10,000, all the steel foundation and frame parts will be purchased in finished form. Beyond 10,000 assemblies per year, in-house fabrication may be economically favorable, but each part must be individually evaluated.

Support Frame

In all field assembly beyond the prototype stage, air-driven wrenches, rivet-sets and other power tools will be used to expedite the placement of fasteners.

Welded mechanical tubing is the lowest-cost suitable structural material. Figures on material properties, wall thickness uniformity, straightness, and ovality indicate that this type of structural member is more than adequate. For the 100,000 per year production level, about 40,000 tons of tubing per year will be required. It will be economically favorable to manufacture these structural members from steel strip at a dedicated central factory facility.

Relatively small quantities of tubing for up to ten concentrators will cost about $.50/lb. Intermediate quantities have been quoted at $.40/lb.

Support Frame Tubing

The structural parts will be manufactured in a tube mill such as that discussed in Appendix B. This facility continuously converts hot-rolled steel coil stock into welded-seam "mechanical" tubing. The mill will be set up with automated cut-off and nosing of tapering stations to shape the ends for rapid on-site assembly. For corrosion protection, the tubing will be cleaned and painted or coated with a type of asphaltic rust preventative similar to that used on automotive frames. Immediately after coating, the tubing will be automatically conveyed to the packaging center where it will be packaged in kit

form along with the other parts.

Support Frame Fabrications

Some of the product of the tube mill will be diverted to the fabrications center where it will be cut into short lengths and further formed for assembly into the various frame connecting fittings.

Fully automated metal-inert-gas (MIG) welding will be used to assemble the fabrications. This process is currently used in the automotive industry. An example is the fully automated welding of tubular steel motorcycle frames. Preformed sections of tubing are automatically jigged and welded without direct labor. Operating personnel are required only for replacing coils of welding wire and equipment adjustments. Welds have very high integrity and reliability because quality does not depend on mood or skill of the operator. MIG welding is a "clean" process which does not leave oxide or slag deposits so that the fabrications can be easily cleaned for application of paint or other corrosion protection.

A possible alternative to the corrosion protection step for the steel frame parts is to produce them in a Cor-Ten or "weathering" steel. This material, which commonly costs 25% more than 1020 or other low-carbon steels, does not "rust away" upon outdoor exposure. It forms a tenacious, thin surface corrosion film which protects against further corrosion. Outdoor exposure in many urban, corrosive environments has proved its excellent resistance to rust. It is probable that the receiver mount and support above the reflector would be painted or coated, however, to prevent staining of the reflector surface, but even this painting may not be necessary, since the reflector will be stowed face-down on rainy days.

12.3 High Volume Production Requirements

In order to produce 100,000 concentrators per year, a daily production rate of 400 concentrators will be needed. Summarized in Table 12-1 and 12-2, are the processing capacity and fabrication centers that will be needed to manufacture 400 7-meter concentrators per year.

12.4 Facility Economics

Once the production levels are established, a facility can be sized and costed for fabricating 400 concentrators per day. Such a factory is depicted in Figure 12-1 and the supporting costing is summarized in Table 12-3. It is important to note that this is not a large facility. Even though the pounds of material being processed is high, the material residence resistence time is short. Secondly, amortizing a 12 million dollar facility over 100,000 concentrators at 15% per year, only contributes $18 to the cost of the concentrator. The information contained in Table 12-3 resulted from numerous vendor contacts. Records of these contacts are contained in Appendix B.

Table 12-1. Production Requirements
(7-Meter Reference)

● Processing Capability - 100,000 Units/Year - 400 Units/Day

MATERIAL	DAILY PROCESSING, lb
STEEL	800,000
Aluminum	80,000
Plastic	350,000
Purchased Parts	160,000
Paint	6,000

Table 12-2. Fabrication Centers

FACILITY	DAILY CAPACITY
● Tube, Minimum	144,000 feet of Tube (27 Miles)
● Fitting Fabrication	8,000 Pieces
● GRD Gore Fabrication	6,800 Pieces
● Rib Fabrication	3,200 Pieces
● Paint Shop	18,000 Pieces
● Packaging for Shipment ● Pallet Storage ● Incoming Material Storage	3 Day Output

Table 12-4 presents the results for the high volume concentrator. The total cost represents a factory price and includes a price to the user plus installation. It is important to note that there will be an escalation in this price due to the distribution chain. A typical distribution chain for this class of hardware would be one which deals directly with the utility. For this type of distribution chain, approximately 20 to 30 percent would have to be added to the factory price to cover such items as applications engineering support, sales, and transportation.

12.5 Volume Sensitivities

Figure 12-2 shows the principal costs as a function of yearly production rate.

At the 100,000 concentrators/yr. production level, the major manufacturing cost is the cost of the material. For example, the plastic reflectors will cost $1,000 for materials and $25 for fabrication labor. A similar relationship holds

12-6
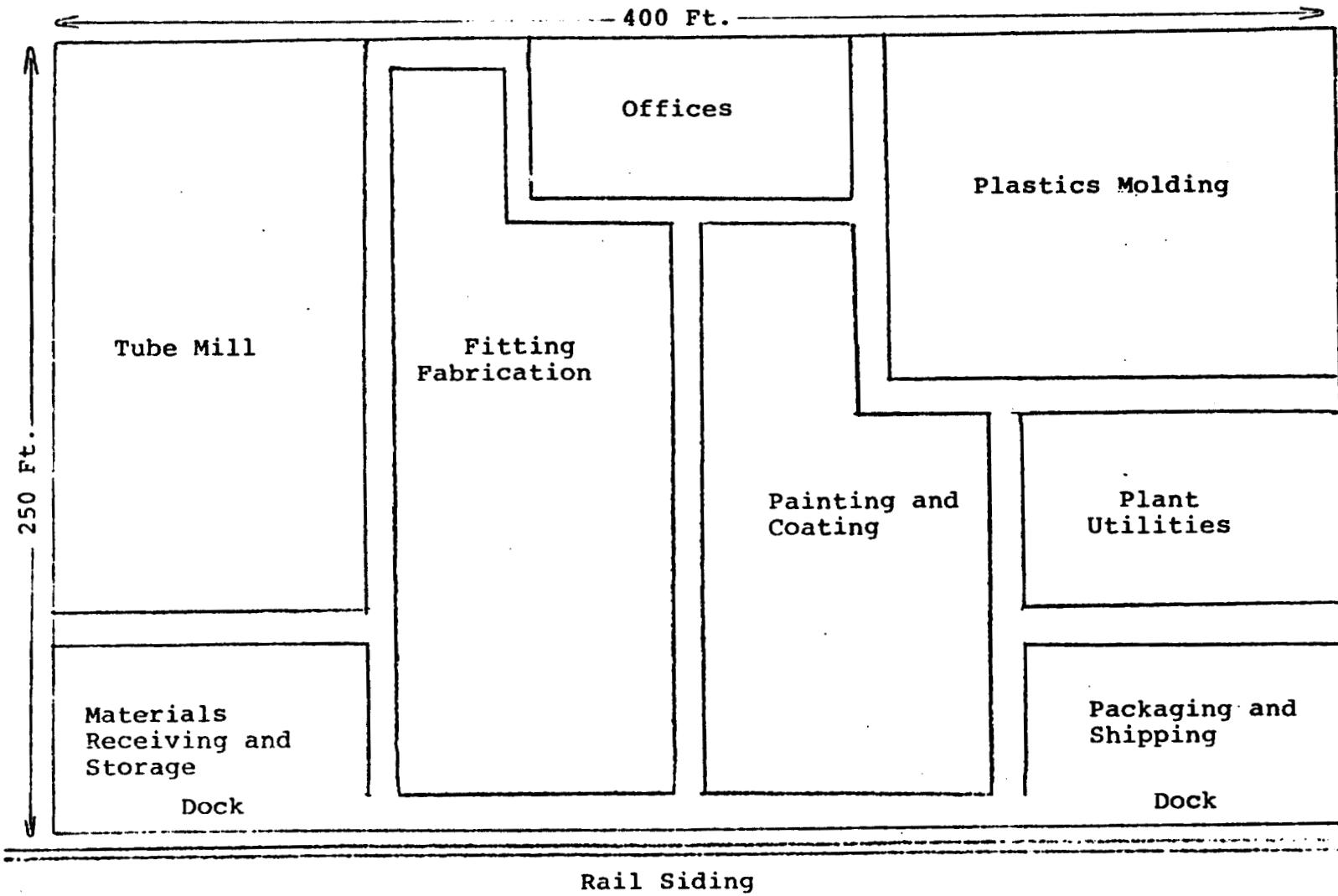
Figure 12-1.
Conceptual Layout of Factory
For Production Level of 100,000 Per Year

Table 12-3.

Factory Equipment and Facilities for Production of 100,000 Concentrators per Year

(Assume 2 Shift Operation - 7-Meter Reference)

EQUIPMENT	CAPITAL INVESTMENT (Dollars)	TOOLING $ (Initial)	TOOLING $ (Yearly)	FLOOR SPACE (Sq. Ft.)	OPERATING PERSONNEL PER SHIFT (Direct Labor)
Plastic Molding	3,750,000	1,000,000	100,000	10,000	25
Tube Mill	1,315,000	65,000	30,000	15,000	4
Fitting Fabrication	1,000,000	200,000	50,000	10,000	10
Rib Fabrication	400,000	100,000	20,000	5,000	10
Painting/Coating	300,000	100,000	20,000	10,000	10
Packaging-Shipping	300,000	50,000	10,000	10,000	15
Parts and Materials Storage & Conveyance	1,000,000	100,000	50,000	10,0C0	5
Building	4,000,000	--	--	--	--
TOTAL	12,065,000	1,615,000	280,000	100,000	79

(Includes aisles, offices, etc.)

Table 12-4. Collector Unit Cost (100,000/Yr)

Subsystem Breakdown

SUBSYSTEM	MATERIAL	WEIGHT #	COST $/LB	TOTAL SUBSYSTEM COST
DISH	GRP	870	1.25	1087.00
REFLECTCR				85.00
MOUNT - RIBS	ALUMINUM	176	1.00	
- FRAME	STEEL TUBE	866	0.35	
- FITTINGS	STEEL WELDMTS	191	0.50	588.40
- BALLAST	CONCRETE	600	0.023	
DRIVE	PURCHASED			412.00
CONTROL	PURCHASED			310.00
FOUNDATION	STEEL SHAPE	873	0.40	
	STEEL FRITTING	24	0.50	614.80
	CONCRETE	11028	0.023	
SITE ASSEMBLY				447.00
TOTAL				3544.20

for the support frame steel and the aluminum ribs for the reflector.

Field assembly will account for a high percentage of the total installed cost especially at low levels of production, although every effort has been made to minimize field assembly labor. Considerable savings were obtained by minimizing the weight of the structure through efficient design, thereby reducing the weight and strength requirements of the foundation.

Another area which will contribute to high costs at the prototype stage is the cost of tooling (molds, fixtures). Even low cost "temporary" tooling represents a major portion of the cost of the reflector plastic and the reflector ribs. At high yearly rates, on the other hand, tooling costs become minor compared to material costs. For example, the mold to produce five reflectors by hand lay-up will cost $5,000, reflector materials will cost $2,000 per reflector, and labor $1,000 per reflector.

Items in which cost is least sensitive to production volume are standard purchased materials and parts, such as steel tubing and plastic resin. Note above that the resin and reinforcement for one prototype reflector will cost about $2,000, while at the 100,000 per year level, resin and reinforcement cost is $1,000 per reflector, still 1/2 the prototype cost. Likewise, steel tubing in relatively small quantities will cost about $.55 - $.60/lb. while at even the highest production rates, its cost will be about $.30/lb.

It is interesting to relate the "energy cost" per concentrator to the concentrator output. The following are estimated energy costs:

Steel	.3 tons	3600 Kw hr.
Aluminum	.09	5250
Plastic	.4	6077
Fabrication	2%	} +3% ————>15375 Kw hr
Installation	1$	

12-10

If the output is taken as 12,000 Kw hr/yr., the energy payback period for the reflector and support frame is 1.28/yr.

12.6 Concentrator Cost/Performance Ratio

With the price for high volume concentrators and the performance estimates of Section 3, the $/Kw$_{th}$ can be computed. The result is shown in Figure 12-3. The $/Kw$_{th}$ is presented as a function of reflector performance, once again to reinforce the agrument that silvered systems offer advantages if the cost comes down. It is also important to note that even with the low cost aluminum films, the goals established by JPL can be met.
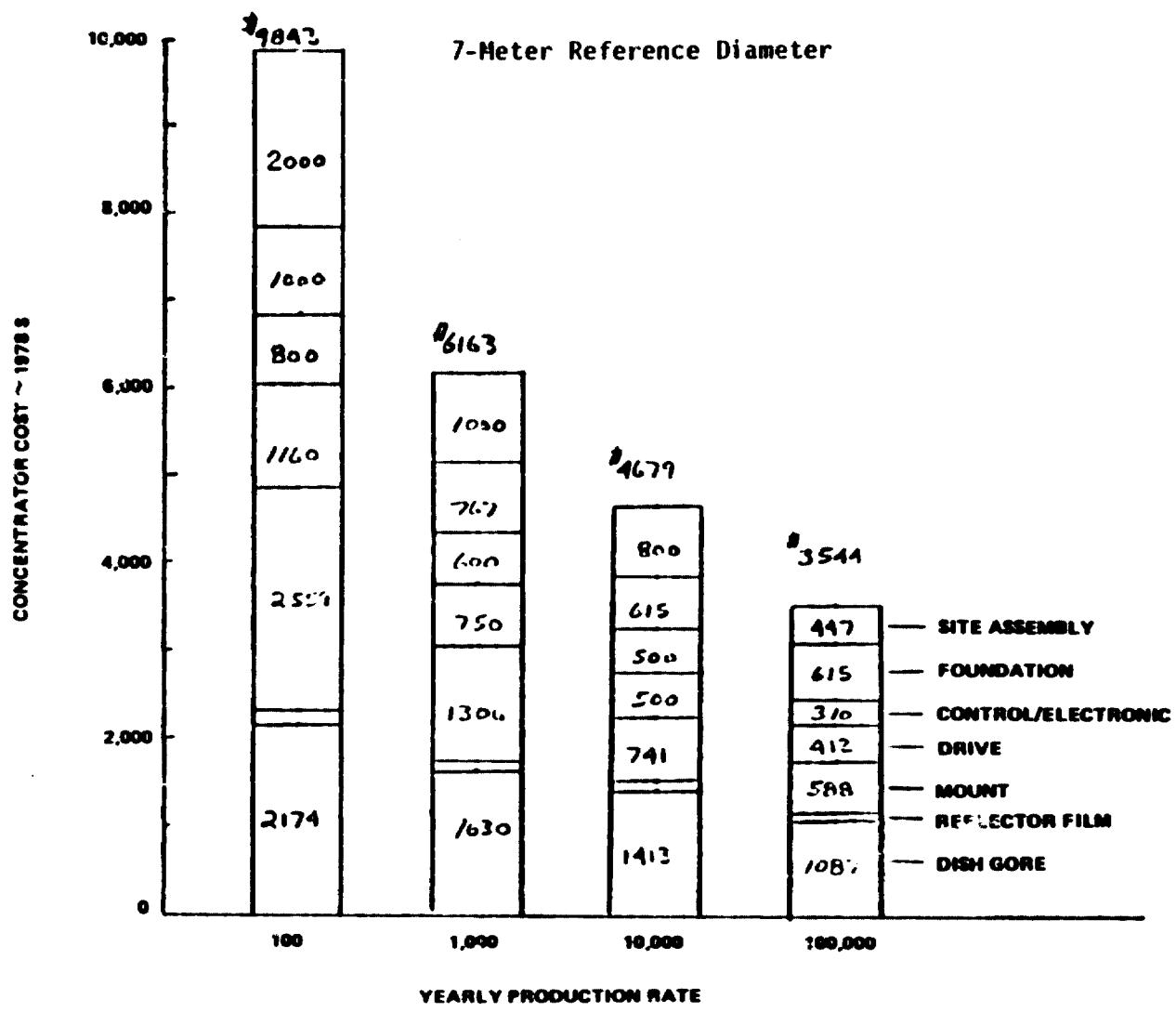
Figure 12-2. Concentrator cost vs. Volume

REFLECTOR EFFICIENCY =
TOTAL REFLECTANCE & EFFECTIVE AREA

SUN

RECEIVER INTERCEPT FACTOR

RECEIVER LOSS

●7 METER DIAMETER
●F/D = 0.5
●$8.55/FT^2
●800 WATTS/m^2

200

180

160

140

120

100

80

TYPICAL ALUMINUM FILMS

SILVERED FILMS

RFP GOAL

Λ

V

CONCENTRATOR #/km Tp

80   90   100

TOTAL REFLECTANCE ~ %
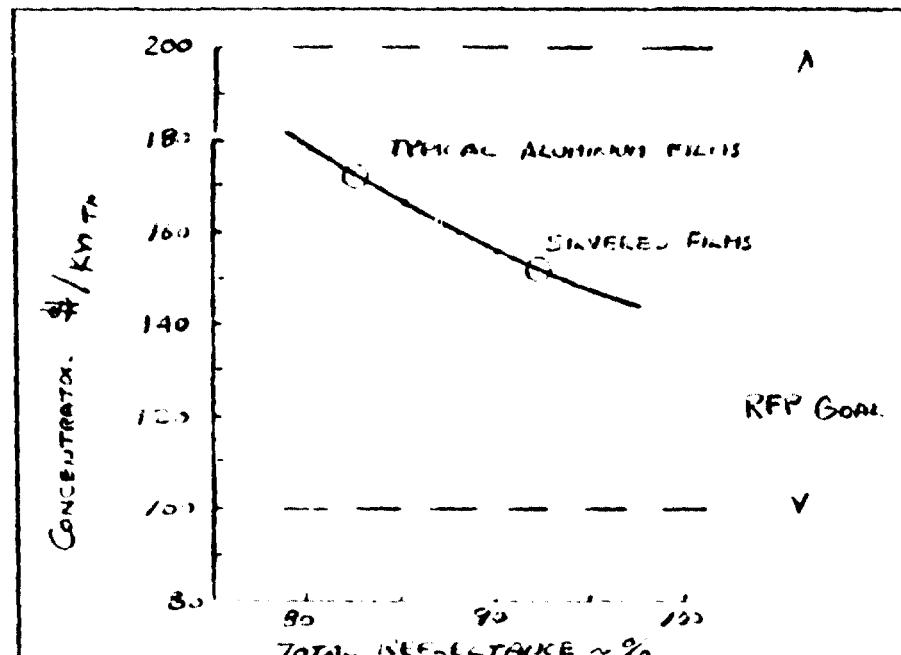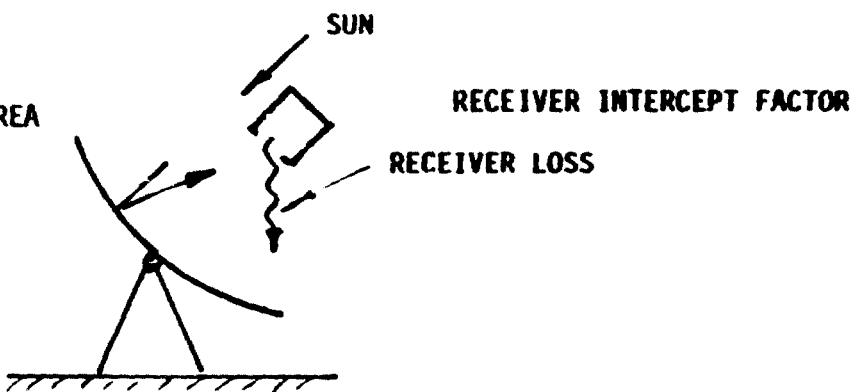
● TODAYS ALUMINUM FILMS MEET JPL
  GOALS

● INCENTIVE TO DEVELOP SILVERED
  FILMS

Figure 12-3. Concentrator Cost/Performance Ratio

SECTION 13.0

DESIGN SCALING

13.0 DESIGN SCALING

13.1 Diameter Scaling

In an effort to determine the effects of dish diameter on subsystem costs in $/ft^2, the seven meter concept was scaled up to eleven meters. For the dish gores the same analysis technique was used for the nine and eleven meter dishes as was used on the seven meter dish. In a similar manner the mount and foundation size, weight and costs were obtained. The results of this study are shown in Figures 13-1 and 13-2. These results along with similar estimates for the effects on controls, drive system, reflector and site assembly were then used to calculate the subsystem costs in $/ft^2 which is presented in Figure 13-3. Summing these individual costs results in the total concentrator cost in $/ft^2 as shown in Figure 13-4. There is a gradual decrease in specific cost with increases in dish diameter but certainly not strong enough to pick a final optimum diameter without knowing more about the entire system requirements including electrical, instrumentation and control requirements for the receiver engine and the power distribution or collection network.

Figure 13-4 also shows the effect of diameter on $/KW$_{thermal}$ based on reflector films of aluminum or silver being assumed to be equivalent in cost. It shows the obvious potential of the high reflectivity of silver as compared to aluminum. However, the only proven method available to environmentally protect silver is with glass which makes the choice of glass/silver less cost effective due to its present high cost.

Other design considerations that became apparent as a function of dish diameter were the manufacturing limitations on gore size relating to manufacturing processes. Figure 13-5 can be used to develop data on the impact of process vs. size. Present day technology for high volume cost effective part production
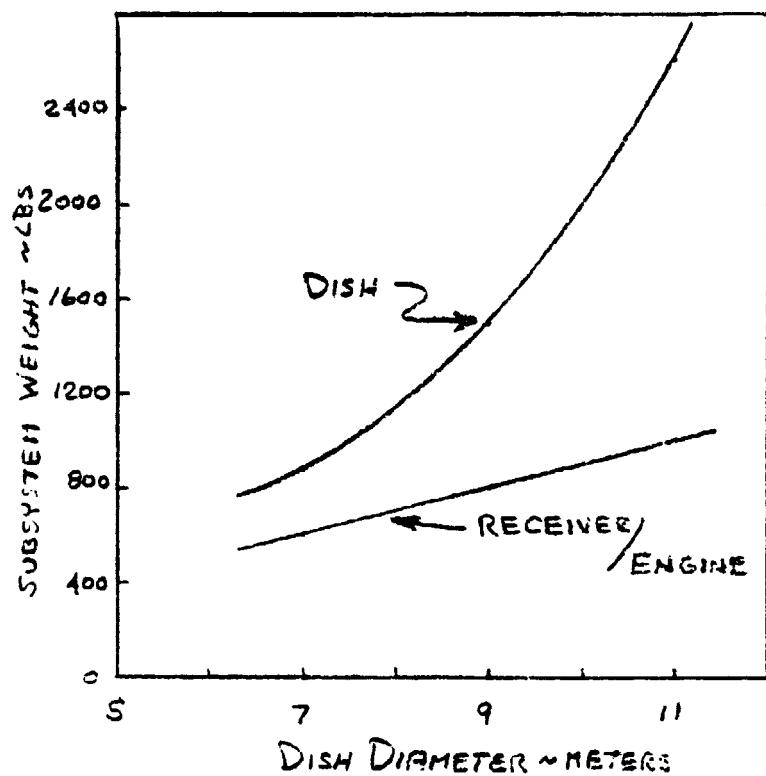
Figure 13-1.
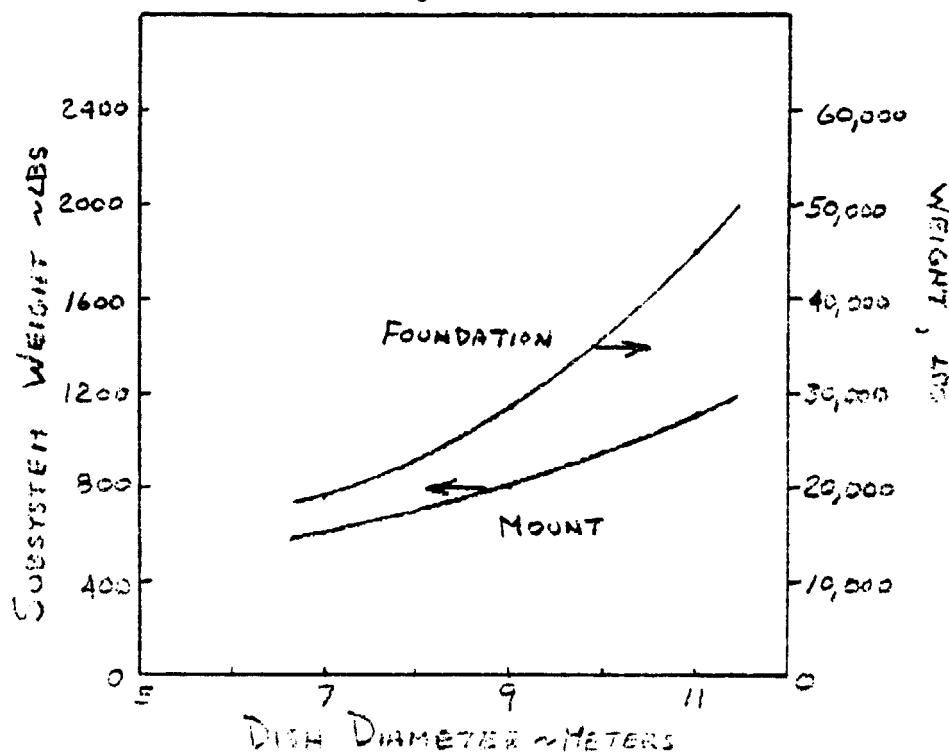
Figure 13-2.
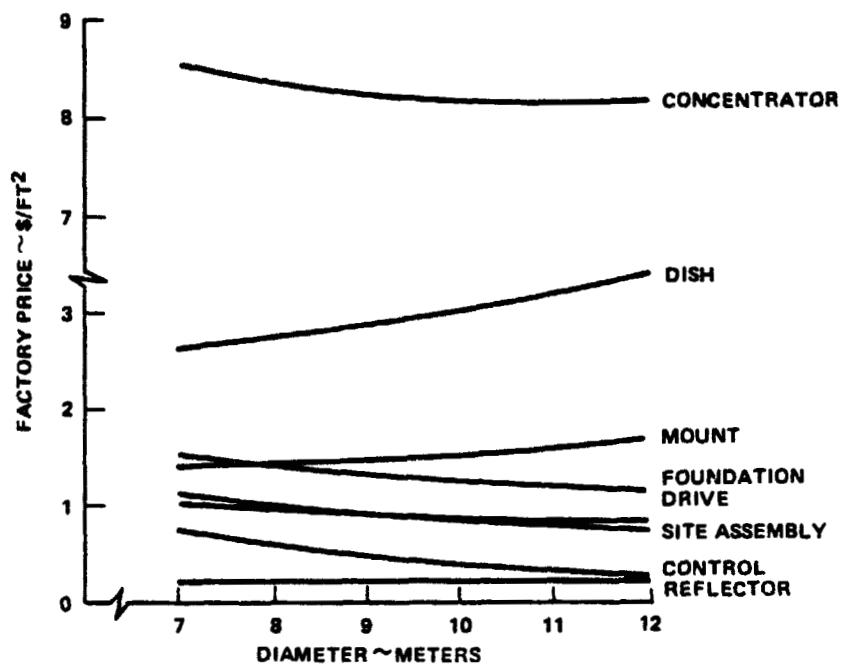
Figure 13-3.   Subsystem Cost Trends
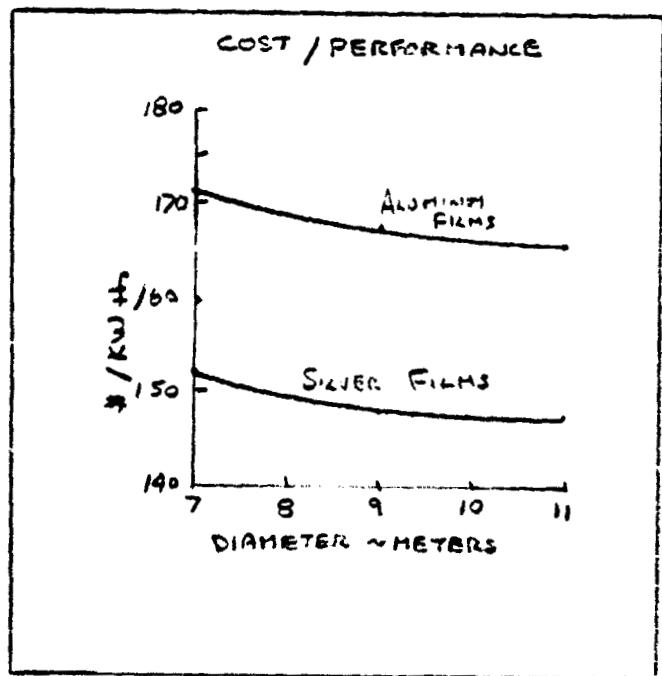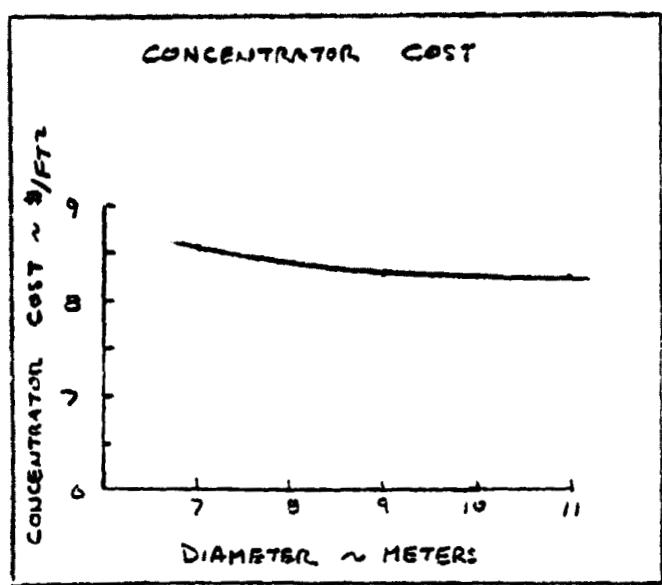
Figure 13-4. Concentrator Cost Trends
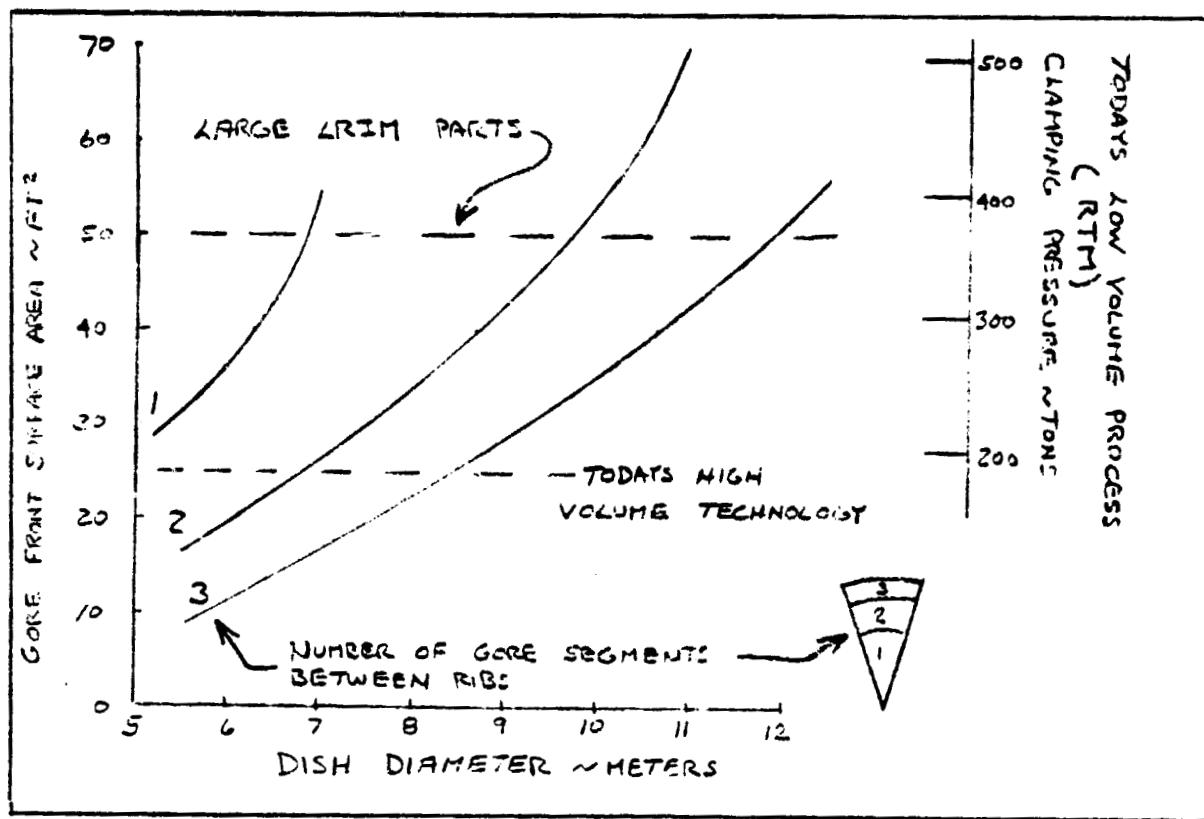
Figure 13-5. Diameter Limitations

requires that gore front surface area be a maximum of 25 ft^2. As can be seen, this corresponds to two equal area pieces to make a seven meter dish or three pieces to be able to make an eight meter dish. Dish diameters larger than this mean more pieces would be required, perhaps four or five pices for an eleven meter dish. More pieces means more joints, more molds, and longer assembly times which translates to higher \$/ft^2. To make fewer pieces now but be able to make larger dishes, to 12 meters, would require the application of the Resin Transfer Molding technique which is applicable for low volume production. The attainment of high volume production of large diameter dishes will be possible when the Liquid Reaction Injection Molding (LRIM) process, presently under development, becomes available.

Table 13-1 summarizes the design scaling implication as a function of process, dish production quantity and production time reference. Specifically, Table 13-1 states that near-term production of large diameter dish prototypes can be accomplished with the Resin Transfer Molding. Present limitations of available high volume molding processes will be extended when the LRIM process is available.

13.2 Impact of 1200°F Cavity

By reducing the cavity temperature from 1700°F to 1200°F the thermal losses from the receiver are reduced substantially and the slope error and concentration ratio changed accordingly. The optical analysis is presented in Figure 13-6. As can be seen, there are two approaches that can be taken. The first would hold the performance levels of the baseline design and decrease the cost due to the less accuracy. The second approach would not alter the design but take the higher concentrator performance associated with the lower receiver temperature. Table 13-2 presents an assessment of these two approaches. In approach 1 less dish

Table 13-1. Diameter Scaling Conclusions

PROCESS QUANTITY TIMING	PROTOTYPES RESIN TRANSFERS <100 0-2 YEARS	LOW PROD COMPRESSION 100-1000 2-5 YEARS	HIGH PROD RIM 10,000-100,000 >5 YEARS
DIA(m) 6-8	YES	YES	YES
8-10	YES	?	YES
10-12	YES	NO	YES
>12	YES	NO	?
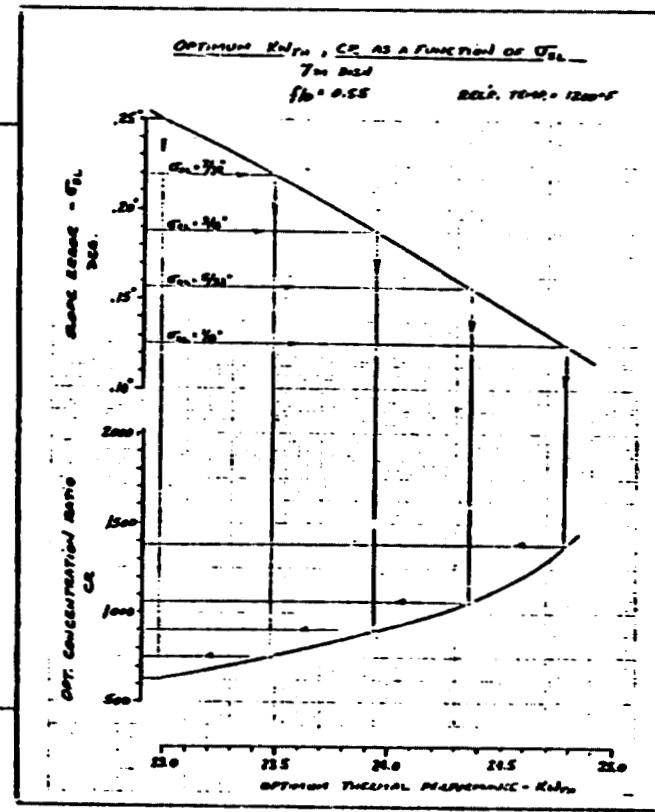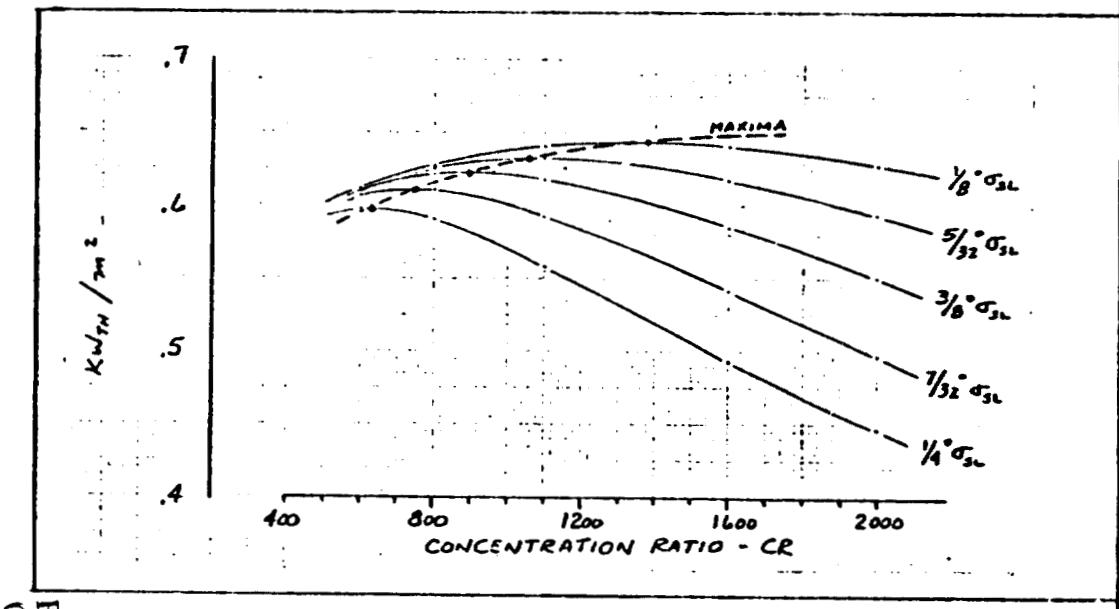
MESSAGES

- APPROACH 1: HOLD PERFORMANCE, DECREASE COST

- APPROACH 2: HOLD COST, INCREASE PERFORMANCE

Figure 13-6.   Effect of 1200°F Cavity -- System Analysis

Table 13-2. Effect of 1200°F Cavity -- 7 Meter Reference

PARAMETER	APPROACH 1	APPROACH 2
SLOPE ERROR, DEGREES	1/4°	1/8°
GORE DEFLECTION, DEGREES	0.4°	1/4°
CONCENTRATION RATIO	650	1800 .
DISH THICKNESS, INCH	.145 INCH	.165 INCH
DISH COST, $/FT	2.30	2.63
SYSTEM COST, $/FT	8.22	8.55
PERFORMANCE, KW_{th}	22.2	24.0
$/KW_{th}$	153.3	147.5

MESSAGE

- COST EFFECTIVE APPROACH WOULD BE TO NOT CHANGE DESIGN AND UTILIZE THE HIGHER PERFORMANCE ASSOCIATED WITH THE LOWER RECEIVER TEMPERATURE

material would be necessary since more deflection would be allowed with the lower concentration ratios. On a $/KW_{TH}$ basis, approach 2, i.e., no change in design, would be the most cost effective.

13.3 Impact of Receiver Weight

The effect of increases in the receiver/engine weight is to increase the loads into the receiver/engine supports, mounts and foundation. The mount and foundation are doubly affected because for every pound of weight increase in the receiver/engine, the ballast or counterbalance must be increased by the same amount. Figure 13-7 lists the effects of doubling the weight of the receiver/engine. Included in the increased concentrator cost are dollar estimates for the increased cost of drive motor and brake system required by the increased mass moment of inertia. Even with these increases, the cost effect is about a dollar per square foot of collector aperture, which is not insignificant.

Figure 13-7. Effect of Receiver/Engine Weight

- Impact on Mount and Foundation Subsystems
- Doubling Weight
    - Increases Mount Loads by 2400 Lbs
    - Increases Foundation Loads by 2900 Lbs
    - Increases Mount Member Weight by 300 Lbs
    - Increases Foundation Weight by 10,000 Lbs
    - Increases Concentrator Cost by $400

SECTION 14.0

PROTOTYPE CONCENTRATORS

14.0 PROTOTYPE CONCENTRATORS

A key objective in the Program was to establish an approach to the manufacturing of prototype concentrators. The main differences between prototype concentrators and the mass produced versions lie in the areas of processing. The major processing variation is the molding of the plastic dish gore. The rest of the concentrator will be composed of the same materials and configurations, however, certain compromises will be made in order to use all purchased hardware. For example, the mount members will be sized to use off the shelf tubing instead of the mass produced tube mill product envisioned for the high volume concentrators. Another compromise would be to use commercially available clamping and joining systems for the mount as opposed to the specialized weldments that would be specified in the mass produced version. These are, however, differences of processes and labor content, not design approaches.

14.1 Resin Transfer Molding Process

As discussed in Section 11, the choice of molding process for GRP depends on production volume. For prototype quantities, the process of choice would be hand lay-up or some other form of low pressure room temperature molding. The process that is recommended for Phase III of the Concentrator Program is the Resin Transfer Molding process. This process offers the advantages of closed mold processing as opposed to the open mold in hand lay-up. The major disadvantage is that the molding costs are slightly higher ($25,000 versus $10,000). This cost differential is warranted considering the decrease in labor required to make the parts.

Resin Transfer Molding (RTM) has become an effective technique for the production of many Fiberglas reinforced plastics. The size of parts that can be produced in RTM is generally limited by the relative cost of constructing

14-1

molds and clamping equipment. Typical parts range from 1 square foot to 45 square feet, although parts up to 100 square feet have been made. The RTM system is inherently cleaner than open-mold techniques. In addition, once the part is designed and its material systems specified and developed on a prototype basis, final production requires a lower level of operator skill. RTM defines both surfaces of the part and, with proper molds and mold-clamping devices, part thickness is highly reproducible on a part-to-part basis. Part reproducibility allows the designer to consider the use of structural adhesive bonding and other assembly techniques. The RTM closed-mold process also affords the opportunity to integrate rib inserts, as well as metal and wood attachment plates. Specific directionally-oriented reinforcements can be located in highly stressed areas.

A further advantage results from the rapid introduction of the catalyzed resin. This feature allows much faster gel and cure than normally associated with open molding. A faster curing cycle allows a high rate of output per RTM mold, compared to a spray-up or hand lay-up mold. The faster cure also minimizes "alligatoring" or gel coat attack by the back-up resins.

Other features of the RTM process are:

- Mobile pumping equipment to allow sequential molding of a variety of part shapes and sizes;

- Closely-controlled material consumption and pumping time to reduce waste;

- The ability to get coat, pigment, post-finish, and mold parts in conjunction with a thermoplastic skin (comoform).

The reflector for the near term prototypes is the aluminized Martin Processing Film presented in Section 5. As demonstrated in the small dish

part development, the film will stretch readily to the degree of curvature needed with no less in reflective performance.

14.2 Prototype Performance

Using the reflector properties of the Martin Processing film, the concentrator performance has been calculated and is presented in Figure 14-1. The reflector efficiency, i.e., the total reflectance times the active concentrator area, is calculated to be 0.769. With a 97% intercept factor and the specified receiver losses, the resultant concentrator efficiency is 66%. A silvered reflector concentrator representative of a mass produced version is carried for ~~composition.~~ Comparison

14.3 Prototype Cost and Schedule

A preliminary costing exercise and scheduling of a near term prototype program was made to ensure that the selected concept was indeed within the schedule goals of JPL and at a cost compatible with near term hardware availability. Figure 14-2 presents an estimated prototype cost based on vendor quotes for prototype quantities for both the 7 meter size and an 11 meter concentrator. The estimated schedule is shown in Figure 14-3.

In conclusion, the approach for the prototype concentrators differs only in the area of processes, substituting more labor intensive operations for the automated ones envisioned for the high production rates. Numerous vendor contacts, both with metal fabricators and plastic molding operators, have substantiated the near term viability of the design approach.

REFLECTOR EFFICIENCY =
TOTAL REFLECTANCE *EFFECTIVE AREA

0.8 KWATTS/M^2
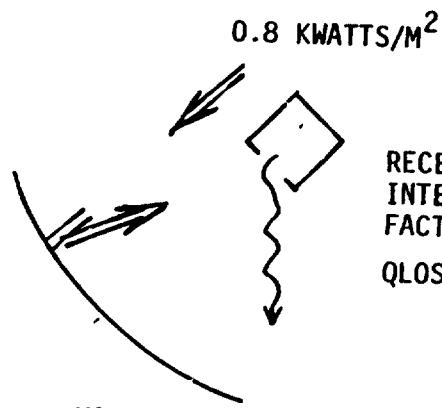
RECEIVER
INTERCEPT
FACTOR

$QLOSS = \dfrac{119}{CR} = 0.066$ KW/M^2

	MASS PRODUCTION	PROTOTYPE
INSOLATION - KW/M^2	0.8	0.8
REFLECTOR EFFICIENCY	SILVER 0.92 x 0.938 = 0.863	ALUMINUM 0.82 x 0.938 = 0.769
RECEIVER INTERCEPT FACTOR	0.97	0.97
RECEIVER LOSS ~ KW/M^2	0.066	0.066
HEAT INTO ENGINE ~KW$_{th}$	0.0604	0.531
CONCENTRATOR EFFICIENCY ~ %	75.5%	66%

Figure 14-1. Prototype Performance

7 METER

FABRICATED ASSEMBLY	MATERIAL	TOOLING	LABOR	PURCHASED PARTS
MOUNT MEMBERS	500	---	500	---
FITTINGS	100	1000	2500	---
GORES	2000	50000	800	---
DRIVES				1160
WHEELS, FASTENERS				300
CONTROLS, ELECTRONICS				1000
PACKAGING, HANDLING	100	---	900	---
FOUNDATION	1000	2000	1000	---
TOTAL	3700	53000	5700	2460

11 METER

FABRICATED ASSEMBLY	MATERIAL	TOOLING	LABOR	PURCHASED PARTS
MOUNT MEMBERS	1400	---		
FITTINGS	275	1500	3000	
GORES	6000	75000	1200	
DRIVES	2500			2500
WHEELS, FASTENERS				330
CONTROLS ELECT				1100
PACKAGING, HANDLING	250		1200	
FOUNDATION	2000	2500	2000	
TOTAL	12425	79000	7400	4300

MESSAGE

CONCEPT LENDS ITSELF TO NEAR TERM
HARDWARE AVAILABILITY

Figure 14-2. Prototype Costs

14-5

Figure 14-3. Prototype Schedule

APPENDIX A

OPTICAL ANALYSIS

APPENDIX A-1

OPTICAL MODEL

A-1.1   Derivation of Optical Model*

Summary

A method is described for finding the flux distribution of reflected radiation at the receiver located at the focus of a parabolic dish. Equations are derived which give the spatial spread of the reflected energy as a function of the optical error and the collector rim angle. The energy intercepted by a receiver of a given size can then be obtained, and the optically optimum rim angle derived.

The analysis follows that of Liu and Jordan** [1965] for a flat plate receiver. An error in Liu and Jordan's analysis was found and corrected, leading to different results from those presented in their paper.

Optical Analysis

The major assumption in this analysis is that the optical error is random in nature and can be described by a Gaussian distribution function. It is further assumed that the reflected beams are symmetric with respect to their respective axes. Consider the reflection of the incident parallel rays from a ring-shaped sector of the parabolic mirror, dA, which makes an angle θ with the dish axis and extends a small angle $d\theta$. (See Figure A-1)

---

* Memo from A. C. Ku to Dr. A. Koenig 9/19/78.

** "Performance and Evaluation of Concentrating Solar Collectors for Power Generation", by B. Y. Liu and R. C. Jordan, J. of Engineering for Power, Jan. 1975.

FIGURE A-1 PARABOLIC DISH GEOMETRY
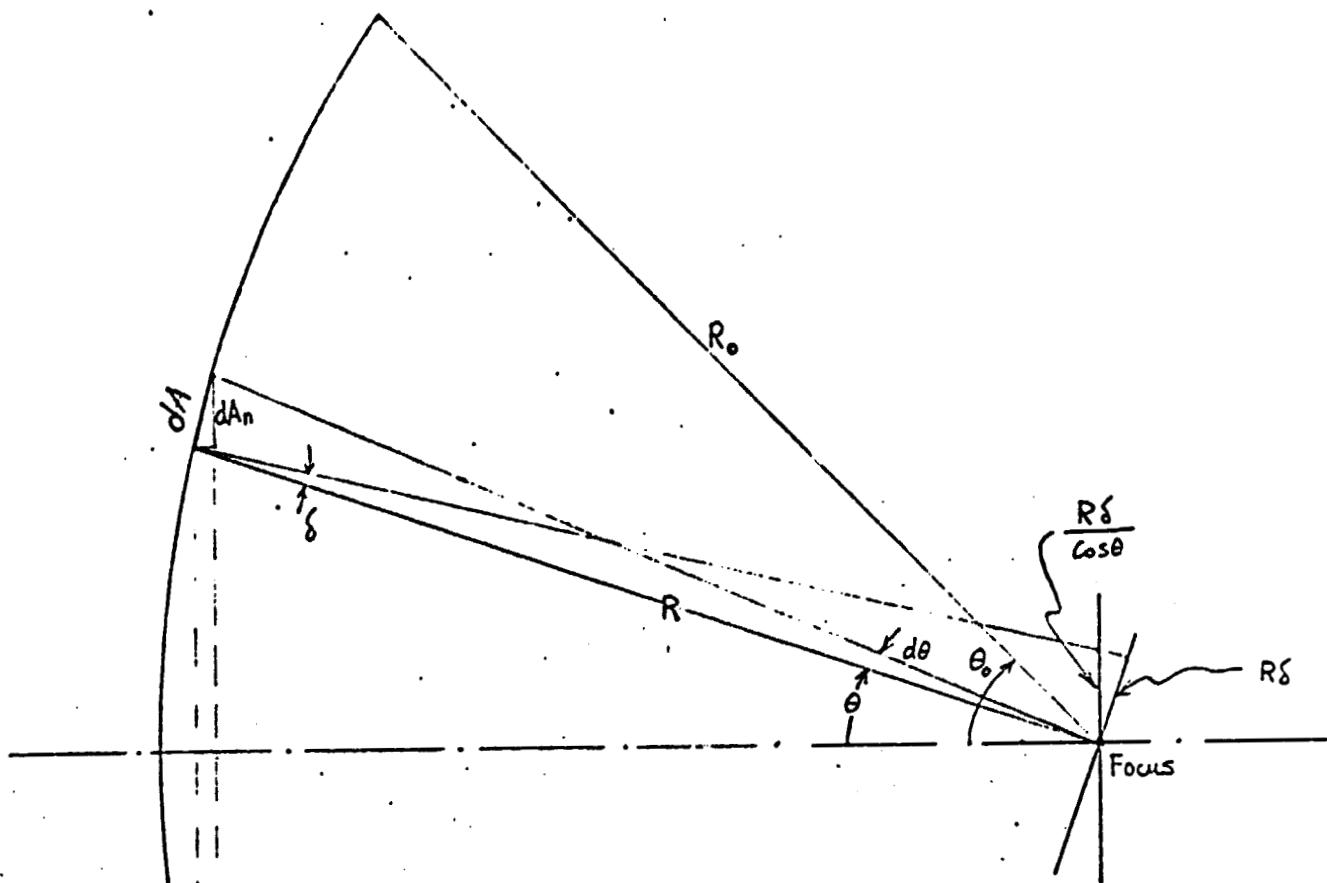
$$dA_n = 2\pi y \, dy$$
$$= 2\pi (R\sin\theta)\left[\sin\theta \, dR + R\cos\theta \, d\theta\right]$$
$$= 2\pi R\sin\theta\left[\sin\theta\left(\frac{1}{R}\frac{dR}{d\theta}\right) + \cos\theta\right] R \, d\theta$$
$$\overset{*}{=} 2\pi R^2 \sin\theta \, d\theta\left[\sin\theta\left(\tan\frac{\theta}{2}\right) + \cos\theta\right]$$
$$\overset{**}{=} 2\pi R^2 \sin\theta \, d\theta\left[1 - \cos\theta + \cos\theta\right]$$
$$= 2\pi R^2 \sin\theta \, d\theta$$

$* \quad \because R = \dfrac{2f}{1+\cos\theta}$

$\dfrac{dR}{d\theta} = -\dfrac{2f}{(1+\cos\theta)^2} \, d(\cos\theta + 1) = \dfrac{2f}{(1+\cos\theta)^2} \sin\theta$

$\therefore \dfrac{1}{R}\dfrac{dR}{d\theta} = \dfrac{1+\cos\theta}{2f} \cdot \dfrac{2f}{(1+\cos\theta)^2} \sin\theta = \dfrac{\sin\theta}{1+\cos\theta} = \tan\dfrac{\theta}{2}$

$** \quad \tan\dfrac{\theta}{2} = \dfrac{1-\cos\theta}{\sin\theta}$

A-2

Let δ be the standard deviation of the optical error (rad.) which is independent of θ. Then

$$\sigma_\theta = \frac{R \delta}{\cos \theta} \tag{1}$$

where σ_θ = Standard deviation of spatial distribution of reflected flux from dA, ft.

R = Distance between dA and the focus, ft.

θ = Polar angle of reflection, degree.

For a parabola in polar coordinates with the origin at the focus, it can be shown that

$$R = \frac{2f}{1 + \cos \theta} \tag{2}$$

where f = focal length, ft. This equation shows that the mirror-to-focus distance increases as dA moves away from the apex.

Combining (1) and (2), we have

$$\sigma_\theta = \frac{2f \delta}{(1 + \cos \theta) \cos \theta} \tag{3}$$

It should be noted that energy collected from dA is proportional to its projected area on a plane normal to the axis of the dish dA_n. Therefore, the variance of the reflected flux at the focal plane, σ^2, is the weighted average of the variance σ_θ^2 :

$$\sigma^2 = \frac{\int \sigma_\theta^2 \, dA_n}{\int dA_n} = \frac{\int \sigma_\theta^2 \, dA_n}{A_\circ} \tag{4}$$

Where $A_\circ$ is the aperture area of the dish. For a more vigorous derivation of Eq. (4), refer to the original analysis of Liu and Jordan.

The parabolic dish collector aperture area is

$$A_o = \pi \left(R_o \sin \theta_o \right)^2$$

where θ_o is the dish rim angle and R_o is the rim-to-focus distance. It can be shown that

$$dA_n = 2\pi R^2 \sin\theta \, d\theta$$

(Note: In Liu and Jordan's original paper an incorrect expression for dA_n was used). By Eqs (3), (4), (5), and (6), we have

$$\sigma^2 = \frac{\int \sigma_\theta^2 \, dA_n}{A_o}$$

$$= \frac{\int \left[\frac{2 f \delta}{\cos\theta (1+\cos\theta)} \right]^2 2\pi R^2 \sin\theta \, d\theta}{\pi \left(R_o \sin \theta_o \right)^2}$$

$$= \frac{8 f^2 \delta^2}{\sin^2\theta_o} \int \left(\frac{R}{R_o} \right)^2 \frac{\sin\theta}{\cos^2\theta \, (1+\cos\theta)^2} \, d\theta$$

From Eq. (2)

$$\frac{R^2}{R_o^2} = \frac{\left(1 + \cos\theta_o \right)^2}{\left(1 + \cos\theta \right)^2}$$

Hence

$$\sigma^2 = 8 f^2 \delta^2 \frac{\left(1 + \cos\theta_o \right)^2}{\sin^2\theta_o} \int_0^{\theta_o} \frac{\sin\theta \, d\theta}{\cos^2\theta \, (1+\cos\theta)^4}$$

$$= 8 f^2 \delta^2 \frac{\left(1 + \cos\theta_o \right)^2}{\sin^2\theta_o} \int_0^{\theta_o} \frac{-d\cos\theta}{\cos^2\theta \, (1+\cos\theta)^2}$$

The integration can be evaluated using the following formula:

$$\int \frac{-dx}{x^2(1+x)^4} = \frac{1+x}{x} - 4\ln\left|\frac{1+x}{x}\right| - \frac{6x}{1+x} + \frac{2x^2}{(1+x)^2} - \frac{x^3}{3(1+x)^3}$$

Therefore:

$$\sigma^2 = \frac{8f^2\delta^2(1+\cos\Theta_0)^2}{\sin^2\Theta_0}\left\{ \frac{1+\cos\Theta_0}{\cos\Theta_0} - 4\ln\left|\frac{1+\cos\Theta_0}{\cos\Theta_0}\right| \right.$$

$$\left. - \frac{6\cos\Theta_0}{1+\cos\Theta_0} + \frac{2\cos^2\Theta_0}{(1+\cos\Theta_0)^2} - \frac{\cos^3\Theta_0}{3(1+\cos\Theta_0)^3} + 3.3143 \right\} \qquad (7)$$

Since

$$f = \frac{R_0(1+\cos\Theta_0)}{2}$$

Eq. (7) relates the spread of reflected flux to the rim angle θ_0 for a given dish radius.

Intercept Factor

The Gaussian distribution of the reflected flux at the focus is

$$I = I_{max} e^{-\frac{r^2}{2\sigma^2}}$$

where I_{max} = (total reflected energy)$/(2\sigma^2 \pi)$, w/m^2

  r = distance from focus, ft.

  σ = standard deviation of concentrated flux distribution at focus, ft.

For the cavity receiver, I_{max} is the peak focal plane flux.

The energy intercepted by a receiver of a given radius is

$$\int_0^r I \, 2\pi r \, dr$$

while the total reflected energy is

$$\int_0^\infty I \, 2\pi r \, dr$$

The intercept factor is defined as

$$\gamma = \frac{\text{reflected energy intercept by a receiver of radius } r}{\text{total reflected energy}}$$

Therefore $\quad \gamma = \dfrac{\displaystyle\int_0^r I\, 2\pi r\, dr}{\displaystyle\int_0^\infty I\, 2\pi r\, dr}$

$$= \dfrac{\displaystyle\int_0^r I_{max}\, e^{-\frac{r^2}{2\sigma^2}}\, r\, dr}{\displaystyle\int_0^\infty I_{max}\, e^{-\frac{r^2}{2\sigma^2}}\, r\, dr}$$

$$\gamma = \dfrac{I_{max}\, \sigma^2 \left(-e^{-\frac{r^2}{2\sigma^2}}\, r\, dr\right)}{I_{max}\, \sigma^2}$$

Finally,

$$\gamma = 1 - e^{-r^2/2\sigma^2} \tag{8}$$

Knowing the magnitude of σ^2 from Eq. (7), the intercept factor for a cavity receiver of radius r can then be calculated.

A-1.2   Experimental Verification of the Area Weighted Optical Model

From an analytical standpoint their are several ways to model the optical characteristics of the paraboloidal dish. A very precise way is thru the use of a computerized ray trace where a beam or ray, from the sun is deflected by a local slope error and spread due to the reflectors specular characteristics. By performing this trace around the dish, a focal plane energy profile is possible. The major drawback of this approach is that it is time consuming and does not lend itself readily to systems trade-off analysis.   Several closed form mathmatical approaches have been suggested (as discussed in A-1.1) and while they provide for managable equations for analysis, this validity must be checked experimentally. Such a model calibration was conducted on other ongoing GE programs, the results of which are discussed below.

A prototype parabolic dish collector has been designed and constructed as the first step in the development of point focus solar concentrators. The dish is constructed of 24 die stamped aluminum "petals" with a reflective tape applied to the parabolic surface. The dish diameter is 3.77 meters with a focal length to diameter ratio of 0.5. Two types of optical measurements have been done on this prototype dish, laser ray trace of the individual petals and flux mapping of the assembled dish. The laser ray traces indicate a RMS slope error of approximately 0.65 degrees. Using this value, a RMS specular spead of 2 mrads and a sun source error, the closed form models of Duff and of ku were used to predict the percentage of focal plane energy captured by the cavity receiver as a function of aperature size (or concentration ratio).

Flux mapping was performed on the assembled dish. A gang of thermal flux sensors were mounted on a track at the focal plane and then moved across the plane to record the flux profile. This raw data was fed into a computer and a three dimensional flux profile was reconstructed and then integrated to determine the amount of energy at the focal plane. Figure A-2 shows the computer reconstructed flux distribution at both the geometric focal plane and at a plane 3" forward of this. As can be seen the profile has a "normal" shape, thus indicating some validity to the RMS treatment of slope errors. Figure A-3 presents the results of numerical integrations of the flux profile when centered over a receiver of 8 thru 12" diameter. As can be seen, the method of Ku, ie the area weighted derivation, agrees excellently, and somewhat conservatively, with the measured flux profile from the prototype collector. This close agreement lends validity to the optical models used in the parameter analysis.

FIGURE A-2

GENERAL ELECTRIC

RECONSTRUCTED ENERGY FLUX PROFILES

GE ENGINEERING PROTOTYPE COLLECTOR

LOW COST CONCENTRATORS
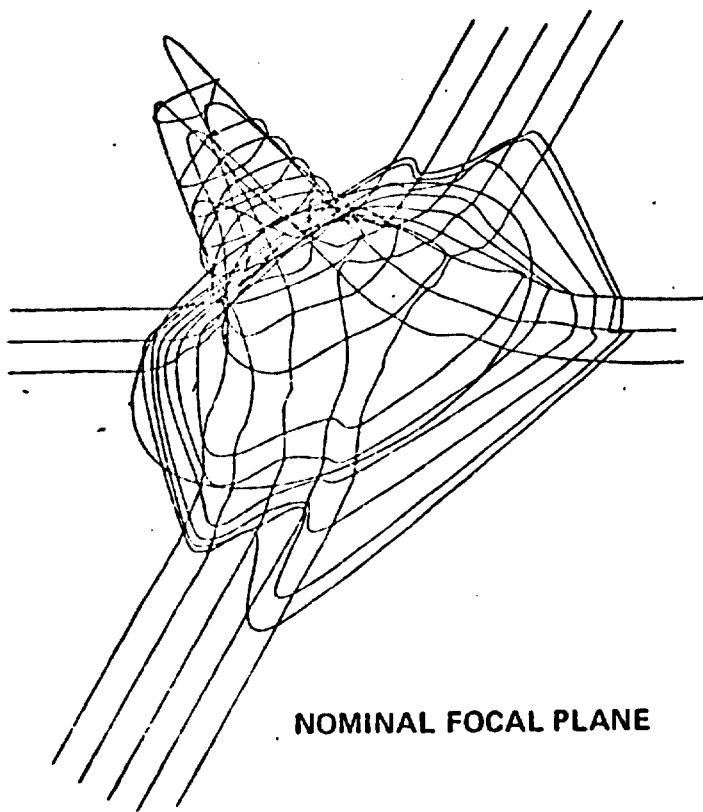
NOMINAL FOCAL PLANE
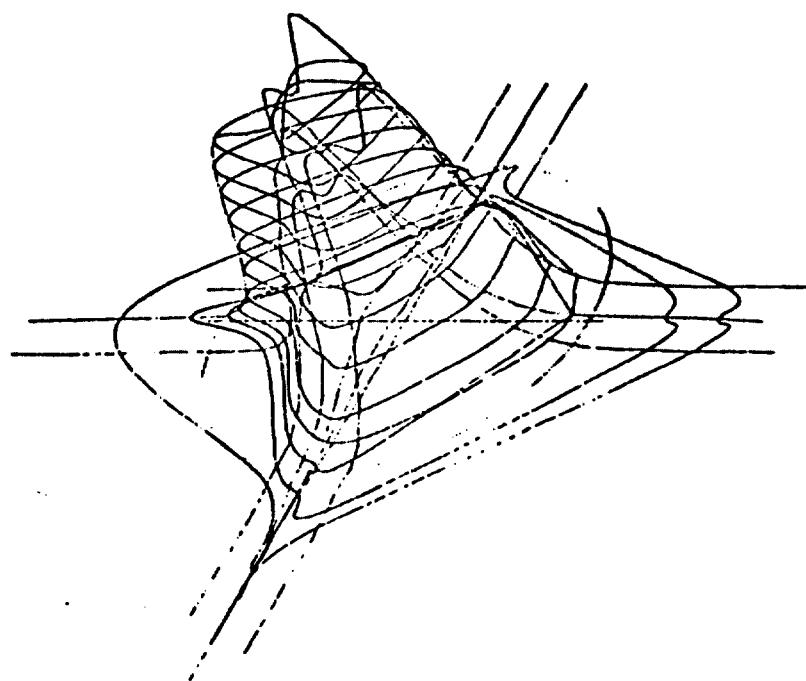
3" FORWARD

GENERAL
ELECTRIC

OPTICAL INTERCEPT FACTOR

LOW COST
CONCENTRATORS

A-11

INTERCEPT FACTOR

DUFF EQUATION

NOMINAL FOCAL PLANE

AREA WEIGHTED RESULT

APERTURE DIA. (INCHES)
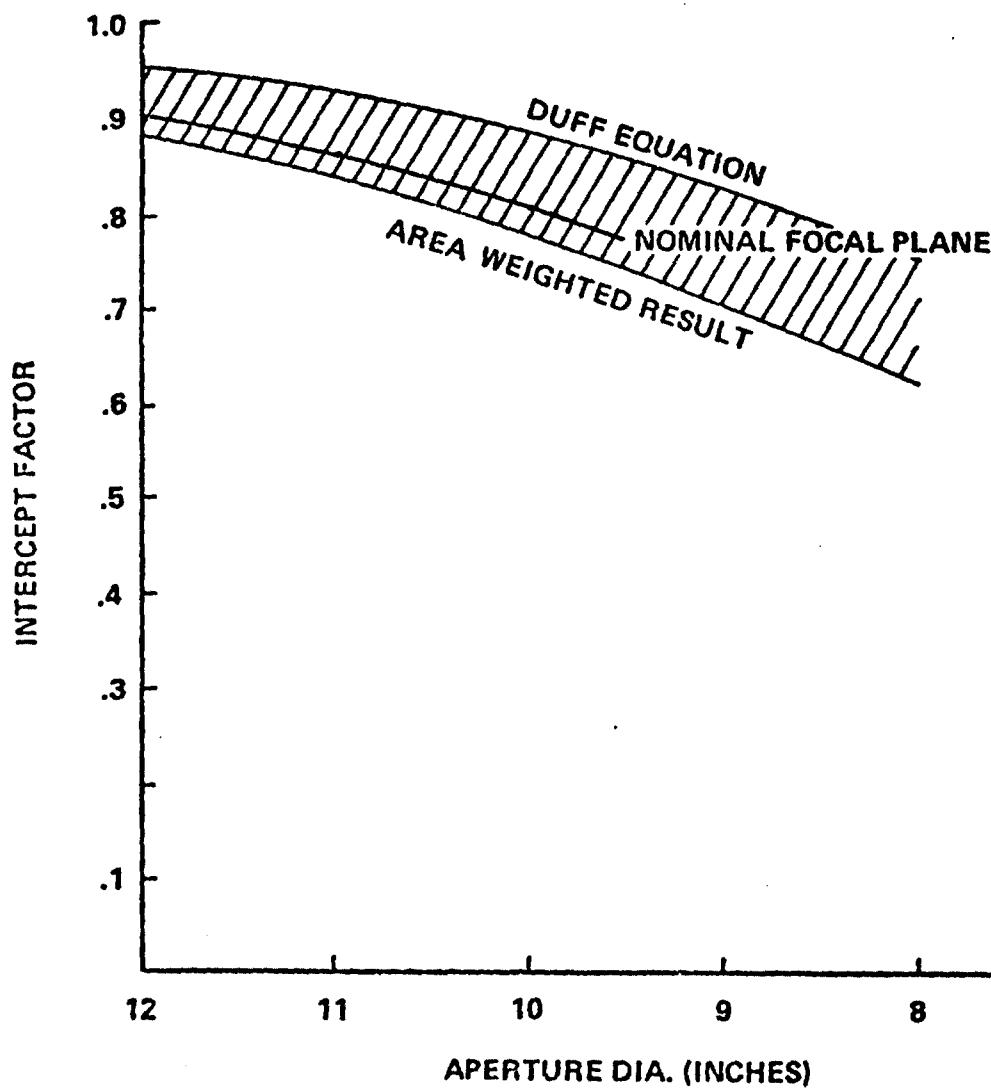
APPENDIX A-2

OPTICAL DEFLECTION ANALYSIS

INTRODUCTION & SUMMARY

The Energy distribution in the image plane of a paraboloidal concentrator with randomly distributed surface errors is usually described by two dimensional Gaussian spacial distribution. In the case of the low cost concentrating collector concept, eight sections or petals, each having a two dimensional paraboloidal contour are joined together to form a paraboloid of revolution. Precise alignment of these petals to insure that the center of the individual image distributions from each petal are co-located is necessary if the smallest distribution width is to be achieved. Maintaining such an alignment in the presence presents of environmentally induced loads such as those caused by winds requires stiffening of the structure with the associated cost increase. Depending on the amount of lost energy under various loading conditions it may be cost effective to allow some spreading of the image distribution under wind loads if a significant amount of structural cost can be eliminated.

This analysis assumes that the energy distribution from each segment of the paraboloid has a two dimentional normal distribution. The spreading will occur symetrically about a central axis through the receiver aperture into eight separate distributions. As the petals open in a similar fashion to that of a rose, the energy falling within the aperture will decrease. The amplitude of the image distribution at any spacial position is given by the sum of the contribution from each of the eight distributions. Total energy within the aperture is given by the weighted sum of all points within the aperture.

A-12

ANALYSIS

The energy distribution from a paraboloidal surface with random errors is assumed to have a radial function given in equation 1.

$$(1) \quad f(r) = \frac{I_0}{\sqrt{3\pi}\,\sigma} \, e^{-\frac{r^2}{2\sigma^2}}$$

where Io is a constraint related to the area of the paraboloid, reflectivity, and the solar intensity.

σ is the standard deviation of the "errors" associated with slope errors, surface specularity and the source function.

It is assumed that each of these sources of image spread can be expressed as Gaussian distributions so that aggregate standard deviation is given by the square root of the sum of the squares of the individual distributions.

$$(2) \quad \sigma_T = \sqrt{4\,\sigma_{SL}^2 + \sigma_{SP}^2 + \sigma_S^2}$$

when σ_T = image standard deviation

σ_{SL} = standard deviation of slope errors

σ_{SP} = standard deviation due to surface specularity

σ_S = effective half width of the sun

As the paraboloid opens, eight separate distributions are formed along axies spaced 45° from one another in the image plane. The amount of energy at a given position in the image plane is given by the sun of the contribution from each of the individual distributions

$$f(r) = \sum_{n} e^{-\frac{(r - r_0)^2}{4\sigma_T^2}}$$

where

r_n = position of the mean of distribution n

each of the distributions from a single petal is no longer circularly symmetric but forms an ellipse about its axis of symmetry. The apparent width of the

distribution is greatest along the axis of symmetry of the petal and is a minimum in the transverse axis as shown below:
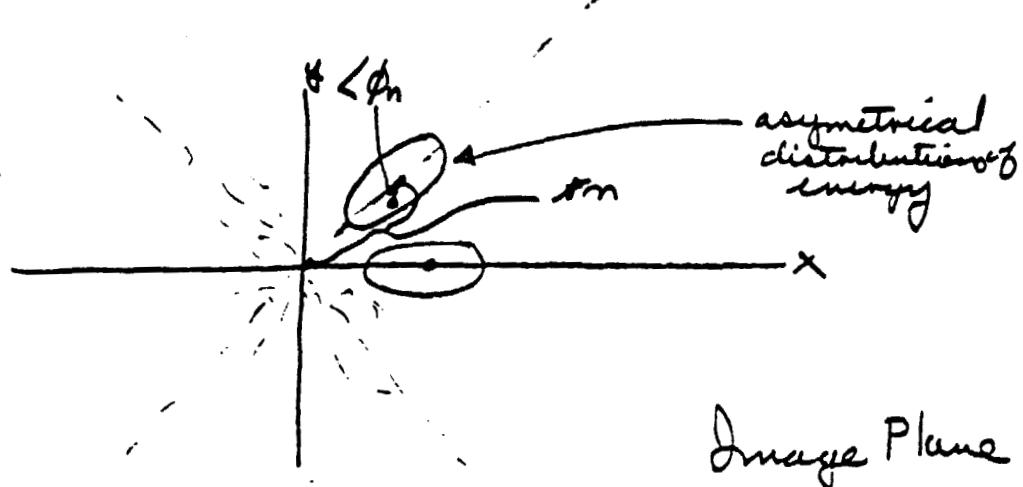
The variation in the apparent σ_T as a function of the angular position ϕ_n is approximately

$$\sigma_{T_n} = \sigma_T \left[\cos \theta_{max} \sin^2 \phi + \cos^2 \phi \right]$$

where θ_{max} is the rim angle of the collector

         ϕ_n is the angular position within a given distribution n.

RESULTS

The amount of energy falling within a given aperture radius can now be determined as a function of image spreading. The computation consists of determining the summation of the contributions of each distribution to each point within the aperture, weighing each point by the area function ($r\,dr\,d\phi$) and summing over the aperture area. Figure 1 shows the results for several spreads (in σ_T's) as a function of aperture radius (in σ_T's)

Fraction of Energy Collected by different Apertures for various displacement errors of eight petal configuration

Apertures Radius (Sigmas)

3.0

2.5

2.0

Fraction of Energy Collected

Petal Displacement (Sigmas)
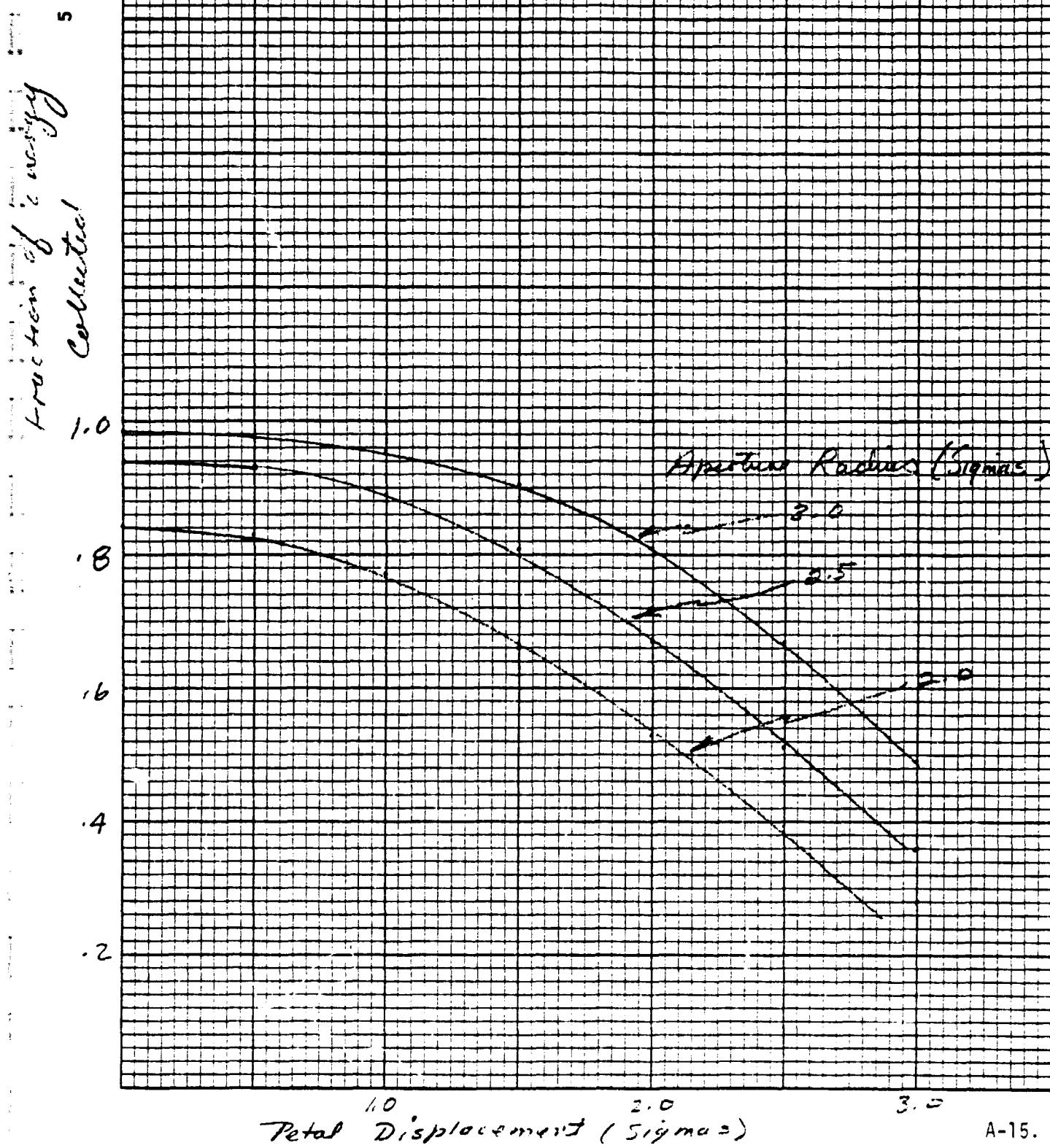
APPENDIX B

SUPPORTING PRODUCTION ASSESSMENT MATERIAL

B-1   MOUNT MEMBER TUBING

SCHUMAG MACHINERY, INC.

COMBINED TUBE WELDING AND DRAWING LINE FROM SCHUMAG

General Description

Escalating costs of labor and materials have increased
interest in production methods that will bring offsetting
savings. A critical look at the conventional tube-welding
and tube-drawing lines for precision tubing reveals that
these production lines involve a disproportionately larger
amount of material-handling, labor, floor space etc., than
needed in many other automated metal-forming systems.

Our engineers speculated that the Schumag continuous
drawing machine for wire drawing could be adapted to form a
simplified tube-welding and drawing line. If so, the drawing
machine would control stock movement through the tube-forming,
tube-welding and tube-drawing steps, eliminating the material-
handling between welding and drawing steps.

Research into this feasibility has led to development of
a one-pass, combined tube-welding and drawing machine. The
first five production versions of the machine have now been
installed and put into operation, with operating results
exceeding expectations.

The combined tube-welding and drawing machine eliminates the calibrating operation for restoring welded-tube roundness and sizing the tube. It also eliminates the need to cut tubing to length and to point the lengths before drawing. Instead, one length of material continues from the coiled strip, through the welder, through the drawing unit, and through the straightener. Only after straightening is the drawn tubing cut into commercial lengths. Figure 1 shows the contrast between this new machine and the conventional line.

Although the initial investment for the new, combined tube-welding and drawing line from Schumag is similar to that for a conventional line, operating costs are considerably lower.

Among the factors reducing operating costs are:

- Changeover to a different tubing size of cross-sectional shape is done in approximately one-tenth of the time;

- Only one operator and one helper are needed instead of the usual five to seven workers;

- Elimination of calibrating rolls and operation with fewer forming rolls halves tooling costs;

- Scrap in the form of cut ends is reduced to a tenth of the usual rate; and

- Floor space required for the new line is about 2,100 square feet rather than approximately 7,500 square feet.

Machine Description

The design and operation of the new, one-pass tube-welding and drawing machine are most easily explained by describing the sequential steps that transform stainless or carbon-steel, aluminum or copper strip stock into precision-drawn tubing. The seven basic steps are (A) forming, (B) welding, (C) weld-bead removal, (D) cooling and lubricant application, (E) drawing, (F) straightening, and (G) cutting to commercial length.

A. Forming - The tube former (Figure 2) has two non-driven strip-width-control sections, 6 driven forming sections, and 6 non-driven side-roll sections.

    An important feature of the tube former is the provision for quick change-over from one starting diameter to another. Forming rolls are shifted laterally, by pushbutton control from a machine-control console, to align any set of several alternate forming rolls for different starting diameters (Figure 3). Two men are able to make the change-over to a different starting diameter, including exchange of side rolls, in about 40 minutes.

B. Welding - A welding station follows the tube former. Three pairs of non-driven rolls close the tube tightly and guide it. A fixed aligning tab extends up into the slot of the moving tube, before the tube is closed, to prevent axial twisting.

In many respects, the seam-welding operation is similar to that on a conventional line. However, here the welder requires no drive system because the drawing unit pulls the tubing smoothly through the welder, controlling weld speed.

C. Weld-Bead Grinding - For stainless steel an abrasive-belt grinder on the line removes the bead from the seam-weld, smoothing the tubing surface. For carbon steel tubing, an outer seam scarfer is used.

D. Tube Cooling - Welded tubing passes through a trough where it is cooled by a water spray and then dried with compressed air. Drawing lubricant is thereafter applied to the cooled tubing, readying it for drawing.

Between the tube cooler and the drawing unit is a hydraulically operated squeeze pointer. It is used only when starting a new production run of tubing in order to get the pointed lead through the drawing die enabling the gripper jaws to grab it.

E. Tube Drawing - It is the tube-drawing unit that permits tube forming and tube drawing to be combined into one continuous process. This unit consists of a die stand, followed by two drawing carriages with their drives. Pneumatically operated jaws in each reciprocating carriage alternately grip the tubing, pulling it through the die in one smooth, continuous motion.

Cams of special shape impart the reciprocating motion
to the carriages and permit a return stroke that is faster
than the forward pulling stroke. Because of the faster
return, transfer of pulling action from one carriage to
the other occurs shortly before the first carriage slows
down for the return stroke. The result is the smooth and
continuous pulling motion essential for a high-quality weld.

F.   Straightening - After drawing, the tubing passes through
a roller straightener comparable to that on a conventional
line. The operating principle of the straightener is to
bend the tubing around two points of support until the
outer layer has been stretched beyond the elastic limit so
the tubing will not spring back.

For best results in continuous, high-speed operation, the
tubing is straightened several times in the vertical plane
and in the horizontal plane. The first rolls for
straightening in each plane bend the tubing through a
greater angle than do the following rolls.

All upper rolls of the seven-roll vertical straightener
are driven. Only the first four rolls of the seven-roll
horizontal straightener are driven.

Aligning the tube-travel axis of the straightener with the axis of the tube-drawing machine -- essential for straightness -- is simple. Adjustment at two points on the straightener completes alignment: one for vertical alignment and one for horizontal alignment.

G. Flying Saw Cut-Off - A flying saw cuts straightened tubing into commercial lengths. A proximity sensor or length counter triggers the saw cycle.

The movable saw carriage rests on guide rails and is accelerated to line speed by a stroking cylinder. When line speed is attained, clamps on both sides of the saw blade grip the tubing firmly, holding the tubing against the saw carriage. After cutting occurs, the clamps release and the carriage returns to its starting position.

Tubing cut to commercial lengths is discharged automatically onto a roller conveyor at the end of the line.

Machine Advantages

After this description of how the combined tube-welding and drawing machine operates, some of the advantages become clearer.

First, the new machine produces multiple finished tube diameters or cross-sectional shapes from a single starting diameter and strip width. When starting diameter is unchanged, only the drawing unit needs retooling. Retooling consists of changing the die and the drawing jaws, requiring an average of

10-20 minutes. Drawn-diameter reductions can be up to 30-35 per cent.

When starting diameter is changed, time for retooling averages some 40-50 minutes, contrasted with 6 to 8 hours for the conventional line. The time saving is attributable primarily to elimination of calibrating stands and addition of pushbutton control for quick change-over of the tube former rolls. Note the change-over time for the roller straightener is approximately the same for either the new or conventional lines.

The second advantage is savings in labor: Only two workers are needed. The manpower saving comes primarily for elimination of material-handling operations between welding and drawing.

A third advantage of the combined tube-welding and drawing machine is the reduced tooling cost because there are no calibrating rolls and fewer forming rolls. Tooling cost has proven to be 48 per cent of that for a conventional line of comparable capacity.

A scrap rate that is 5 per cent for conventional tube-welding and tube-drawing lines is reduced to 0.5 per cent, chiefly because only one pointed end is discarded: for each new tubing size produced on the combined tube-welding and forming machine.

The fifth advantage is the saving in floor space: 2,100 square feet compared with 7,500 square feet (195 m2 and 700 m2). Size of the floor space needed for the new line is 15 x 140 feet (4.6 x 42.7 m).

Evaluating only two of the cost advantages -- labor and floor space -- with five fewer workers and 5,400 fewer square feet, annual savings of $235,500 can be projected.

5 workers @ $14,700 annually, including

fringes, is $ 73,500

5,400 square feet @ $30/square foot

annually is $ 162,000

Totalling $ 235,500

As explained, the new, combined tube-welding and drawing line is more flexible than a conventional line. A wide range of precision tubing sizes and shapes can be drawn from the same starting size, diminishing the inventory of coiled strip. For size reductions greater than the 30 per cent permissible range, or a larger finished tube, the tube-former rolls are merely shifted laterally for the new strip width selected.

Shape of the finished tube may be round, square, rectangular, oval, or most any special shape required.

Size tolerances and surface finishes for the new and conventional methods are comparable. In production, it has been established that the new line permits tube tolerances to be made tighter .008" (.2 mm), with an improvement in surface finish. With a hollow draft, material saved is calculated to amount to $ 85,000. annually based on carbon steel drawn at a rate of 200 feet/minute (60 m/minute) for 6,000 hours.

Machine Specifications

```
KRZ-I   for Stainless Steel Tubing
     Finished O-Ds          6 - 30  mm
     Wall Thickness         .5 - 2   mm
     Drawpull               14300 lbs.

KRZ-II for Stainless Steel Tubing
     Finished O-Ds          10 - 42 mm
     Wall Thickness         1 - 3   mm
     Drawpull               22000 lbs.

KRZ-III for Stainless Steel Tubing
     Finished O-Ds          16 - 76 mm
     Wall Thickness         1 - 3.5 mm
     Drawpull               33000 lbs.

KRZ-I   for Carbon Steel Tubing
     Finished O-Ds          8 - 30  mm
     Wall Thickness         .5 - 2   mm
     Drawpull               14300 lbs.

KRZ-II for Carbon Steel Tubing
     Finished O-Ds          10 - 42 mm
     Wall Thickness         1 - 3   mm
     Drawpull               22000 lbs.

KRZ-III for Carbon Steel Tubing
     Finished O-Ds          16 - 76 mm
     Wall Thickness         1 - 3.5 mm
     Drawpull               33000 lbs.
```

Finished lengths from 3 meters (10 feet) upwards length · tolerance max. ± 10 mm (.394"). Max. line speeds are 100 meters (320 feet) per minute for carbon steel (depending on wall thickness and % reduction).

For stainless steel the limits are presently at 5 meters (16 feet) per minute, where the speed is controlled by the welder.

Applications

Tubing for a wide range of markets and purposes can be produced readily and economically on the same combined tube-welding and drawing machine. In addition to round tubing of stainless steel for food and beverage processing, tubing of other cross-sectional shapes may be used for business and residential furniture.

Additional applications include heat exchanges, high pressure tubing, mechanical piping, etc.

2:78

Combined Tube Welding and Drawing Line, Type "KRZ"

SCHUMAG

ELEC. CONTROL CABINETS

DRAWING + Straight.

Flying SAW

ELEC. CASING TURNING

WELDING

20' Tubes
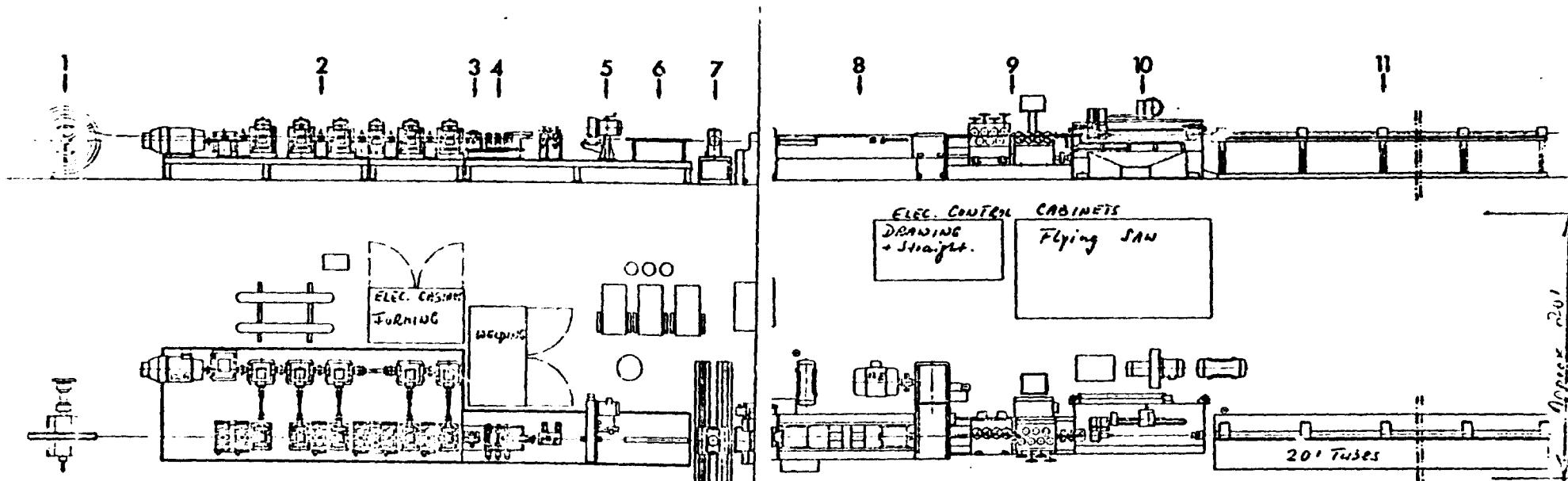
Approx. 20'

| 1 – Pay-off | 2 – Tube Former | 3 – Guide for the slot before the weld | 4 – Welder | 5 – Weld Bead Removal (belt grinder) | 6 – Cooling Trough | 7 – Squeeze Pointer | 8 – Drawing Unit | 9 – Roller Straightener | 10 – Flying Saw | 11 – Roller Conveyor |

Approx. 150'

Total sq/Ft = Approx 3000

0922 A75.07.11

SCHUMAG MACHINERY, INC.   Q U O T A T I O N #H-553

General Electric Company
Schenectady, New York   February 6, 1979

"SCHUMAG" Combined Tube Welding and Drawing Line, Type KRZ III

For in line forming, welding, drawing (sinking pass), straightening
and cutting to length of carbon steel tubing.

Working Range:

Finished Tube Diameters: .630" - 3.00"

Wall Thickness: .039" - .140" (depending on O-D)

Max. Drawbar Pull: 33,000 lbs.

Line Speed: 25 - 328 ft./min.

Min. Finished Length: 20 ft.

Max. Length Tolerance: +.394"

BASIC MACHINE PRICE: $ 819,898.--
per drawing 0922 A75.07.11   ============
including tooling for one finished
diameter, w/o welder

Consisting Of:

Dual Reel Pay-Off   Pos. 1 $ 32,602.--

Tube Forming Unit   Pos. 2 $ 188,370.--

Tube Positioner   Pos. 3   Incl. in Pos. 2

External Weld Bead Scarfer   Pos. 5   Incl. in Pos. 2

Cooling Tower   Pos. 6   Incl. in Pos. 2

Hydraulic Squeeze Pointer   Pos. 7 $ 41,469.--

Drawing Unit with Single
Speed Gear Box   Pos. 8 $ 246,612.--

Vertical & Horizontal
Straightener   Pos. 9 $ 93,880.--

Flying Saw   Pos. 10 $ 138,000.--

Driven Exit Roller
Conveyor, 23' long   Pos. 11 $ 17,250.--
DC Drive Complete   Pos. 12 a & b $ 61,715.--

REFERENCE X-31557

ON

YODER

W-35 TUBE MILL

FOR

GENERAL ELECTRIC COMPANY
SCHENECTADY, NEW YORK

FEBRUARY 15, 1979

PRODUCT

             3" O.D. by .125" wall to
             5" O.D. by .125" wall maximum

cut-to-length tube made from cold rolled, hot rolled pickled or hot
rolled unpickled low carbon steel in coiled form slit accurately to
width.   The maximum wall specification is based on strip hardness
not exceeding 75 Rockwell B or a maximum yield strength of 45,000 psi.

SPEED

             50 to 200 feet per minute.

The speed at which a particular tube can be run depends upon the
quality of material, operator technique, wall thickness, and the
diameter of the tube. Approximate attainable welding speeds are
listed below:

TUBE SIZE	WELDING SPEEDS FOR 150 KW, 450 KHz INDUCTION WELDER
3" O.D. x .125" wall	160 FPM
5" O.D. x .125" wall	130 FPM

MILL DIRECTION
The tube mill line will be for right to left hand operation.

ELECTRICAL SPECIFICATIONS
460 volt, 3 phase, 60 hertz, Power Supply.
110 volt, 1 phase, 60 hertz, Control Voltage.

UTILITIES REQUIRED (Approximate)
Electric Power   --   700 KVA.
Cooling Water   --   50 GPM at 75°F (For R.F. Weld Power Unit)
Cooling Water   --   60 GPM (Cooling Trough and Weld Area)
Air   --   10 CFM at 80 psi.

PAINT
All equipment will be painted Conolac Industrial Enamel #80
Blue Gray.

Number of men required to run line - four (4).

Approximate floor space required - 250' long x 25' deep
plus space required for material storage and handling.

EQUIPMENT SUMMARY

ITEM	DESCRIPTION	
1	Double Swivel Coil Reel	
2	End Detector	
3	Shear & End Welder	
4	Strip Storage System	
5	W-35-7 Tube Forming Machine	
6	Welder Mechanicals	
7	Tube Cooling Section	
8	W-35-3 Tube Sizing & Straightening Machine	
9	Drive Connections	
10	Rotary Cutoff Machine	
11	Runout Table	
12	Drive Electrics	
13	150 KW Induction Welder	
	TOTAL BALL PARK INVESTMENT --	$800,000

14   Tooling
One complete set of roll tooling will be
approximately $25,000 to $65,000 per set,
depending on tube size to be made. Roll
material would be high-carbon, high-chrome
tool steel.

FWC:ah

TELEPHONE CALL RECORD

xXx
From Frank Canda
The Yoder Company
Office Cleveland, Ohio

Date 2/13/79   **Time:**

Customer

Phone 8*216/631-0520

Ref. No.

Subject Tube Mill for Producing 40,000,000 ft./yr. of 4-1/2" x 1/8
Wall Mechanical Steel Tubing.

Equipment:	$800,000	
Tooling :	$ 65,000	$25,000/yr. Tooling Maintenance
Facilities:	700 KVA	
	50 gal./min. water	
	10 cu.ft./min 85 Psi air	

| Labor | : | 4 men - 2 shifts |
| Space | : | 250 ft. x 40 ft.   10,000 sq. ft. |

+

5,000 sq.ft. material storage

Action required: (Yes) (No)

Copies to:

Shields M. Bishop
Signed

The Copperweld Tubemakers

OHIO STEEL TUBE COMPANY

Shelby, Ohio 44875 U.S.A.
Birthplace of America's Seamless Steel Tube Industry

DIRECT MILL REPRESENTATIVES
200 SOUTH SERVICE ROAD
ROSLYN HEIGHTS, NEW YORK 11577
TEL.: (916) 484-2550

Quotation

to   Corporate Consulting Services
General Electric Company
One River Road   Bldg 10A Rm. 127
Schenectady, N. Y. 12345

Attn: Mr. Shields M. Bishop
        Consultant Metals Processing

Date   March 9, 1979

Reference:

TERMS: ½ OF 1% 10 DAYS. NET 30 DAYS APPLYING ON NET F.O.B. SHELBY VALUE. F.O.B. SHELBY, OHIO, FREIGHT COLLECT
UNLESS OTHERWISE SPECIFIED. FREIGHT ALLOWANCES, IF ANY, WILL BE INDICATED BELOW.

ORDERS PLACED AGAINST THE FOLLOWING QUOTATION ARE SUBJECT TO THE CONDITIONS PRINTED ON THE BACK HEREOF

WE APPRECIATE SINCERELY THE OPPORTUNITY TO QUOTE ON YOUR REQUIREMENTS.

Gentlemen:

     This will confirm prices quoted on February 22, in connection
with the Solar Energy Collector.

SPECIFICATION: "Custom Made Copperweld Steel Tubing" 1020 Hot
rolled, electric welded, inside welding flash-
in, type 1 unannealed and conforming to ASTM A 5 13

PRICES: Size 4.500" O.D. X .120 wall
           ±.020   +.003
                       -.013

10 UNITS				142 UNITS			
60 pcs	11 ft.	$191.08	C/ft	852 pcs	11ft.	$167.59	C/ft
40 "	17 "	$191.08	"	568 "	17 '	$167.59	"
20 "	13 '	$191.08	"	284 "	13'	$167.59	"
40 "	15 '	$191.08	"	568 "	15'	$167.59	"
10 "	40 '	$216.14	"	142 "	40'	$192.65	"

Size 3.000" O.D. X .120 wall
           ±.000   +.004
                       -.012

10 UNITS				142 UNITS		C/ft
100 pcs	7 ft.	$131.77	C/ft	1420 pcs 7 ft.	$103.90	
70 pcs	12 ft.	$128.80	"	994 pcs12 ft.	$106.01	

SHIPMENT: Will be develop at time you are ready to order.

The Copperweld Tubemakers

OHIO STEEL TUBE COMPANY

Shelby, Ohio 44875 U.S.A.
Birthplace of America's Seamless Steel Tube Industry

DIRECT MILL REPRESENTATIVES
200 SOUTH SERVICE ROAD
ROSLYN HEIGHTS, NEW YORK 11577
TEL.: (516) 484-2550

Quotation

to

Corporate Consulting Services
General Electric Company
One River Road Bldg 10 Rm 127
Schenectady, N. Y. 12345

Date March 9, 1972

Reference:

Attn: Mr. Shields M. Bishop
Consultant, Metals Processing

TERMS: ½ OF 1% 10 DAYS. NET 30 DAYS APPLYING ON NET F.O.B. SHELBY VALUE. F.O.B. SHELBY, OHIO, FREIGHT COLLECT
UNLESS OTHERWISE SPECIFIED. FREIGHT ALLOWANCES, IF ANY, WILL BE INDICATED BELOW.

ORDERS PLACED AGAINST THE FOLLOWING QUOTATION ARE SUBJECT TO THE CONDITIONS PRINTED ON THE BACK HEREOF

WE APPRECIATE SINCERELY THE OPPORTUNITY TO QUOTE ON YOUR REQUIREMENTS

DELIVERY: Prices quoted are f.o.b. mill, all transportation
charges collect. In the absence of a specified routing
the most economical method of transportation
available will be used. A transportation allowance
effecting equalization or item #1 Oil City, Pa
on item #2 Brooklyn, N. Y. and predicated on the
actual method of transportation used, will be
shown separately in billing.

Yours very truly,

OHIO STEEL TUBE COMPANY

James M. Cunningham

JMC/ck

B-2 MOUNT FITTINGS

THE UTICA STEAM ENGINE & BOILER WORKS

726-806 Whitesboro Street

UTICA, NEW YORK

February 22, 1979

General Electric Co.
Shields Bishop
Building 10A
Room 127
Schenectady, N.Y.   12345

Dear Mr. Bishop:

This will confirm our "ballpark" price for
trunion fittings for the Solar Concentrator.

Castings of either aluminum or cast iron,
will be approximately $40.00 each with a one
time charge of about $1200.00 for pattern
equipment. Fittings fabricated from steel
tubing will also be approximately $40.00.

Fittings for other parts of the concentrator
will be about the same, depending on complexity.

These prices are valid for prototype quanti-
ties of less than 200 per style. Greater quan-
tities of castings should probably be separately
priced for die casting or other high production
methods.

Sincerely,

THE UTICA STEAM ENGINE & BOILER WORKS

E. Burrell Fisher
Assistant Secretary

EBF:me

Memo - 3/12/79

AUTOMATED WELDING EQUIPMENT COSTS

Mr. J.D. Carey, Manager, Metal Joining, Manufacturing Technology Development and Applications, General Electric Co., Schenectady, N.Y. (Phone 518/385-3056) was consulted concerning the cost of automated welding equipment for the fabricated hardware of the solar concentrator. Based on recent pricing of this type of equipment, Mr. Carey estimated the following costs for the equipment required:

MIG-TIG Welding Machines - $ 7,000 ea. x 15 = $105,000

Control Robots   - $50,000 ea. x 15 = $750,000

Total = $855,000

SM Bishop

TELEPHONE CALL RECORD

From R. Swett
        Swett & Swett Welding
Office Schenectady, NY

Phone (518) 393-0336

Date   3/1/79   **Time:**

Customer

Ref. No.

Subject Cost Estimate for LCC frame

Exclusive of the ribs for the reflector, Swett estimated a total cost of $4,500 for the <u>moving</u> part of the steelwork. Foundation cost would be additional.

He estimated five weeks delivery after order placement.

(This firm does a large part of steelwork fabrication for Automation Equipment Systems, Schenectady, Bldg. 10)

Action required: (Yes) (No)

Copies to:

Signed   Shields M. Bishop

B-3 DISH RIBS

LAVELLE AIRCRAFT COMPANY

Manufacturers of Airplane Parts

NEWTOWN, BUCKS COUNTY, PENNSYLVANIA 18940 • (215) 968-3838
TWX 510-667-2255

February 26, 1979

General Electric - Energy Systems
Building 10 A, Room 127
Schenectady, N. Y.   12345

Attention: Mr. Shields Bishop

Dear Mr. Bishop:

In response to your request of our Ronald Wilks, we are pleased
to offer to manufacture and form the lower rib caps to a radius
(to be defined) described by G.E. drawing "LCC Preliminary Concept
#2 - 7 Meter Dia." dated 18 January 1979. In summary the cost for
accomplishing the tasks outlined are:

	Cost per pc.	Tooling
Cap (made from Sheet metal	$ 62.62	$ 800.00
Set of parts plus assembly of rib	462.38	1,500.00
Total -	$525.00	$2,300.00
Cap (made from extrusion)	68.12	1,450.00
Set of parts plus assembly of rib	456.88	1,500.00
Total	$525.00	$2,950.00
1 set of 8 ribs	$525.00 each	$4,200.00 total
2-5 sets of 8 ribs	475.00 each	3,800.00 total
6-10 sets of 8 ribs	435.00 each	3,480.00 total

The above prices do not include end pieces since we have too little
information on the designs.

If the caps are to be made from sheet metal, we'd recommend the use
of 6061T4 aluminum sheet; if extruded, we recommend 6063T6. The
prices above include material.

Tooling costs include:

Stretch dies - $ 800.00
Extrusion die -   650.00
Assembly jig -   1,500.00

The extrusion die and assembly jig would be usable in producing large quantities, the stretch die would not.

For purposes of planning you should safely expect to have parts within 16 weeks after placement of the order, assemblies within 20 weeks.

As discussed with Mike Concannon, we have several suggestions which you might consider for production. These include ideas which I believe Ron has already transmitted; e.g., assembly at the site in specially designed trailers and extruding the cap. In addition, please consider the design attached. It provides the capability for keeping the reflector base uniform in thickness rather than requiring a thick edge. Additionally, it permits rapid assembly. If you have any questions, please feel free to call either Ron Wilks or me. Ron will be on the west coast until Monday, 3/2/79.

I hope this meets your needs; we are looking forward with great anticipation to working with you on this project. If we can be of any other assistance, please call on us.

Very truly yours,

LAVELLE AIRCRAFT COMPANY

Richard Ludwig
President

RL:ac
enc.

Copy: M. Concannon, G. E.
       R. Wilks, H. Platon, J. Magalhaes, S. Evans, Lavelle Aircraft

EXTRUSION

FOAM-IN-PLACE PLASTIC

PLASTIC PETAL
WITH REFLECTIVE LAYER

FEEDER HOLE

ALT. #1

EXTRUSION #1

PLASTIC PETAL
WITH REFLECTIVE
LAYER

RUBBER GASKET

EXTRUSION #2

ALT #2
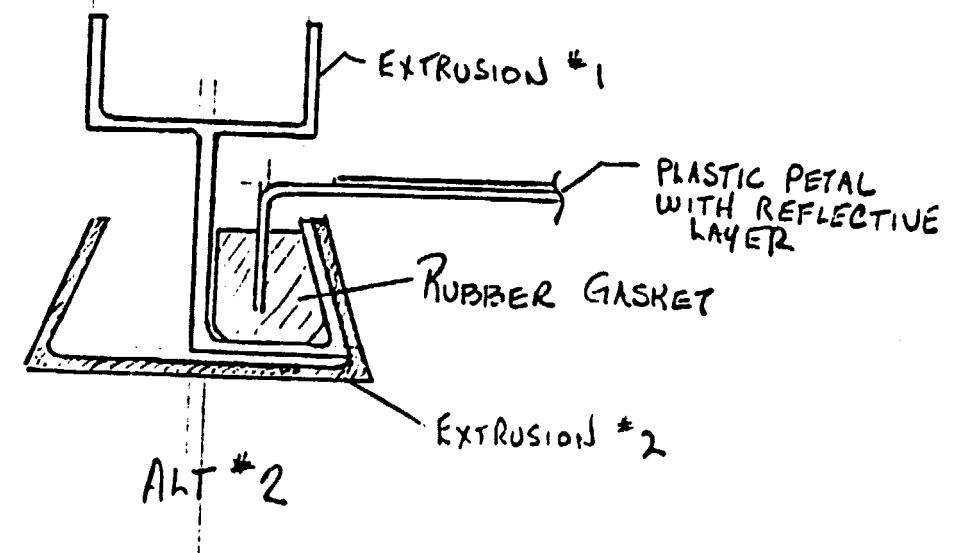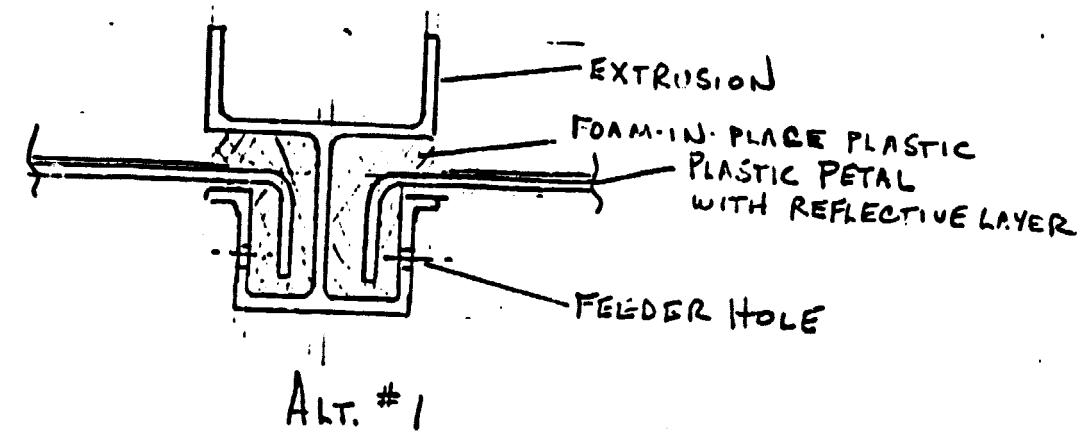
LAVELLE AIRCRAFT CO
R. LUDWIG 2/26/79

B-4   GORES

New England Boat Builders, Inc.

Mar. 2, 1979

Mr. Shields M. Bishop
Consultant, Metals Processing
Building 10A, Room 127
General Electric Co.
One River Road
Schenectady, NY 12345

Dear Shields:

This will confirm our telephone conversation of 3/1/79 regarding the parabolic reflectors.

The prices we have arrived at are tentative and are based on parts that are solid polyester-fiberglass or epoxy-fiberglass, 1/4" thick, with a 1/8" thick flange on the sides that have to be fastened together and a similar flange on the perimeter edge for stiffening and strengthening. Prices have also been based on, a. one mold for each part, b. two molds for each part.

Material	Part	a. One mold each:	b. Two molds each:
Polyester/glass	Perimeter	$185.00	$150.00
" "	Center	165.00	130.00
Epoxy/glass	Perimeter	270.00	215.00
" "	Center	240.00	185.00

Since we are currently making parabolic reflectors for Sylvania in polyester/glass, I feel that the polyester prices above should be pretty close. The only problem with them might be the future price of polyester resin, which went up about 8% late last year and is scheduled for a similar increase before June and some suppliers are predicting that by the end of the year the price of resin could be 50% higher than it was last year. The price of fiberglass also was raised by about 10% late last year and will probably do the same again some time this year.

Based on some calculations we did, the perimeter pieces should weigh approximately 62 lbs. ea. and the center pieces 44 lbs. ea., including flanges.

In regard to tooling, this would be the procedure:
1. Make a model (reversed) of a complete 1/8 section.
2. Make masters parts (2) from the model.
3. Make molds from the masters.

Tentative prices for these are as follows:

Model: $3300.00
Masters: 600.00 ea., 2 req'd.
Molds: 600.00 ea., at least 2 req'd.

The finish on the model, and subsequently the masters, molds, and parts, would be about equivalent to the mold finish for the boats we make or the reflectors. This finish, which will have to be more accurately defined, is not mirror shiny. The degree of finish has a great bearing on the price of the model, depending as it does on the number of man hours of polishing by hand.

If as many as 1600 parts were required in one year, at least 6 molds of each part would be required, 8 of each would be better. Of course, this would also have the effect of lowering the price of the parts, possibly as much as 25%.

These parts, in polyester/glass, would be approximately equivalent in strength properties to epoxy/glass, and would have somewhat better weathering properties. We work with both of these materials and find the polyester easier to handle and also present less health problems. If you wanted epoxy/glass, it would probably be a good idea to test at least one reflector in polyester/glass as a comparison.

In regard to the engineering of the reflector, it is possible to make lighter and stronger parts by including some type of core, such as honeycomb, end grain balsa or foam. However, it probably is best to start with the simplest type of construction and go on from there.

I would like to thank you for the opportunity to work with you on this project and look forward to hearing from you again.

Sincerely Yours,

John Feroce

John Feroce, President

TELEPHONE CALL RECORD

Xrox

From John Feroce
New England Boat Builders, Inc.
Office Mattapoisett, Mass.

Date 3/2/79   Time:

Customer

Phone   8*617/758-9050

Ref. No.

Subject   LCC Plastic Reflector Parts

For prototype, hand lay-up reflector gores, the following

costs would apply:

Model $3,300)
Master Part   600) $5,100 tooling cost
Molds (2)   1,200)

Gores would cost $ 185 Outer
                 $ 165 Inner   for the first
                   Polyester

                 $ 270 Outer
                 $ 240 Inner
                   Epoxy

80 pieces (5 reflectors)
Each reflector would cost $2,800 in polyester
and $4,080 in epoxy. For 5 reflectors, tooling would
cost $1,020 each.

Letter confirming will follow.

Action required: (Yes) (No)

Copies to:

Signed   Shields M. Bishop

TELEPHONE CALL RECORD

To   Dr. S.H. Schroeter
From   Dr. J.V. Crivello   Date 2/12/79   Time:
        Polymer Studies Branch
Office CR & D   Customer

Phone 5-8806
                                    Ref. No.

Subject   Reaction Injection Molding of Large Epoxy Partswith Reinforcement.

    Experimental moldings have been made in epoxy 28" x 18",

    but production is several years in the future. The epoxy at

    current costs, will be about $1.25 to $1.50/lb. The molding

    cycle will be about 2 minutes minimum. Pressure requirements

    will be about 50 to 100 psi, resulting in relatively light

    equipment.

Action required: (Yes) (No)

Copies to:

                                    Signed   Shields M. Bishop

TELEPHONE CALL RECORD

To
Rrox J.W. Arnold, Process Engineer Date 3/2/79 Time:
General Motors Manufacturing Development
Office Warren, Michigan Customer

Phone 8*313/575-8993 Ref. No.

Subject

Precision attainable in Reaction Injection Molding of urethane
plastic automotive fascias.

Arnold estimated precision of large RIM molded parts as with a
range of .25%. He referred me to Mobay for further information
on RIM.

(Arnold is author of:

> AUTOMATION OF REACTION INJECTION MOLDING OF
> AUTOMOBILE FASCIAS

a paper which appeared in Journal of Cellular Plastics, May/June, 1978)

Action required: (Yes) (No)

Copies to:

Signed Shields M. Bishop

TELEPHONE CALL RECORD

To
Bruce Niekamp   Date 2/9/79   Time:

Office **Plastics Business Div.**   Customer
Pittsfield, Mass.
Phone **8*236-4178**   Ref. No.

Subject **Metallized Plastic Films**

Niekamp said that .003" Lexan film would cost 4¢/sq.ft.

A "super" protective coating (proprietary) is under development

which will make the Lexan U.V. and weather resistant for "many

years". The plan is to get the "super" coating down to

35¢/sq.ft. Based on these figures, it is conservative to

estimate a Lexan metallized film @ 50¢/sq.ft.

Niekamp referred me to:

Metallized Products Div.
King Seeley Thermos Co.
37 East St.
Winchester, Mass. 01890

8* (617) 729-8300
Robert W. Steeves, Plant Manager

Action required: (Yes) (No)

Copies to:

Signed   Shields M. Bishop

TELEPHONE CALL RECORD

To
From R.W. Steeves   Date   2/9/79   Time:
      Metallized Products Div.
Office King Seeley Thermos Co.   Customer
      37 East St., Winchester, Mass, 01890
Phone 8*(617) 729-8300   Ref. No.

Subject Cost & Quality of Metallized Plastic Film

A typical rate for metallized film is $300/roll. For 26" D roll

x 6 ft. wide of .003" Lexan this is .34¢/sq. ft.

Steeves said King Seeley has developed and is patenting an

inorganic coating for the aluminum on metallized plastic film.

This inorganic film which is more transparent than other films

is not degraded by UV and is very corrosion resistant. He has

many samples under test in various locations such as seashore,

industrial, and desert areas.

Action required: (Yes) (No)

Copies to:

Signed   Shields M. Bishop

B-5   DRIVE GEAR MOTOR

INTER-OFFICE MEMO

TO: Stu Young

FROM: Jim Evans

DATE: February 15, 1979

SUBJECT: GE SPACE DIVISION
           Sergie Onufreiczuk

Stu:

Milt and I have discussed this particular unit in great detail
and while Sergie would like to work with the VW77 or a similar
worm gear drive it is going to increase his cost tremendously.
The reduction required in a worm gear unit would have an overall
efficiency of approximately 28% to 30%. This means with a 1/6
H.P. motor, which could be totally enclosed and still run for
duty cycle in the night mode or return mode, would not produce
the 4000+ inch pounds that may be required. It would take at
least a 1/4 H.P. motor and possibly more because of the ineff-
iciencies.

The 1/6 H.P. PSC Motor could be used on the VW47 as we have
suggested and produce approximately 6,000 inch pounds with no
problem at all.

To tool the gearmotor we would not amortize the piece price but
would charge tooling up front as usual. It would be between
$20,000-$30,000. The piece price of the unit self estimated would
be about $85-$95 depending upon the motor cost when we got into
production.

As we have mentioned on the VW47, the brake to prevent back driving
we know will withstand better than 500 inch pounds back driving
force. We believe it would be better designed, better motor, better
unit all the way around.

The questions which Sergie asked me concerning in rush current,
gear size and mass, or motor time full speed, gear box time at
full speed, and output torque or motor output torque and gear
efficiency are not available because we do not yet have that
motor. The present 1/6 H.P. PSC motor was designed to duplicate
the shaded pole motor but with the feature of reversing. It has
a 43 ounce inch starting torque and 112 ounce inch running torque.
This is not adequate for what they need.

In terms of efficiencies the VW47 has approximately 60% through
the geartrain, a worm gear unit approximately 28%-30%. We still
believe that the VW47 with a brake would be the correct way to
go and price wise would be less expensive than the worm gear drive
under any conditions. You can figure approximately $85 in quantity
for the VW47 and it is possible in the 100,000 lot he is looking
for this could be dropped to about $65.00.

JE:de

(Dictated but not read)

TELEPHONE CALL RECORD

Xox

From L. Snyder
Specialist- Rates & Routes
Office Schenectady Utilities Oper.

Phone 8*235-4634

Subject Shipping Cost for LCC

Date 3/2/79 **Time:**

Customer

Ref. No.

Snyder said that the class 45 (machinery) rail freight rate for Louisville, Ky. to Los Angeles, CA. is $12.32/100 lbs. in carload quantities.

Small numbers (less than 10) would get a lower rate by motor truck, because the railroads do not ship less than carload quantities. However, shipping costs, even in small numbers should not exceed $15/100 lbs. for transportation from Louisville to Los Angeles.

Action required: (Yes) (No)

Copies to:

Signed Shields M. Bishop